**DEPARTMENT OF ELECTRICAL ENGINEERING AND COMPUTER SCIENCE**
**SCHOOL OF ENGINEERING AND SCIENCE**

**NEW YORK UNIVERSITY**

**UNIVERSITY HEIGHTS BRONX, NEW YORK 10453**

TECHNICAL REPORT 403-22

# DIGITAL COMPUTER TRANSFORMATIONS FOR IRREGULAR LINE DRAWINGS

Giovanni B. Reggiori

April 1972



Prepared by

NEW YORK UNIVERSITY
School of Engineering and Science
Department of Electrical Engineering and Computer Science
University Heights, Bronx, New York 10453

Prepared for

OFFICE OF NAVAL RESEARCH
INFORMATION SYSTEMS BRANCH
Contract N00014-67-A-0467-0010

iia

UNCLASSIFIED
Security Classification

**DOCUMENT CONTROL DATA - R & D**

(Security classification of title, body of abstract and indexing annotation must be entered when the overall report is classified)

| | |
|---|---|
| 1. ORIGINATING ACTIVITY (Corporate author)<br>NEW YORK UNIVERSITY, School of Engineering and Science<br>Department of Electrical Engineering and Computer Science<br>University Heights, Bronx, New York 10453 | 2a. REPORT SECURITY CLASSIFICATION<br>UNCLASSIFIED<br>2b. GROUP |

3. REPORT TITLE

DIGITAL COMPUTER TRANSFORMATIONS FOR IRREGULAR LINE DRAWINGS

4. DESCRIPTIVE NOTES (Type of report and inclusive dates)

Technical Report

5. AUTHOR(S) (First name, middle initial, last name)

Giovanni B. Reggiori

| | | |
|---|---|---|
| 6. REPORT DATE<br>April 1972 | 7a. TOTAL NO. OF PAGES<br>163 + xv | 7b. NO. OF REFS<br>37 |
| 8a. CONTRACT OR GRANT NO<br>N00014-67-A-0467-0010, NR 049-274<br>b. PROJECT NO<br><br>d. | 9a. ORIGINATOR'S REPORT NUMBER(S)<br>TECHNICAL REPORT 403-22<br>9b. OTHER REPORT NO(S) (Any other numbers that may be assigned this report)<br>None | |

10. DISTRIBUTION STATEMENT

"Reproduction in whole or in part is permitted for any purpose of the United States Government."

| | |
|---|---|
| 11. SUPPLEMENTARY NOTES | 12. SPONSORING MILITARY ACTIVITY<br>Office of Naval Research<br>Code 437<br>Washington, D.C. 20360 |

13. ABSTRACT

This report describes a parametric quantization scheme for irregular line drawings. With this scheme, different quantized versions of the same drawing can be obtained by changing the values of the parameters. Three figures of noise are proposed for evaluating the quality of quantized drawings and design formulae are developed for the parameters of the quantization scheme as functions of bounds on the figures of noise.

The degradation of the quality of a quantized drawing resulting from a coordinate transformation and requantization is studied in terms of transformed figures of noise. Also, it is shown theoretically and by means of a number of examples how to choose the parameters of the quantization scheme in order to meet the requirements on the transformed figures of noise. This enables one to quantize a preprocessed satellite picture so that after computation of a Mercator projection, the resulting geographic map will have the required quality.

The theory presented in this report is applicable to any irregular line drawing and to any transformation defined by a pair of functions that are continuous together with their partial derivatives.

DD FORM 1 NOV 65 1473

UNCLASSIFIED
Security Classification

| 14. KEY WORDS | LINK A | | LINK B | | LINK C | |
|---|---|---|---|---|---|---|
| | ROLE | WT | ROLE | WT | ROLE | WT |
| line-drawing processing<br>computer graphics<br>map processing<br>Mercator projections<br>line-drawing encoding<br>quantization noise | | | | | | |

## ACKNOWLEDGMENT

The work described here was supported by the Information Systems Branch, Office of Naval Research, under contract N00014-67-A-0467-0010, Professor Herbert Freeman, Principal Investigator.

The author wishes to express his debt of gratitude to Professor Herbert Freeman for his guidance and encouragement in the present investigation.

ABSTRACT

An irregular line drawing is an abstraction of an image which can be defined as a set of planar curved arcs. The geometric features of these arcs are implicitly defined in the output of the preprocessing operations which generated the drawing from the image.

In order to process such a drawing with a digital computer, it is necessary first to describe it to the machine in a suitable language. Such a description is complete if and only if it includes all the desired features of the drawing. The precision of a complete description is then related to the precision with which each of the preprocessed features is represented in it. To represent a feature means essentially to substitute for it a feature for which a standard machine description already exists. Therefore, the quality of a description of a preprocessed irregular line drawing is completely determined by the resolution of the quantization scheme used.

Many quantization schemes have been studied in the past. In these schemes, the resolution is chosen independently from the type of processing to be done later on the quantized drawing. For example a particular resolution may be chosen because the user wants the quantized version of a curved arc to appear to him as smooth as the arc itself.

No mention exists in the current literature of the more general problem of choosing the resolution of the quantization scheme so that the quality of the quantized drawing after processing is satisfactory in some specified sense. This thesis describes an approach to the solution of this problem when the required processing is a coordinate transformation. A general

purpose quantization scheme is presented in a parametric form. Different quantized versions of the same drawing can then be obtained by changing the values of the parameters governing the quantization scheme. An optimal encoding scheme is described which utilizes the patterns in the quantized drawing.

Three figures of noise are introduced for describing three different aspects of the quality of the quantization scheme. The first figure of noise is related to the average area between the quantized version of the drawing and the drawing itself. It also provides an indication of the difference between the length of the drawing and that of its quantized version. A second figure of noise describes the average maximum displacement between the quantized version of the drawing and the drawing itself. A third figure of noise serves as a measure of the so-called staircase effect. It should be noted that although many references to the staircase effect can be found in the literature, there has been no known scheme for quantifying it.

A figure of cost is presented for evaluating how much "cost" has been expended in transforming the quantized version of a given drawing.

A figure of merit is defined to indicate how much has been spent (figure of cost) for achieving the given quality (figure of noise) after transformation.

The effect of a coordinate-transformation on the three figures of noise is evaluated together with the non-reversible contribution due to the requantization following the transformation.

The thesis concludes with a comparison between the proposed quantization scheme and other schemes on the basis of their figures of merit. Bounds on the distortions in angle and length occurring when the drawings are quantized accordingly to a variety of quantization schemes are derived.

TABLE OF CONTENTS

| | | Page |
|---|---|---|
| ACKNOWLEDGMENT | | ii |
| ABSTRACT | | iii |
| LIST OF ILLUSTRATIONS | | viii |
| GLOSSARY | | x |
| I. | INTRODUCTION | 1 |
| | 1.1 Statement of the Problem | 2 |
| | 1.2 Literature Survey | 5 |
| II. | THE QUANTIZATION METHOD | 13 |
| | 2.1 Definitions for Irregular Line Drawings | 14 |
| | 2.2 Algorithm for Approximating an S-continuous Arc | 16 |
| | 2.3 Approximation of an Irregular Line Drawing | 23 |
| | 2.4 Square Grid Quantization of an Approximated Line Drawing | 24 |
| | 2.5 Relations Among the Precision Parameters | 30 |
| | 2.6 Concluding Remarks | 33 |
| III. | THE ENCODING METHOD | 34 |
| | 3.1 General Considerations | 34 |
| | 3.2 Chains for Segments of Class I | 37 |
| | 3.3 Chain Computation by Substitution | 37 |
| | 3.4 Chains for Segments of Class II | 38 |
| | 3.5 Chains for Segments of Class III | 42 |
| | 3.6 Chain Patterns | 43 |
| | 3.7 Algorithm | 46 |
| | 3.8 Ambiguous Chainlets | 48 |
| | 3.9 Properties of Ambiguous Chains | 51 |
| | 3.10 Translational Invariance of Chain Patterns | 53 |
| | 3.11 The Encoding Scheme | 55 |
| | 3.12 Concluding Remarks | 59 |
| IV. | TRANSFORMATIONS | 62 |
| | 4.1 General Considerations | 62 |
| | 4.2 Approximation of General Transformations | 64 |
| | 4.3 Relations Among Linear Transformations | 66 |
| | 4.4 Standard Decomposition of Class II Transformations | 67 |
| | 4.5 Mercator Projections | 72 |
| | 4.6 Mercator Projections of Circular Arcs | 79 |
| | 4.7 Concluding Remarks | 80 |

| | | | |
|---|---|---|---|
| | | | Page |
| V. | FIGURES OF NOISE | | 81 |
| | 5.1 | Classical Approach to the Definition of a Figure of Noise | 81 |
| | 5.2 | Figures of Noise for Quantized Line Drawings | 83 |
| | 5.3 | Area-Type Noise | 84 |
| | 5.4 | Displacement-Type Noise | 88 |
| | 5.5 | Staircase-Effect-Type Noise | 89 |
| | 5.6 | Concluding Remarks | 94 |
| VI. | TRANSFORMATIONS OF FIGURES OF NOISE | | 95 |
| | 6.1 | General Considerations | 95 |
| | 6.2 | Rotations | 96 |
| | | 6.2.1 Noise after Rotation without Grid Contributions | 97 |
| | | 6.2.2 Noise after Rotation with Grid Contribution | 97 |
| | 6.3 | Isotropic Scalings | 102 |
| | | 6.3.1 Noise after Isotropic Scalings without Grid Contributions | 102 |
| | | 6.3.2 Noise after Isotropic Scalings with Grid Contributions | 104 |
| | | 6.3.2.1 Expansions | 104 |
| | | 6.3.2.2 Contractions | 105 |
| | 6.4 | Non-isotropic Scalings | 107 |
| | 6.5 | Summary of Noise Transformations | 111 |
| | 6.6 | Figures of Cost and Merit | 113 |
| VII. | COMPARISONS WITH OTHER METHODS | | 116 |
| | 7.1 | General | 116 |
| | | Case 1: Grid intersect method | 117 |
| | | Case 2: Square box method | 126 |
| | | Case 3: Rounded coordinates method | 131 |
| | | Case 4: Diamond and circular boxes methods | 132 |
| | | Case 5: Modified grid intersect method | 132 |
| | 7.2 | Comparison Between Modified Grid-Intersect Scheme and Proposed New Scheme | 135 |
| | | Case 1: Area-type Figure of Merit | 136 |
| | | Case 2: Displacement-type Figure of Merit | 136 |
| | | Case 3: Staircase-effect-type Figure of Merit | 137 |

| | | Page |
|---|---|---|
| VIII. | APPLICATION PROGRAM AND RESULTS | 140 |
| | 8.1 General | 140 |
| | A. Input Data | 140 |
| | B. Output Data | 140 |
| | C. General Comments | 141 |
| | 8.2 Results of the Program | 141 |
| | A. Direct Approach | 144 |
| | B. Intermediate Approach | 146 |
| | C. Inverse Approach | 148 |
| | D. Concluding Remarks | 150 |
| IX. | SUMMARY AND CONCLUSIONS | 157 |
| | 9.1 General | 157 |
| | 9.2 Specific Contributions of this Research | 158 |
| | 9.3 Future Extensions | 160 |
| REFERENCES | | 161 |

## LIST OF ILLUSTRATIONS


| Fig. No. | | Page |
|---|---|---|
| 1 | Preprocessing of an Image | 3 |
| 2a,2b | Transformation of Quantized Curves | 6 |
| 3 | Examples of Locally Disjoint Points | 15 |
| 4 | Illustration of Arc and Chord of a Curve | 17 |
| 5 | Arc with Constant Radius of Curvature | 17 |
| 6 | Two Adjacent Arcs and Chords | 21 |
| 7 | Length and Angular Distortion of a Straight Line Segment Due to Quantization | 26 |
| 8 | Segment and Plotted Chain | 35 |
| 9 | Plotter Movements and Chain Elements | 36 |
| 10 | Chain for a Class II Segment | 39 |
| 11 | Chain for a Class II Segment | 40 |
| 12 | Chain for a Class II Segment | 41 |
| 13 | Block Diagram | 47 |
| 14 | Ambiguous Chainlet | 49 |
| 15 | Area Associated with a Segment and a Chain | 52 |
| 16 | Proposed Code | 60 |
| 17 | Non-commutativity of Transformations | 68 |
| 18 | Spherical Reference Frame | 75 |
| 19 | Schematic of Mercator Maps | 78 |
| 20 | Example of Symbolic Difference (areas) | 85 |
| 21 | Arc and Approximating Chord | 87 |
| 22 | Staircase Effect in Quantized Drawings | 92 |
| 23 | Arc and Chord Before and After Rotation | 98 |
| 24 | Arc and Chord Before and After an Isotropic Scaling | 103 |
| 25 | Arc and Chord Before and After a Non-Isotropic Scaling | 108 |
| 26 | Angular Variations Due to Non-Isotropic Scalings | 110 |
| 27 | Example of Non-linear Transformation (Mercator Projection) | 114 |

| Fig. No. | | Page |
|---|---|---|
| 28a,28b | Distortions Due to Grid Intersect Requantization | 118 |
| 29 | Angular Distortion | 120 |
| 30 | Length Distortion | 121 |
| 31a,31b | Length and Angular Distortion for a Pair of Orthogonal Elements | 122 |
| 32a,32b | Distortions for Pair of Elements with Different Length | 124 |
| 33 | Distortion for a Pair of Elements Forming an Angle Larger than $90^{\circ}$ | 125 |
| 34 | Ambiguous Case | 127 |
| 35a,35b | Distortions Due to Square Box Method | 128 |
| 36 | Length Distortions | 130 |
| 37a,37b | Distortions Due to Diamond Box Method | 133 |
| 38a,38b | Distortions Due to Circular Box Method | 134 |
| 39 | Block Diagram | 142 |
| 40a,40b, 40c,40d | Program Results for Rotation | 145 |
| 41a,41b, 41c,41d | Program Results for Non-isotropic Scaling | 147 |
| 42a,42b 42c,42d | Program Results for Mercator Projection | 149 |
| 43 | Coastline | 151 |
| 44 | Quantized Coastline | 152 |
| 45 | Transformed Coastline | 154 |
| 46 | Transformed Quantized Coastline | 155 |

GLOSSARY

| | | |
|---|---|---|
| 1. | $a$ | relative coordinates of the terminus of a segment with respect to the initium |
| 2. | $\bar{a}$ | size of a square containing L |
| 3. | $a'$ | ratio between $\bar{a}$ and the minimum length-detail parameter $\ell$ |
| 4. | $a_c, a_\ell$ | areas associated with a chain and a segment |
| 5. | $a_i$ | area associated with the i-th segment of a P-structure |
| 6. | $A$ | initium of a segment |
| 7. | $\bar{A}$ | matrix |
| 8. | $A(P)$ | region containing a rotated chain element |
| 9. | $A_j$ | initial point of the j-th arc |
| 10. | $\alpha(P_j)$ | angle between the directions of the tangent to $s_j$ at $P_j$ and the reference axis |
| 11. | $\alpha_i, \alpha_{ix}, \alpha_{iy}$ | i-th chain element and the x and y components associated with it |
| 12. | $\alpha'_j$ | angle between the tangents at $A_j$ to $s_j$ and $A_{j+2}$ to $s_{j+1}$ |
| 13. | $\alpha_{min}$ | minimum angular discontinuity measured at the cusps of L |
| 14. | $\bar{\alpha}_{min}$ | application specified parameter |
| 15. | $\alpha'_{min}$ | minimum possible value of $\alpha_{min}$ |
| 16. | $b$ | relative coordinate of the terminus of a segment with respect to the initium |
| 17. | $b_o$ | integer identifying the first half of the first octant |
| 18. | $\vec{b}_1$ | tangent to a parallel |
| 19. | $B$ | terminus of a segment |
| 20. | $B_c$ | number of bits required for storing the information contained in a P-structure of N vertices, in the chain code |

| | | |
|---|---|---|
| 21. | $B_{incr}, B_{mc}, B_p$ | number of bits required for storing the information of quantized data according to three different schemes |
| 22. | $B_S$ | number of bits required for storing the information of quantized data according to the slope-length scheme |
| 23. | $B_1, B_2$ | transformation dependent constants |
| 24. | $\beta_j$ | angle between the direction of the j-th segment and the reference |
| 25. | $\beta'_j$ | angle between the j-th segment and the tangent to $s_{j+1}$ at $A_{j+2}$ |
| 26. | $c$ | displacement constant |
| 27. | $C$ | chain |
| 28. | $C_1, C_2, C_3, C_4$ | constants for fast algorithm for generating a chain |
| 29. | $d$ | displacement constant |
| 30. | $ds$ | elementary arc of a lossodromia |
| 31. | $\delta$ | smallest of two scale factors (taken in absolute value) |
| 32. | $\delta_j$ | maximum distance between $s_j$ and the j-th segment of the P-structure |
| 33. | $\Delta\alpha_j$ | angular difference between the direction of $\vec{t}_{1j}$ and $\vec{t}_{2j}$ |
| 34. | $\Delta\alpha_{max}$ | precision parameter |
| 35. | $\Delta\beta_j$ | angular difference between the directions of the j-th and the (j+1)-th segments |
| 36. | $\Delta s$ | finite value of an arc of a lossodromia |
| 37. | $\epsilon_u, \epsilon_v$ | percentage errors due to the approximation of a Class III transformation with elementary transformations |
| 38. | $f$ | transformation function |
| 39. | $f_c$ | figure of cost |
| 40. | $f_i, f_g, f_h$ | fractions |

41. $f_{m_a}, f_{m_\ell}, f_{m_{S.E.}}$ figures of merit associated with the figures of noise of area-, displacement-, staircase-effect-type

42. $f_x$ derivative of a function f with respect to one of its variables, x

43. $f_w$ figure of noise

44. $f_{w_a}, f_{w_\ell}, f_{w_{S.E.}}$ figure of noise of area-, displacement-, staircase-effect-type

45. $g$ transformation function

46. $\bar{g}$ integer

47. $\gamma$ largest between two scale factors (taken in absolute value)

48. $\bar{\gamma}$ angle of a lossodromia

49. $h, i$ integers

50. $I_k$ position of the last zero in C before the k-th one

51. $\bar{j}$ index of the arc $s_{\bar{j}}$ whose minimum radius of curvature is the minimum for the entire line drawing

52. $k, k_\alpha, k_\ell$ precision parameters

53. $K_{max}$ constant for fast algorithm for generating a chain

54. $K_p$ cost for transforming the coordinates of a single point

55. $\bar{K}$ constant for fast algorithm for generating a chain

56. $\ell$ minimum length-detail parameter

57. $\ell_j$ length of the j-th segment of the P-structure

58. $\ell_k$ number of zeros between the k-th and the (k+1)-th ones in a chain

59. $\ell_{max}$ precision parameter

60. $\ell_{min}$ smallest of the distances between the extremes of any S-continuous arc

| | | |
|---|---|---|
| 61. | $\overline{\ell}_{min}$ | smallest of the distances between any two locally disjoint points |
| 62. | $\ell'_{min}$ | minimum possible value of $\ell_{MIN}$ |
| 63. | $\ell_s$ | user defined constant for evaluating the average staircase effect in a quantized line drawing |
| 64. | $\ell_{TOT}$ | length of a quantized line drawing |
| 65. | $\vec{\ell}_1$ | tangent to a lossodromia |
| 66. | L | irregular line drawing |
| 67. | L* | approximated line drawing |
| 68. | $L_{a,b,c,d}$ | linear transformation |
| 69. | $\lambda$ | S-continuous arc |
| 70. | m | rational slope value |
| 71. | m' | logarithm base two of the number of rows (or columns) of a uniform square grid contained in the smallest square containing an irregular line drawing |
| 72. | $m_1,m_2$ | coefficients specifying the structure of the formula for evaluating the staircase-effect-type of noise |
| 73. | M | constant related to the number of vertices in a closed P-structure |
| 74. | $M_r$ | regular transformation |
| 75. | n | precision parameter |
| 76. | $n_o,n_1$ | number of zeros and ones in a chain |
| 77. | $n_h,n_{h-1}$ | numbers of sequences of zeros in C with lengths h and h-1 |
| 78. | $\vec{n}_1$ | normal to a sphere |
| 79. | N | number of chain elements in the shortest segment of a P structure |
| 80. | $N_{min},N_{max}$ | minimum and maximum number of chain elements |

81. $P_i$ — i-th point in a given list

82. $p_\ell$ — length precision constant

83. $p_\theta$ — angular precision constant

84. $Q_j$ — j-th node in a sequence of grid nodes

85. QL — quantized line drawing

86. r — largest displacement of a point due to quantization

87. $r_j$ — ratio between the minimum values of the radius of curvature of $s_j$ and that of $s_{\bar{j}}$ ($\bar{j}$ denotes the arc containing the smallest radius of curvature of the drawing)

88. $r_m$ — maximum radius of curvature in the drawing

89. $R_j$ — constant radius of curvature

90. $R_\lambda$ — rotation by an angle $\lambda$

91. R(S) — subset of the plane which is characteristic of the given quantization scheme

92. s — ideal signal

93. $s_j$ — j-th S-continuous arc associated with the j-th segment of the P-structure

94. $S_\alpha$ — isotropic scaling with a factor equal to $\alpha$

95. $S_{\alpha,\beta}$ — non-isotropic scaling with factors equal to $\alpha$ and $\beta$

96. t — grid ratio; ratio between the values of the grid sizes used before and after a transformation

97. $\vec{t}_1$ — tangent to a meridian

98. $\vec{t}_{1j}, \vec{t}_{2j}$ — unit vectors tangent to $s_j$ at its extreme points

99. T — grid size

100. $T_1, T_2$ — grid sizes used before and after a transformation

101. $\theta$ minimum angular-detail parameter

102. $\theta_s$ user defined constant for evaluating the average staircase effect in a quantized line drawing

103. $\theta_{TOT}$ global angular variation defined by a quantized line drawing

104. $w$ noise

105. $(x_i, y_i)$ X-Y coordinates of the i-th point in a list

# I. INTRODUCTION

The problem of developing techniques for the computer processing of pictures has received increasing attention in recent years. Currently most of the effort is dedicated to two classes of problems: the processing of images and the processing of line drawings.

As the term will be used here, an <u>image</u> is a two-dimensional representation of a scene, and its information is given by spatial variations of brightness and color. In contrast, a <u>line drawing</u> is an abstraction of an image. The information it contains is given solely by the shape of thin curves appearing on a contrasting background, where neither the actual thickness of the curves nor the nature of the background are relevant.[15]

The abstraction of a line drawing from a given image is a subjective matter. For instance, given a blurred aerial photograph of an island, it is subjective to decide what the exact shape of the coastline is. Once this has been decided, that is, once a thin line has been drawn to represent the coast, then it can be said that a line drawing has been abstracted from the image. In doing this abstracting, all the detail that is regarded as noise is filtered away. The line drawing is then simply an assembly of smooth curves with possible slope discontinuities at points where two curves are joined.

The abstracting process described here belongs to a class of operations that are commonly referred to as <u>preprocessing</u>. In the following we will refer to a line drawing L as a drawing consisting of a set of smooth thin curves containing inflections, separated by cusps, and linked by invisible arcs. Moreover it will be supposed that the curves are described in such a way as to permit the measurement of their geometric features (i.e., the radii of curvature, the slopes, etc.) to any required precision. Examples of line drawings are provided by contour maps generated from preprocessed terrain photographs, high energy particle tracks obtained from bubble-chamber pictures, and the outlines of individual cells in biomedical-application images.

## 1.1 Statement of the Problem

In order to process a line drawing L by means of a digital computer, it is necessary to describe it first to the machine in a suitable language. Such a description is complete if and only if it includes all the desired features of the drawing. Description implies quantization, and the precision of a complete description is dependent on the precision with which each of the preprocessed features is represented in the description. To represent a feature means essentially to replace it by one for which a standard machine description already exists. Ultimately, the precision of a description of a preprocessed line drawing is determined by the resolution fineness of the quantization scheme used.

In order to clarify the concepts of preprocessing and quantizing, consider the example of Fig. 1. The figure shows a blurred photograph of a coastline which allows the detection of details to a precision of one meter. Now suppose that a map is to be produced with a precision of 30 meters. By a precision of 30 meters we mean that there is a circle of uncertainty of radius 30 meters about any point in the map.

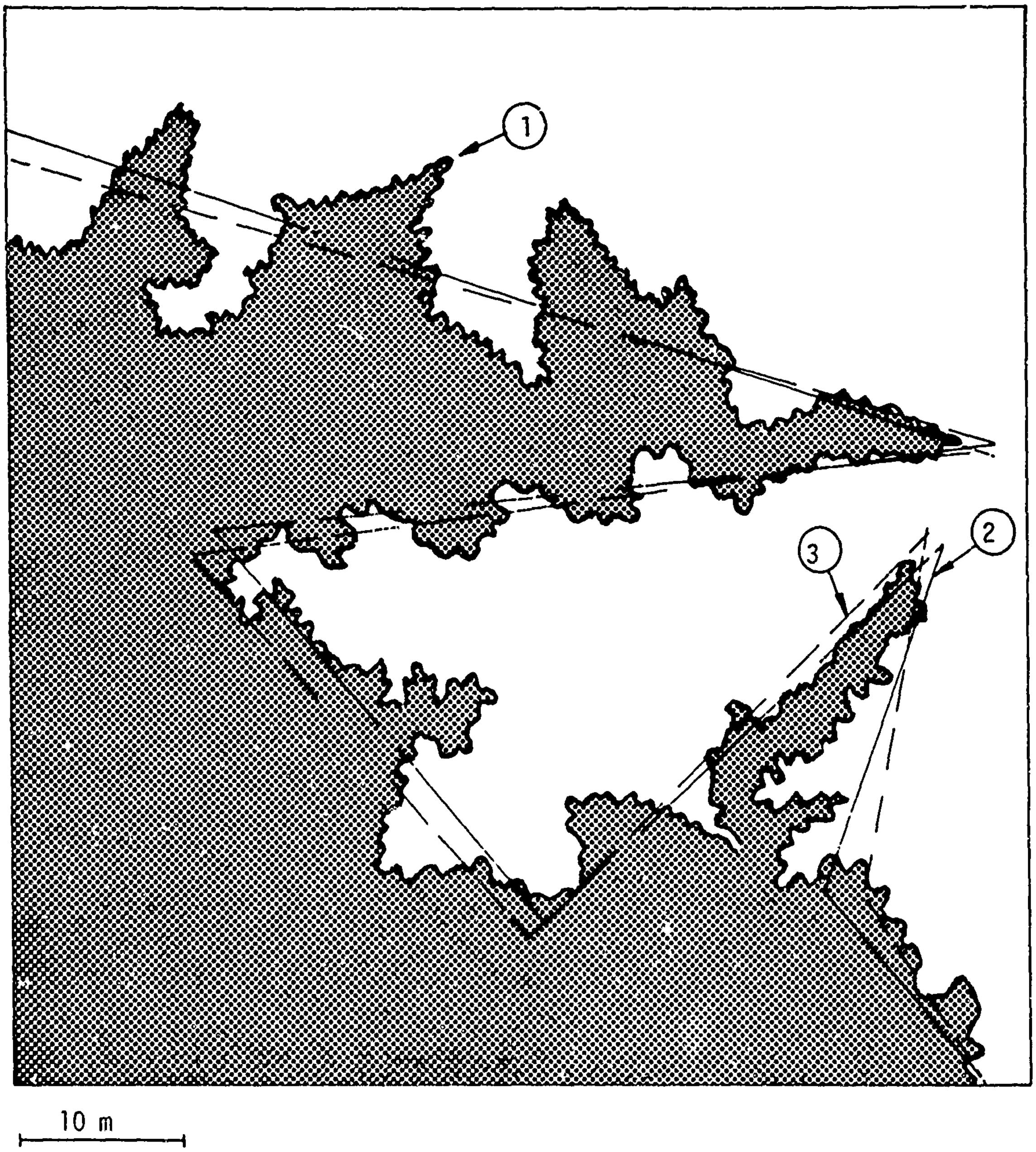


1. User Abstracted ILD Coastline (Preprocessing)
2. First Quantization Step (User Generated Curves)
3. Second Quantization Step (Approximation with "Namable" Entities)

FIG. 1

AN IRREGULAR LINE DRAWING WITH USER GENERATED CURVES AND THEIR APPROXIMATION

The first operation (preprocessing) to be carried out is then the one of identifying a coastline (line drawing) in the given picture.[36] This may require filtering to remove noise, thickening, thinning, and finally edge detection.[4,7] Next the extracted line drawing is approximated by a sequence of straight line segments in such a way that the maximum distance of a coastline arc from its approximating segment does not exceed, say, 25 meters. This can be regarded as the first line drawing quantization operation. There was, of course, a prior image quantization when the data was input in the computer through a digital scanning device.

The coordinates of the extreme points of each segment are next truncated so that they can be expressed by numbers with the agreed-upon number of digits. This operation can be regarded as a second line drawing quantization step, and it leads to a displacement of each segment. If such a displacement does not exceed 5 meters, then the new segment will be within 30 meters of the coastline and the required precision will be achieved. Further, the new segment can now be described by the coordinates of its end points to exactly the desired resolution (number of digits).

Many line-drawing quantization schemes have been studied in the past and proposed in the literature.[9,14] However, no mention exists of the problem of how to quantize a line drawing so that the features of interest will be retained to the desired precision even after a coordinate-transformation. This thesis offers a working solution to this problem.

In designing the quantization scheme one must take into account the type of transformation to be applied to the quantized drawing. This is illustrated by the following example. Let L be a line drawing consisting of a straight line segment, and consider two approximations of it, C and P, as indicated in Fig. 2a. Now suppose that the required processing of L is to be uniform scaling by a factor of three. If C represents the only available information about the line drawing, the result is C', whereas if P is given, the result is P', as shown in Fig. 2b. The ideal result is L', which has been plotted in Fig. 2b by computing the position of a large number of points of L. L' appears to be better represented by P' than by C' since P' retains the straight-line feature. The shape deformation presented by C' is referred to as "staircase effect".

In this thesis a general-purpose quantization scheme is presented and an efficient encoding scheme is described. Three figures of noise are proposed for describing three different aspects of the quality of the quantization scheme and a related figure of cost is defined. The effect of coordinate-transformations on the quality of line-drawing descriptions is studied, and bounds are shown to exist that relate the feature qualities before and after a transformation.

## 1.2 Literature Survey

This section reviews some of the past work by others relating to the problem of transforming quantized planar curves. It is divided into three sections, each dealing with a different aspect of the problem.

### Quantization of Smooth Curves

The problem of quantizing a closed smooth curve has been treated by many authors by quantizing the planar region whose border is the closed curve.

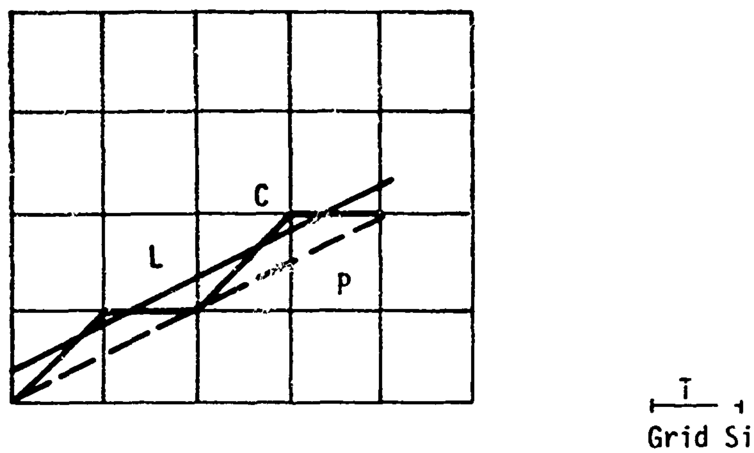


FIG. 2a

TWO QUANTIZATION EXAMPLES

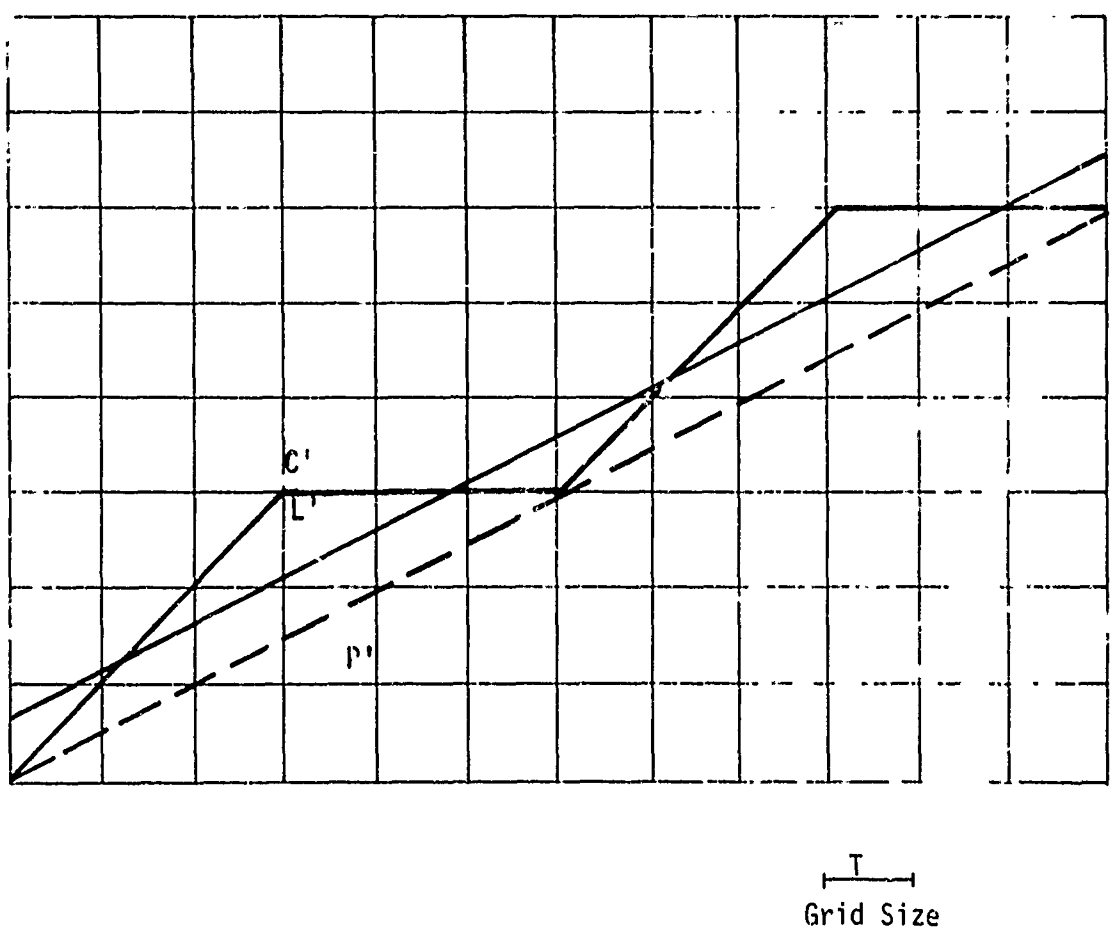


FIG. 2b

EFFECT OF A TRANSFORMATION ON QUANTIZED CURVES

Cheng and Ledley[7] consider digitizations of pictures using a flying spot scanner and propose an error-bounded digitization scheme. Using a least mean-square criterion, they established the precision of their reconstructing method. An example of a mechanical scanner is given by Pilipchuck[26] for off-line picture digitization. Neither of these papers, however, is particularly applicable to the work of interest here because the curves with which we will be concerned may be either closed or open.

Freeman[15] stresses the distinction between an image and a line drawing, and clarifies the problems of line-drawing quantization and encoding. A useful method for quantizing both closed and open curves was described in detail by Freeman.[9] He considers various methods for quantizing arbitrary planar curves, with specific emphasis on the grid-intersect quantization method. He also proposes the so-called chain code, in which a chain represents a translation-invariant encoding of a curve quantized on a square grid. Combined quantization and encoding is achieved by superimposing a grid on the given curve and selecting the closer of the two grid nodes, $Q_j$, lying to either side of the intersections between the curve and the grid. The relative position of $Q_{j+1}$ with respect to $Q_j$ can be defined simply by an octal digit. The sequence of selected nodes can thus be represented by a sequence of octal digits. This is sufficient for encoding the quantized curve with a precision depending only on the grid size.

In the following, use will be made of Freeman's encoding scheme for efficiently encoding a quantized curve and directing a digital plotter for drawing it.

Freeman[15] presents a comparison between the so-called array digitization and the chain quantization and encoding of the border of finite planar regions, with many interesting remarks on border length and smoothness. Freeman[12] discusses a fast algorithm for generating the chain of a circle. Freeman and Glass[14] propose a criterion for selecting the appropriate grid size to be used for chain encoding a curve. The curve is interpreted as an elastic beam under flexure and the elementary grid size is selected so that the curve can be represented by a beam of minimum strain energy. The problem of reconstructing a curve from its chain is a very complicated one, and a method is proposed by the authors for approximating the actual solution with cubics. However, even this approximation leads to very involved computations, especially in the case of a curve with several points of inflection, selfintersections or cusps.

Glass[17] presents a note on the quantization of two-dimensional line drawings which shows that the chain quantization process acts as a source of uniformly distributed noise, and Montanari[20] discusses some limit properties of digitization schemes with emphasis on continuity requirements for curve digitization.

Raudseps[27] presents a new type of quantization by describing a curve as a function of tangent angle vs. arc length. From this, the curve can be reconstructed uniquely. Quantization is achieved by taking the coefficients of the truncated Fourier transform of the function. Some of the ideas contained in this work are applicable to the quantization scheme presented here, especially those related to the definition of a figure of noise.

Analysis and Pattern Recognition of Quantized Planar Curves

From the point of view taken by this thesis, the problem of recognition of patterns in quantized curves is fundamental to the one of transforming them. Two approaches are known to the author. The first one deals with the properties of quantized curves directly; the second one first transforms the curves into another representation, called skeletons, and then applies pattern recognition techniques to the skeletons.

Basic work has been done by Freeman[10], who studied different algorithms for checking the topological properties of chains, such as closure, symmetry, and intersections, and geometric patterns such as length, area, moments, etc.

Freeman[11] presents an analysis of chain patterns in terms of a chain directionality spectrum which shows the relative amount of the octal digits of various types in a given chain, and difference sequence functions which are defined on the differences of adjacent octal digits in a chain and which are related to the curvature of the chain.

Freeman[13] proposes a classification scheme based on a hierarchy of chainlet levels. Freeman and Feder[8] present a contour correlation algorithm for the problem of curve matching. Bodin[1] presents computer program routines for evaluating chain cross- and auto-correlations for each possible value of the shift index. Socci[35] describes a special correlation technique based on the chain difference functions and proves its invariancy with respect to chain rotation. Finally, for the case of array digitized regions (i.e., closed curves), two works deserve to be mentioned. In the first, Rosenfeld[28] presents definitions of connectivity and order of connectivity, and discusses their topological applications for array digitized planar regions. In the second, Lourie[19] presents two algorithms for identifying and labeling connected regions formed by sets of closed curves in interactive graphics.

The second approach for pattern recognition in quantized curves, using new shape descriptors was originated by Blum[2], who presented a pattern recognition scheme which extracts new descriptors of the shape of a given contour. The contour is interpreted as the origin of a wave front which propagates with constant velocity and extinguishes itself whenever two or more arcs of the same wavefront pass through the same points. These points define the medial axis of the contour line and, together with the time of front extinction defined for each of them, they describe in a compact way the shape of the original contour. A contour can be reconstructed in a unique way starting from its medial axis.

Other works on medial axis or skeletons were presented by Philbrick[25], who proposes a digitized version of Blum's analog propagation. Pfalz and Rosenfeld[24] use a different approach for digitized skeletons based on the idea of neighboring points, and prove the advantage of using digitized skeletons whenever set-theoretic operations are required on the given contour. Calabi and Hartnet[6] present a new definition of skeletons of closed regions, and Montanari[21,23] describes a method for obtaining skeletons using a quasi-Euclidean distance and a special method for generating continuous skeletons from digitized images.

Rutowitz[32] proposes a data structure for handling digitized pictures and a grey-weighted distance for solving digitally the problem of correctly determining the skeleton of a given contour. The possibility of using skeletons for the problem of transformation of quantized curves is not explored in the following. One big disadvantage of using skeletons is that it involves the use of curved arcs (e.g., parabolas) even for the case of polygonal contours.

A classic book on decision-making processes in pattern recognition is the one by Sebestyen[34] in which are derived linear and non-linear methods for separating patterns from one another.

Transformations of Quantized Planar Curves and Noise Filtering

Butt and Snively[4] present the PAX II picture processing system as a collection of routines for curve manipulation such as scaling and rotation, and Butt and Wells[5] present a set of studies in visual texture manipulation and synthesis including smoothing of expanded pictures, rotation techniques, and picture enhancement algorithms based on the interpolation of grey levels. This kind of approach to the problem of transformation is, however, different from the one taken here in the sense that in those works the patterns to be transformed are those of the quantized curves and no attempt is made to determine the relation between the features of the quantized curves and those of the original curves. Moreover, no theoretical proof is given to show the advantage of smoothing and filtering after transformation as compared to the case in which such filtering is done before transformation to remove the quantization noise. This last approach was presented for instance by Montanari[22].

Montanari proposes a filtering of the border of array-digitized regions using polygonal reconstruction of quantized contours. The polygon used is the one with minimal length and a proof of its uniqueness is given in detail.

Rosenfeld, Lee etc.[29] present various methods for curve enhancement. A non-linear method is also presented for enhancing smooth continuous curves. An example shows that their methods work even with levels of noise of 24%.

Rosenfeld, Strong etc.[24] present a noise cleaning algorithm as a modification of the classical scheme, which changes a one into a zero if the number of zeros within a given distance exceeds a given threshold. They also present a propagation process and show that it will give optimal results which can be justified theoretically. As a general reference on picture processing, see Rosenfeld.[31]

Finally it should be noted that the problem considered here is of interest not only because of its theoretical aspects, but also because of very real practical applications. This last point is well presented in the Proceedings of the Symposium on Map and Chart digitizing[18], where many real-life problems of transforming digitized curves were discussed in detail.

## II. THE QUANTIZATION METHOD

The quantizing of line-drawing data to place the data into a form suitable for computer processing, storage, and display is usually a two level process. In the first step the line drawing is derived from the source image (e.g., photograph), either by scanning or by tracing. The resulting "given" line drawing is often subjected to some preprocessing to remove noise, and then quantized once more into a more compact representation, efficient in terms of storage requirements but yet faithful in its preservation of the significant features. This thesis is primarily concerned with the second level of quantization, occurring after preprocessing. In the scheme to be described, a given irregular line drawing is first approximated by a set of polygonal structures whose vertexes belong to the drawing. Next these vertexes are shifted to the nearest nodes of a square grid and a new set of polygonal structures is generated. For the sake of simplicity, a polygonal structure will be called a P-structure in the subsequent discussion.

The criterion governing the generation of the first set of P-structures is the one of guaranteeing a "shape" precision by requiring that for each smoothly curving arc of the given line drawing there be at least one distinct segment of a P-structure. The "positional" precision is guaranteed by choosing the fineness of the square grid in such a way that the length and angular variations due to the grid quantization of the segments of the first set of P-structures are limited to a specified tolerance. This assures that the final set of P-structures will be "close" to the original drawing in both "shape" and "position".

## 2.1 Definitions for Irregular Line Drawings

Definition 1: An irregular line drawing I is a finite set of smooth curves of finite dimensions and infinitesimal thickness, containing inflections and separated by cusps and invisible arcs.

Definition 2: The elementary line drawings are:

1. a point
2. a continuous slope varying (S-continuous) arc
3. a straight line segment

Note that any irregular line drawing can be regarded as a continuous curve composed of an ordered sequence of S-continuous arcs separated at a given point by a cusp or linked by invisible straight line segments.

Definition 3: The features of the elementary line drawings are:

1. the position of a point
2. the sequence of angles of the tangents, with respect to a reference axis, of an S-continuous arc
3. the length and angle, with respect to a reference axis, of a straight line segment

Definition 4: Two points $P_i$ and $P_j$, belonging to an irregular line drawing are called locally disjoint points if there is no visible curve connecting them in at least one of the two circular regions with radius $P_iP_j$ and center in one of them.

Examples of locally disjoint points are illustrated in Fig. 3.

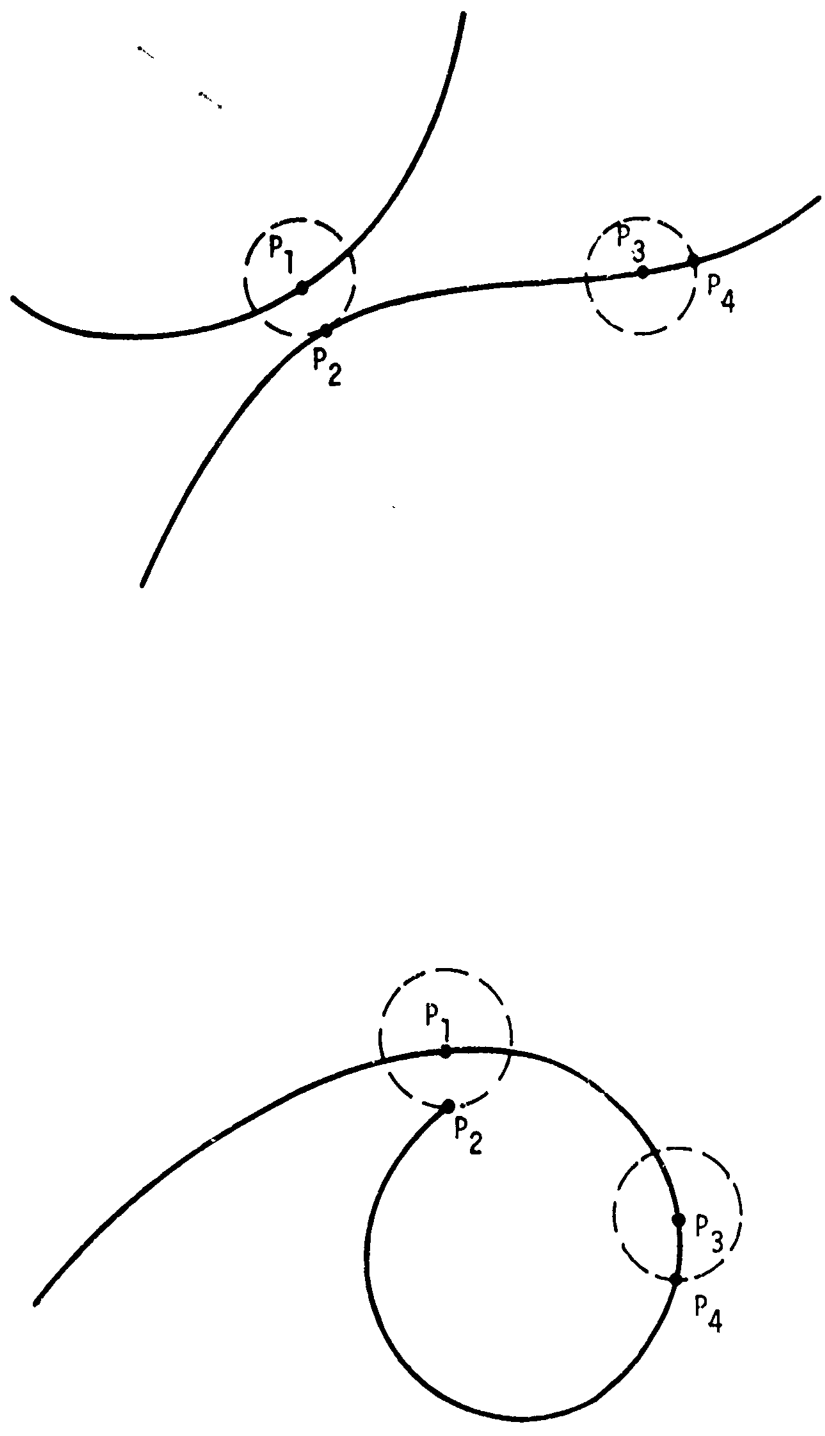


$P_1, P_2$ Locally disjoint points
$P_3, P_4$ Non Locally Disjoint Points

FIG. 3

EXAMPLES OF LOCALLY DISJOINT POINTS

Definition 5: The features of an irregular line drawing are:

1. the features of its elementary line drawings
2. the angular discontinuities defined by its cusps
3. the distances between the extreme points of S-continuous arcs
4. the distances between any two locally disjoint points

In the following an algorithm is presented which allows one to generate a P-structure for approximating an S-continuous arc with a required precision (i.e., for approximating its features with the required precision). Then the problem of approximating an irregular line drawing (i.e., its features) is reduced to the one of finding with which precision to approximate its S-continuous arcs.

The minimum values of the features (2), (3), (4) of the irregular line drawing will play a fundamental role in determining such precision. Next the so-found P-structure is replaced by another one whose vertices are nodes of a square grid. A design formula for the elementary size of the grid will be given and the relations among the various precision parameters will be derived. It will be shown that the precision with which an irregular line drawing is represented by its quantized version is dependent on a length and an angle measurable on the drawing itself, on the elementary size of the square grid and on a precision parameter.

## 2.2 Algorithm for Approximating an S-continuous Arc

A P-structure will now be constructed on a finite number of points of an S-continuous arc. The notation is illustrated in Fig. 4.

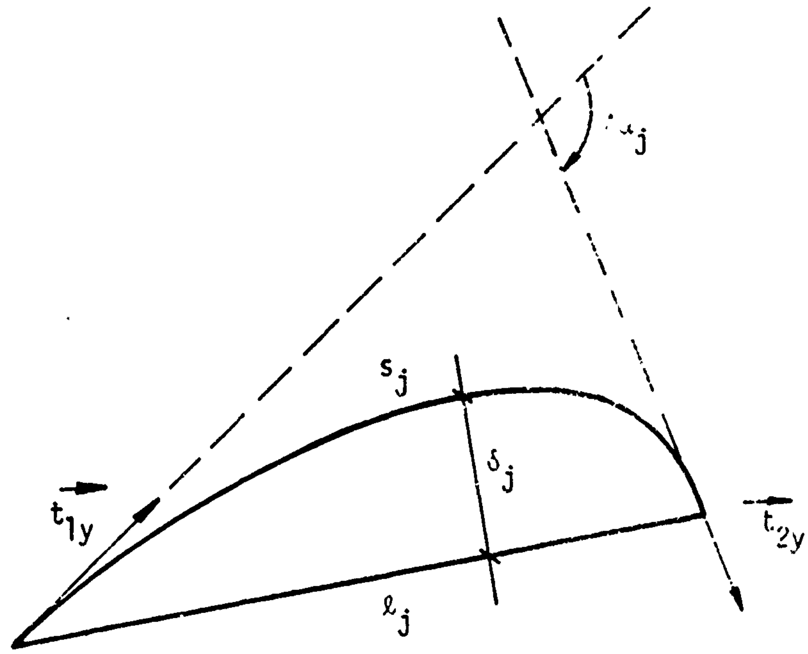


FIG. 4

ILLUSTRATION OF ARC AND CHORD OF A CURVE

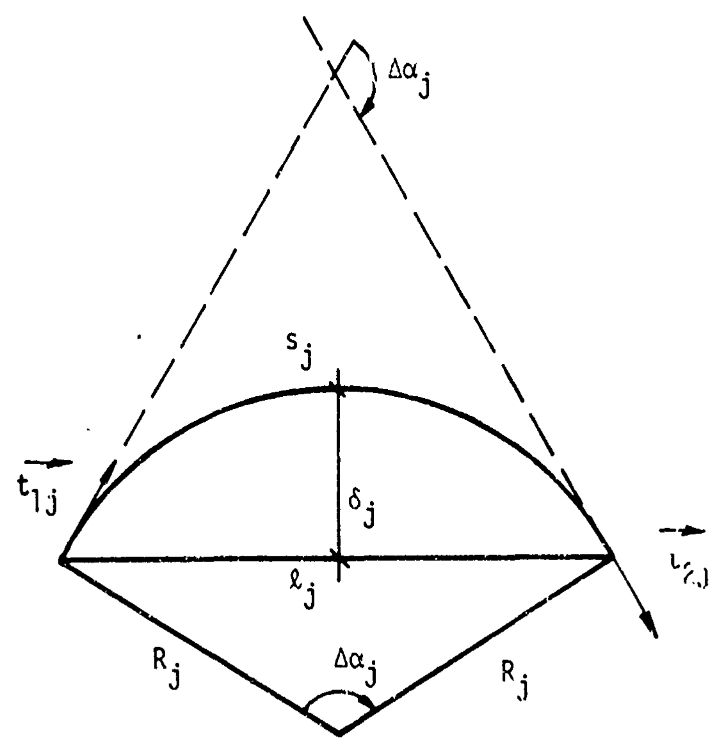


FIG. 5

ARC WITH CONSTANT RADIUS OF CURVATURE

| | |
|---|---|
| $s_j$ | the j-th S-continuous arc associated with the j-th segment of the P-structure |
| $\vec{t}_{1j}, \vec{t}_{2j}$ | the unit vectors tangent to $s_j$ at its extreme points |
| $\Delta\alpha_j$ | the angular difference between the directions of $\vec{t}_{1j}$ and $\vec{t}_{2j}$ |
| $\delta_j$ | the maximum distance between $s_j$ and the j-th segment of the P-structure |
| $\ell_j$ | the length of the j-th segment of the P-structure |
| $\bar{j}$ | index of the arc $s_{\bar{j}}$ whose minimum radius of curvature is the minimum for the entire line drawing |
| $r_j$ | ratio between the minimum values of the radius of curvature of $s_j$ and that of $s_{\bar{j}}$ |

Definition 6: A P-structure $P(\lambda,k,\ell_{max},\Delta\alpha_{max})$ approximating an S-continuous arc $\lambda$ with precision $k,\ell_{max},\Delta\alpha_{max}$ is one whose j-th segment defines an arc $s_j \epsilon \lambda$ such that:

1. $s_j$ has no inflections
2. $\Delta\alpha_j \leq \Delta\alpha_{max}$ (2.1)
3. $\delta_{\bar{j}} \leq k\ell_{\bar{j}}$ (2.2)
4. $\ell_{\bar{j}} \leq \ell_{max}$ (2.3)
5. $\ell_j \geq \ell_{\bar{j}} \quad ; \quad \ell_j \leq \sqrt{r_j}\,\ell_{\bar{j}}$ (2.4)

Let us note that for small values of k and $\Delta\alpha_{max}$, the arc $s_j$ will be very close to an arc of a circle with radius $R_j$. The angle associated with $s_j$, as seen from its center of curvature, is equal to the angle defined by the directions $\vec{t}_{1j}$ and $\vec{t}_{2j}$. The notation used here is also shown in Fig. 5.

Since $\delta_j = R_j - R_j \cos(\Delta\alpha_j/2)$ and $\ell_j = 2R_j \sin(\Delta\alpha_j/2)$ then

$$\delta_j/\ell_j = (1-\cos(\Delta\alpha_j/2))/(2\sin(\Delta\alpha_j/2)) = \sin^2 \frac{\Delta\alpha_j}{4}/2 \sin \frac{\Delta\alpha_j}{4} \cos \frac{\Delta\alpha_j}{4} =$$

$$= \frac{1}{2} \tan \frac{\Delta\alpha_j}{4}$$

Since, in general, $\Delta\alpha_{max}$ will be small, it follows that $\sin \frac{\Delta\alpha_j}{2} \simeq \frac{\Delta\alpha_j}{2}$ and $\tan \frac{\Delta\alpha_j}{4} \simeq \frac{\Delta\alpha_j}{4}$ and therefore $\delta_j/\ell_j \simeq \frac{\Delta\alpha_j}{8}$, $\ell_j \simeq R_j\Delta\alpha_j$ and $\delta_j \simeq \ell_j/8R_j$.

Let us now consider two different arcs, such that $R_{j_1} > R_{j_2}$ then $\delta_{j_1}/\delta_{j_2} \simeq (\ell_{j_1}/\ell_{j_2})^2 R_{j_2}/R_{j_1}$ ; further assuming $\ell_{j_2} \lesssim \ell_{j_1} \lesssim \ell_{j_2}\sqrt{R_{j_1}/R_{j_2}}$ then $\delta_{j_2} \gtrsim \delta_{j_1}$. In other words, when dealing with two small arcs it is possible to characterize them in terms of constant radii of curvature, $R_{j_1}$ and $R_{j_2}$. Let us assume that $R_{j_1} > R_{j_2}$, then for a fixed length $\ell_{j_2}$ it is always possible to find for $s_{j_1}$ a value $\ell_{j_1} \gtrsim \ell_{j_2}$ such that its maximum deviation from its chord is $\delta_{j_1} \lesssim \delta_{j_2}$. This observation is used later to show that the procedure for approximating an S-continuous arc with a P-structure always halts and therefore is an algorithm.

<u>Definition 7</u>: The <u>segmentation of an arc</u> is the generation of a pair of arcs, obtained by dividing the original arc at the point of maximum distance from its chord.

The following procedure generates $P(\lambda,k,\ell_{max},\Delta\alpha_{max})$ for a line drawing consisting of a single S-continuous arc $\lambda$ given the values $k,\ell_{max},\Delta\alpha_{max}$.

<u>Procedure</u>

<u>Step 1</u>: The arc $\lambda$ is subdivided into arcs with no inflections.

<u>Step 2</u>: The arc (s) $s_J$ containing the minimum radius of curvature is segmented (in accordance with Definition 7) and this operation is repeated until:
a. the length $\ell_J$ of the chord of $s_J$ is less than $\ell_{max}$
b. $\delta_J \lesssim k\,\ell_J$

<u>Step 3</u>: If $\ell_{\bar{J}}$ is not the smallest among all $\ell_j$'s, continue to segment $s_{\bar{J}}$ until this condition is satisfied.

<u>Step 4</u>: The following tests are made for all values of $j$:
a. $\Delta\alpha_j \leq \Delta\alpha_{max}$
b. $\ell_j \leq \sqrt{r_j}\,\ell_{\bar{J}}$

If they are all satisfied, then the P-structure has been generated correctly and the process ends. Otherwise continue to segment all the arcs that do not satisfy at least one of the tests and return to Step 2.

<u>Comment</u>: It is sufficient to recall previous considerations on the possibility of always finding an $\ell_{j_1} \geq \ell_{j_2}$ such that $\delta_{j_1} < \delta_{j_2}$, for $R_{j_1} > R_{j_2}$. This ensures that the above described procedure always converges to a unique solution in a finite number of cycles.

In order to investigate the precision with which a P-structure approximates an S-continuous arc, let us introduce the following additional notation, illustrated in Fig. 6.

| | |
|---|---|
| $\alpha(P_j)$ | angle between the direction of the tangent to arc $s_j$ in $P_j$ and the reference axis |
| $A_j$ | initial point of arc $s_j$ |
| $\alpha_j$ | $= \alpha(A_j)$ |
| $\alpha'_j$ | angle between the tangents to $s_j$ at $A_j$ and to $s_{j+1}$ at $A_{j+2}$ |
| $\beta_j$ | angle between the direction of the $j$-th segment and the reference axis |
| $\beta'_j$ | angle between the $j$-th segment and the tangent to $s_{j+1}$ at $A_{j+2}$ |
| $\Delta\alpha_j$ | angular difference between the directions of the tangent to $s_j$ at $A_j$ and $A_{j+1}$ |
| $\Delta\beta_j$ | angular difference between the directions of the $j$-th and the $(j+1)$-th segments |

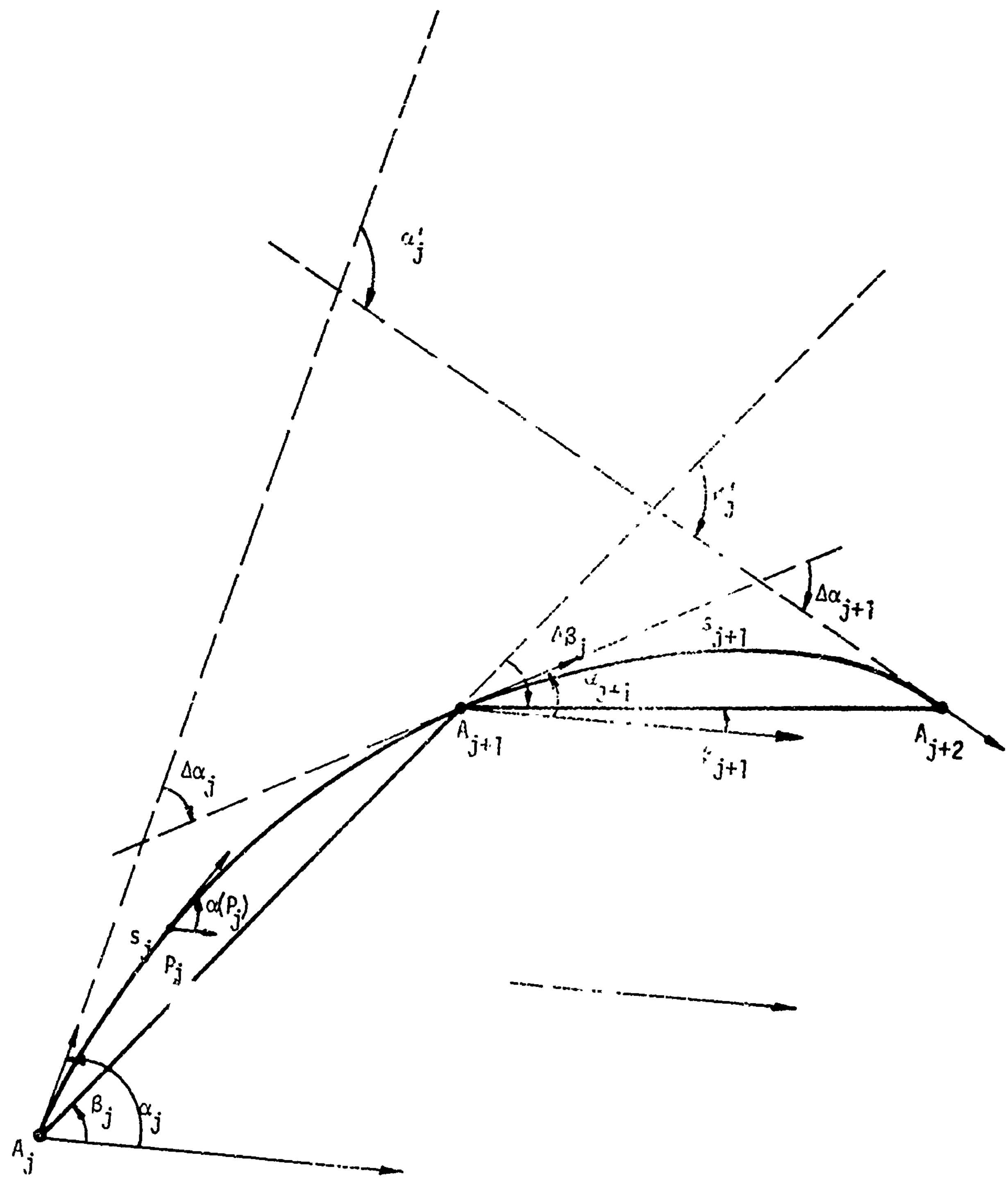


FIG. 6

TWO ADJACENT ARCS AND CHORDS

The following relations hold in general:

$$|\alpha_j - \beta_j| + |\beta_j - \alpha_{j+1}| = \Delta\alpha_j \leq \Delta\alpha_{max}$$

$$|\alpha_j - \beta_j| \leq \Delta\alpha_{max}$$

$$|\beta_j - \alpha_{j+1}| \leq \Delta\alpha_{max}$$

$$|\alpha_{j+1} - \alpha(P_j)| \leq |\alpha_j - \alpha_{j+1}| \quad , \qquad P_j \in s_j$$

$$|\alpha_j - \alpha(P_j)| \leq |\alpha_j - \alpha_{j+1}| \quad , \qquad P_j \in s_j$$

$$|\beta_j - \alpha(P_j)| \leq \Delta\alpha_{max}$$

Therefore it follows that

$$\Delta\beta_j = \beta_j - \beta_{j+1} < \beta'_j < \alpha'_j = \Delta\alpha_j + \Delta\alpha_{j+1} \leq 2\,\Delta\alpha_{max}$$

$$\Delta\beta_j \leq 2\,\Delta\alpha_{max} \quad ; \qquad \Delta\alpha_j \leq \Delta\alpha_{max}$$

It can be concluded that the j-th segment of a P-structure is an approximation of the arc $s_j$ belonging to an S-continuous arc with precision guaranteed by the relations

$$\delta_j \leq \bar{\delta_j} \text{ and } |\beta_j - \alpha(P_j)| \leq \Delta\alpha_{max} \qquad (2.5)$$

Moreover the P-structure approximating an S-continuous arc defines a discrete sequence of angular variations which approximates the continuous sequence defined by the S-continuous arc itself, and with a precision specified by

$$\Delta\beta_j \leq 2\Delta\alpha_{max} \qquad (2.6)$$

To improve the precision with which the P-structure approximates the S-continuous arc, it is sufficient to reduce progressively k and $\Delta\alpha_{max}$.

## 2.3 Approximation of an Irregular Line Drawing

Definition 8: The approximated line drawing $L^*$ of a given irregular line drawing L, is the totality of all the P-structures which approximate the S-continuous arcs of L, with precision $k, \ell_{max}, \Delta\alpha_{max}$ where:

$$\Delta\alpha_{max} = \frac{1}{2k_\alpha} \min(\alpha_{min}, \bar{\alpha}_{min})$$

$$\ell_{max} = \frac{1}{k_\ell} \min(\ell_{min}, \bar{\ell}_{min})$$

$k, k_\alpha, k_\ell$, are precision parameters; $\bar{\alpha}_{min}$ is an application specified parameter; $\alpha_{min}$ is the minimum angular discontinuity defined by the cusps of L; $\ell_{min}$ is the smallest of the distances between the extremes of any S-continuous arc or straight line in L and $\bar{\ell}_{min}$ is the smallest of the distances between any two locally disjoint points of L.

Comment: $\bar{\alpha}_{min}$ is set to $10^\circ$ or $20^\circ$, for examples, in the case of artistic drawings whereas it is set to few degrees in the case of drawings for scientific applications, as was suggested in the Proceedings of the Symposium on Map and Chart Digitizing[18].

Lemma: Any irregular line drawing L can be represented by an approximated line drawing $L^*$ with any specified precision, by choosing appropriate values for $\alpha_{min}, k, k_\alpha, k_\ell$.

Comment: It is sufficient to note that the algorithm for approximating an S-continuous arc with a P-structure and the definition of $L^*$, guarantees that all the features of L(per Definition 5) are approximated with the required precision.

2.4 Square-Grid Quantization of an Approximated Line Drawing

We shall next investigate the precision with which an approximated line drawing is represented by its quantized version defined on a uniform square grid. A design formula is derived for the coarsest grid size which still allows one to quantize the approximated line drawing with a specified precision.

Definition 9: The minimum length-detail parameter of $L^*$ is:

$$\ell = \ell_{\bar{j}} \tag{2.9}$$

Definition 10: The minimum angular-detail parameter of $L^*$ is:

$$\theta = \min_j \Delta\beta_j \tag{2.10}$$

Let us note that $\ell$ and $\theta$ are the smallest details of interest contained in $L^*$. The precision with which the square-grid quantized version of $L^*$ approximates $L^*$ is then completely specified in terms of the precision with which such details are represented in the quantized version. In fact if $\frac{\Delta\ell}{\ell}$ and $\frac{\Delta\theta}{\theta}$ are the maximum percentage errors affecting $\ell$ and $\theta$ as a consequence of the quantization on a uniform square grid with elementary size T, then for all the remaining elements of the P-structures of L, for which in general $\ell_j \geq \ell$ and $\Delta\beta_j \geq \theta$, the percentage errors will be less than $\frac{\Delta\ell}{\ell}$ and $\frac{\Delta\theta}{\theta}$.

Definition 11: A well-quantized approximated line drawing is one in which the percentage maximum variations of $\ell$ and $\theta$ due to the quantization process are bounded by the constants $p_\ell$ and $p_\theta$ (called length and angular precision parameters, respectively).

Let us note that when a point of an irregular line drawing is replaced by a grid node in the quantization process, the maximum possible distance between these two points is

$$r = \frac{\sqrt{2}}{2} T \tag{2.11}$$

In the case of a straight line segment, it is then possible to relate the maximum angular and length errors due to the quantization process to the precision with which the positions of the extreme of the segment are known, as shown in Fig. 7. Indicating with $\ell_j^*$ the length and with $\beta_j^*$ the angle of the j-th segment after quantization and recalling that $\ell_j$ and $\beta_j$ are the corresponding values before quantization, the following relations hold

$$|\ell_j - \ell_j^*| \leq 2r \qquad \text{and} \qquad |\beta_j - \beta_j^*| \leq \tan^{-1} \frac{2r}{\ell_j} \simeq \tan^{-1} \frac{2r}{\ell_j}$$

Also note that in the worst case the angle between the directions of two straight line segments is changed by the quantization process by an amount equal to twice the possible angular variation occurring in quantizing a single straight line segment. Therefore the following relations can be established for $\Delta\ell$ and $\Delta\theta$.

$$\Delta\ell = 2r \tag{2.12}$$

$$\Delta\theta = 2 \tan^{-1} \frac{2r}{\ell} \tag{2.13}$$

<u>THEOREM 1</u>: The largest grid size T such that L* can be well-quantized (per Definition 11) is

$$T = \frac{\sqrt{2}}{2} p\ell \tag{2.14}$$

where

$$p = \min(p_\ell, \tan p_\theta \frac{\theta}{2}) \tag{2.15}$$

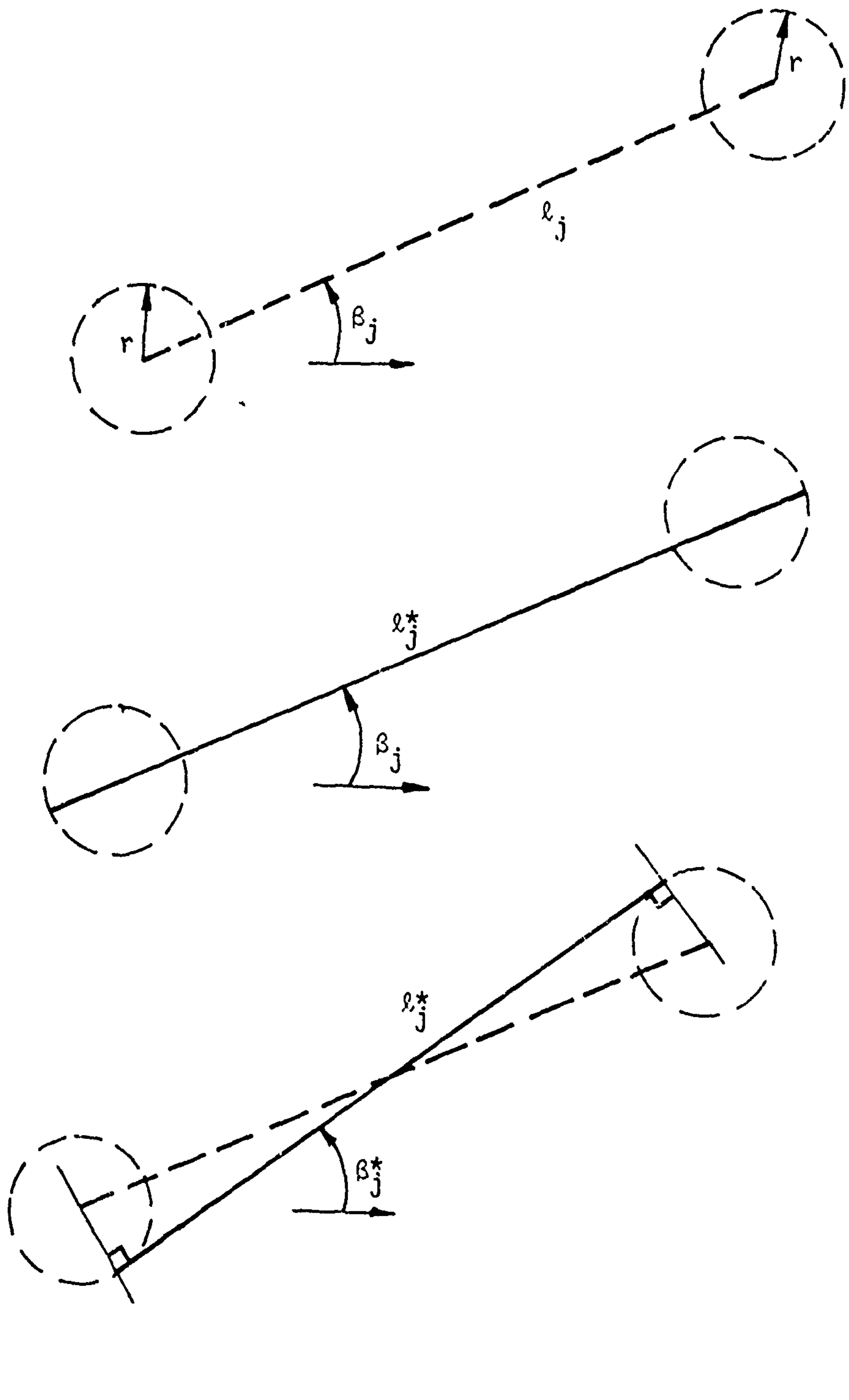


FIG. 7

LENGTH AND ANGULAR DISTORTION OF A STRAIGHT
LINE SEGMENT DUE TO QUANTIZATION

<u>Proof</u>: It is sufficient to note that according to Definition 11, L* can be well quantized if and only if

$$\frac{\Delta \ell}{\ell} \leq p_\ell \tag{2.16}$$

$$\frac{\Delta \theta}{\theta} \leq p_\theta \tag{2.17}$$

or equivalently $\frac{\sqrt{2}T}{\ell} \leq p_\ell$ and $\tan^{-1} \frac{\sqrt{2}T}{\ell} \leq p_\theta \frac{\theta}{2}$

and, therefore, $$\frac{\sqrt{2}T}{\ell} = \min(p_\ell, \tan p_\theta \frac{\theta}{2}) = p \cdot$$

Let us note that in defining L* it has been shown that the maximum deviation $\delta_j$ of the j-th arc of L from its cord fulfilled the relation $\delta_j \leq \delta_{\bar{j}} \leq k\ell_{\bar{j}}$ where $\ell_{\bar{j}}$ is equal to the minimum-length detail parameter $\ell$. If we now write

$$k = \frac{p}{\sqrt{2}\, n} , \tag{2.18}$$

where n is a precision parameter, we have

$$\delta_j \leq \delta_{\bar{j}} \leq p\, \ell_{\bar{j}}/\sqrt{2}\, n = p\, \ell/\sqrt{2}\, n = \sqrt{2}T/\sqrt{2}\, n = \frac{T}{n} \tag{2.19}$$

In other words, if the constant k used in defining L*, is equal to $p/\sqrt{2}\, n$ then the maximum displacement of any curved arc of L from the corresponding cord of L* cannot exceed T/n. Since T is the largest grid size which allows one to well-quantize L*, then in general the grid nodes selected by L and those selected by L* will tend to coincide as the value of n is increased.

This last consideration justifies the use of P-structures as approximations for irregular line drawings. The importance of the precision parameter n will become clearer later when it will be shown that all the precision parameters subsequently introduced are related to n and that bounds on the quality of the description of an irregular line drawing before and after a transformation are function of n only.

Let us note that the minimum and maximum number of chain elements for the shortest straight line segment in L* can be computed as a function of the precision parameter p alone. In fact, the following relations hold for $N_{min}$ and $N_{max}$

$$N_{min} = \left\lfloor \frac{\ell - \Delta\ell}{\sqrt{2}\,T} \right\rfloor = \left\lfloor \frac{1-p}{p} \right\rfloor \tag{2.20}$$

$$N_{max} = \left\lceil \frac{\ell + \Delta\ell}{T} \right\rceil = \left\lceil \sqrt{2}\,\frac{1+p}{p} \right\rceil \tag{2.21}$$

Table I shows the values of $N_{min}$ and $N_{max}$, and the angular variation $\frac{\Delta\theta}{2}$ for a straight line segment as a function of the precision parameter p.

Let us note that if the given irregular line drawing can be enclosed by a square with sides of length $\bar{a}$, and $2^{m'}$ is the number of rows (or columns) of a uniform square grid superimposed on it, then from (2.11), (2.12), and (2.14) the following relations hold:

$$p\ell = \Delta\ell = \sqrt{2}T = \bar{a}\,\sqrt{2}/2^{m'}$$

$$2^{m'} = \sqrt{2}\,\bar{a}/p\ell$$

$$a' = \bar{a}/\ell$$

$$2^{m'} = a'\,\sqrt{2}/p \qquad ; \qquad m' = \log_2(\sqrt{2}\,a'/p)$$

Thus, for instance, if $a' = 10^5$ and $p = 20\%$, then $N_{max} = 9$ and $m' = 19$. Then for representing the most detailed line drawing, that is, the one whose L* contains only segments of the shortest length, the number of bits required

TABLE I

| p | $N_{min}$ | $N_{max}$ | $\frac{\Delta\theta}{2}$ | $\theta$ |
|---|---|---|---|---|
| 50% | 1 | 5 | $26^\circ\ 36'$ | $53^\circ\ 12'$ |
| 40% | 1 | 5 | $21^\circ\ 42'$ | $43^\circ\ 24'$ |
| 30% | 2 | 7 | $18^\circ\ 30'$ | $37^\circ$ |
| 20% | 4 | 9 | $11^\circ\ 21'$ | $22^\circ\ 42'$ |
| 10% | 9 | 16 | $5^\circ\ 36'$ | $11^\circ\ 12'$ |
| 5% | 19 | 30 | $2^\circ\ 52'$ | $5^\circ\ 44'$ |
| 4% | 24 | 37 | $2^\circ\ 18'$ | $4^\circ\ 36'$ |
| 3% | 32 | 49 | $1^\circ\ 37'$ | $3^\circ\ 14'$ |
| 2% | 49 | 73 | $1^\circ\ 9'$ | $2^\circ\ 18'$ |
| 1% | 99 | 144 | $30'$ | $1^\circ$ |
| 0.5% | 199 | 285 | $15'$ | $30'$ |
| 0.1% | 999 | 1,415 | $30''$ | $1'$ |
| 0.05% | 1,999 | 2,840 | $15''$ | $30''$ |
| 0.005% | 19,999 | 28,500 | $0.5''$ | $1''$ |

for storing the coordinates of the N points of the P-structures of L* is $B=2\,m'\,N = 38N$. However, if the P-structures are chain encoded, then the number of required bits becomes $B_c = 2m' + 3N_{max}(N-1) = 38 + 27(N-1)$ and the difference $B_p - B_c = 9(N-1)$ is always positive and increases with N.

Chain encoding tends to be a better solution for encoding the information contained in a well-quantized L*, if a large number of arcs with small curvature is present in it. In the following chapter, patterns are shown to exist in the chain of a segment and advantage is taken of these for improving the efficiency of the chain code.

## 2.5 Relations Among the Precision Parameters

Let us note that the chain of a well-quantized approximated line drawing consists of a sequence of chain-encoded straight line segments. The number of elements in the chain of the shortest straight line will be

$$N \geq N_{min}(p) \tag{2.22}$$

Let us note further that if two consecutive segments form an angle less than $2\Delta\alpha_{max}$ then the vertex of that angle does not correspond to any cusp in L. However if such angle is greater than or equal to $\alpha_{min}$, then its vertex corresponds to a cusp in L. Once vertice have been so classified, the chain can be segmented into chainlets, each corresponding to an S-continuous arc in L. In order to guarantee the separability between the vertices of a well-quantized L*, a relation has to be established between $2\Delta\alpha_{max}$ and $\alpha_{min}$. Let us note that the following relations follow from (2.6),(2.7), (2.10),(2.13),(2.15)

$$\Delta\theta = 2\tan^{-1} p \leq p_\theta\ \theta \leq \theta \leq \Delta\beta_j \leq \frac{1}{k_\alpha}\min(\alpha_{min},\overline{\alpha}_{min}) = 2\Delta\alpha_{max} \tag{2.23}$$

then if all $\Delta\beta_j = \theta$, the minimum possible value $\alpha'_{min}$ of $\alpha_{min}$ can be computed as $\alpha'_{min} = k_\alpha\theta$. Separation is then guaranteed if and only if $\alpha'_{min} > \theta$ and, therefore, $k_\alpha > 1$. Since the largest variation of any angle, due to the quantization process, is $\Delta\theta$, the above relation is maintained after quantization on the square grid if it is at least: $\alpha'_{min} - \Delta\theta \geq \theta + \Delta\theta$ or $\alpha'_{min} \geq \theta + 2\Delta\theta$ and therefore $\alpha'_{min} \geq (1+2p_\theta)\theta$ which leads to the following relation between two precision parameters:

$$k_\alpha \geq 1+2p_\theta \tag{2.24}$$

A similar relation exists between $k_\ell$ and $p_\ell$. In fact the following relations follow from (2.3),(2.8),(2.9),(2.16)

$$\Delta\ell \leq p_\ell\ell \leq \ell \leq \ell_{max} = \frac{1}{k_\ell}\min(\ell_{min},\overline{\ell}_{min})$$

then $\ell'_{min} = \min(\ell_{min},\overline{\ell}_{min}) = k_\ell\ell$. Before quantization on the square grid $\ell'_{min} \geq \ell$. Such a relation is preserved after quantization if and only if $\ell'_{min} - \Delta\ell \geq \ell + \Delta\ell$ and therefore $\ell'_{min} \geq \ell + 2\Delta\ell = (1+2p_\ell)\ell$. This leads to the following relation between two precision parameters:

$$k_\ell \geq 1 + 2p_\ell \tag{2.25}$$

It is now possible to show that all the precision parameters can be computed once the minimum detail parameters $\ell$ and $\theta$ are given and n and T are chosen.

The following is a list of all such relations.

1. $$p = \frac{T}{\ell}\frac{\sqrt{2}}{2} \tag{2.26}$$

2. $$p_\ell \geq p \tag{2.27}$$

3. $$p_\theta \geq \frac{2}{\theta}\tan^{-1}p \tag{2.28}$$

4. $$k_\ell \geq 1 + 2p_\ell \tag{2.29}$$

5. $$k_\alpha \geq 1 + p_\theta \tag{2.30}$$

6. $$k = \frac{p}{\sqrt{2}n} = \frac{T}{\ell n} \tag{2.31}$$

7. $$\min(\alpha_{min},\bar{\alpha}_{min}) \geq k_\alpha\theta \tag{2.32}$$

8. $$\Delta\alpha_{max} \geq (1+2p_\theta)\frac{\theta}{2} \tag{2.33}$$

9. $$\min(\ell_{min},\bar{\ell}_{min}) \geq k_\ell\ell \tag{2.34}$$

10. $$\ell_{max} \geq (1+2p_\ell)\ell/2 \tag{2.35}$$

11. $$\Delta\ell \leq p_\ell\ell = \sqrt{2}T \tag{2.36}$$

12. $$\Delta\theta \leq p_\theta\theta = 2\tan^{-1}p = 2\tan^{-1}\frac{\sqrt{2}T}{\ell} \tag{2.37}$$

13. $$\delta_j \leq k\ell = \frac{T}{n} \tag{2.38}$$

All these relations show that, given an irregular line drawing which is characterized by the minimum-length and angular-detail parameters $\ell$ and $\theta$ and which is described in terms of a quantized version defined on a grid with size T, the precision of its description is solely a function of the precision parameter n. The larger the value of n, the more precise the description will be. This result will actually be proved in a following chapter when the bounds on three different types of quality indicators (i.e., figures of noise) will be shown to be proportional to the inverse of n, both before and after a transformation.

## 2.6 Concluding Remarks

An algorithm for approximating an irregular line drawing and for quantizing it on a square grid has been described. Relations between the precision parameters have been shown to exist which guarantee that the features of the drawing be preserved with the required precision. Also it has been shown that the quality indicator of the description of an irregular line drawing quantized on a given grid is the precision parameter n.

# III. THE ENCODING METHOD

In this chapter, patterns will be shown to exist in the chain of a straight line segment and advantage will be taken of these for compressing the chain code of the segment. Then a comparison with other types of codes will show the advantage of the one proposed here.

## 3.1 General Considerations

Let the segment $\ell$ be defined as the one connecting nodes A and B, and defined to be positive in the direction A to B. Let us define a right-handed coordinate system, X-Y, centered on A and with axes parallel to the grid lines. The coordinates of B will be denoted by the ordered pair a,b, where the unit of measure is the grid size T=1.

To obtain the chain C for the segment $\ell$, one determines the intersections between $\ell$ and the grid, and selects the nodes closest to each intersection[10]. Since a point moving on $\ell$ from A to B crosses these intersections one after the other, the nodes associated with each intersection can be ordered in a sequence. A segment, its chain and the plotter movements (dotted) corresponding to the chain are shown in Fig. 8; the correspondence between all possible chain elements and the plotter movements is shown in Fig. 9. Denoting with $\alpha_i$ the i-th element of C, a compact notation[16] for representing N such elements is

$$C = \mathop{C}_{i=1}^{N} \alpha_i = \alpha_1 \ldots \alpha_N \tag{3.1}$$

The coordinates of the (i+1)-th node relative to the i-th node will be

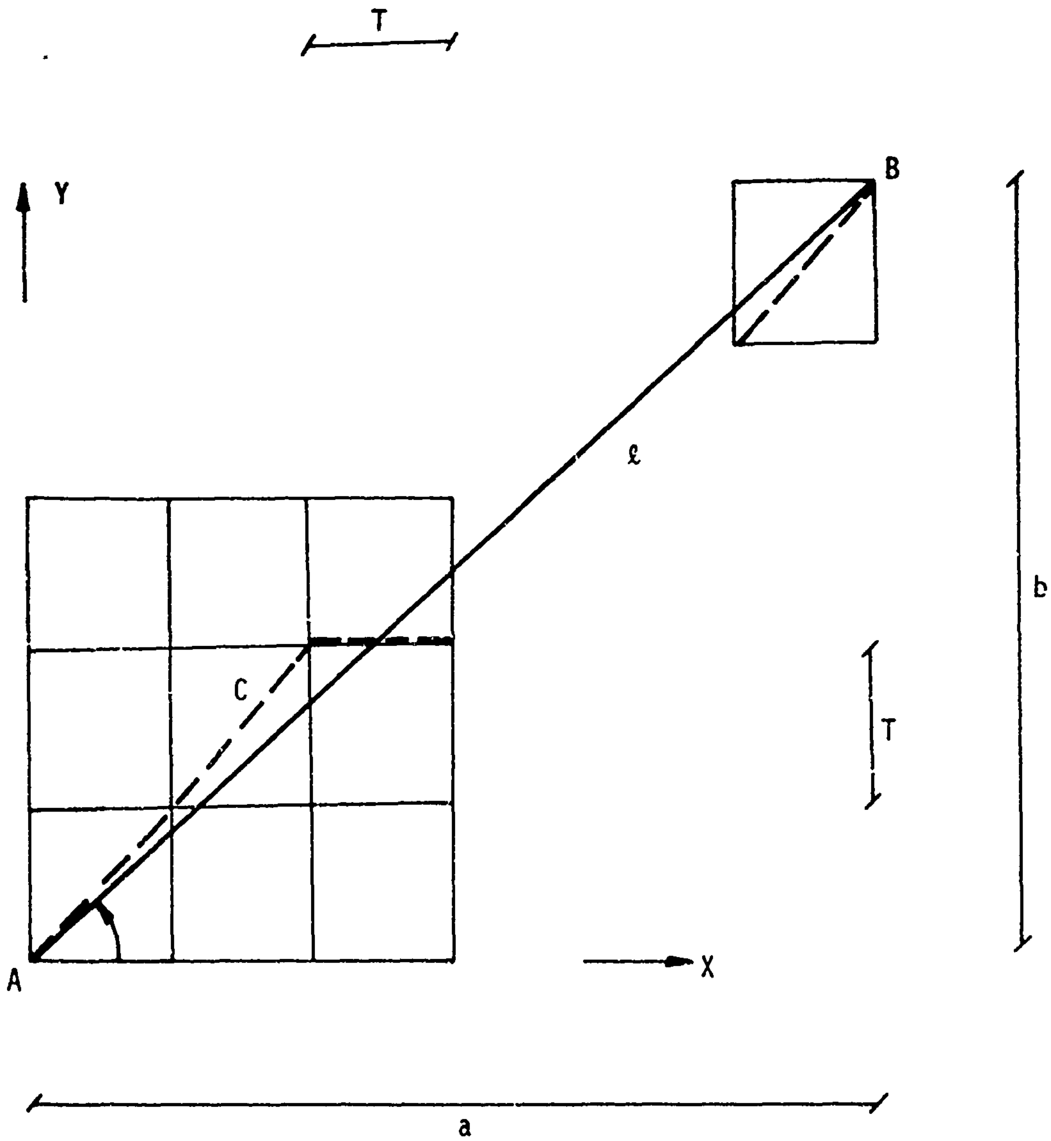


FIG. 8

SEGMENT AND PLOTTED CHAIN

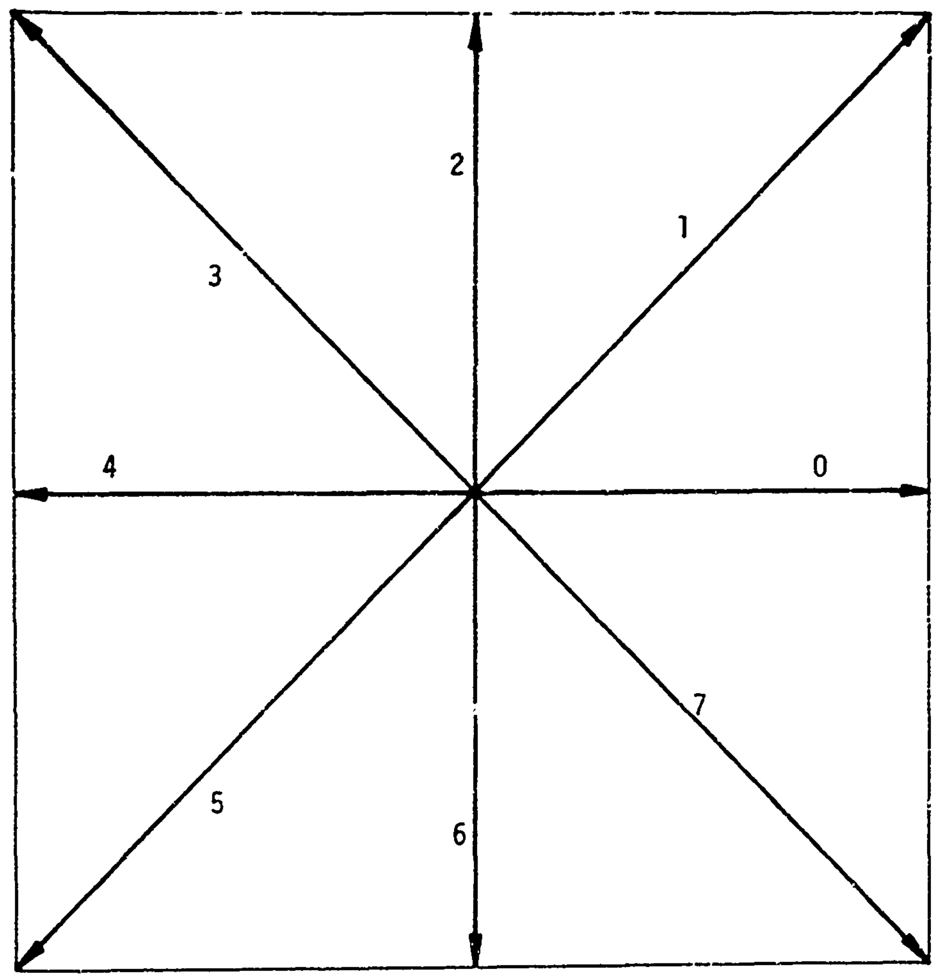


FIG. 9

PLOTTER MOVEMENTS AND CHAIN ELEMENTS

denoted by $\alpha_{ix}, \alpha_{iy}$. In the following, segments are classified into three classes. The determination of C for segments of the first two classes is trivial. For segments of the third class, patterns will be proved to exist and an algorithm given for the fast computation of C.

3.2 Chains for Segments of Class I

Definition 12: A segment of Class I is one for which either $|a| = |b|$ or $a = 0$, $b \neq 0$ or $a \neq 0$, $b = 0$ ($|X|$ is the absolute value of X).

Statement: The elements of the chain C of a segment of Class I are of one type only; that is the chain has the form $C = \underset{i=1}{\overset{N}{C}} \alpha_i$, $\alpha_i = \alpha_{i+1}$ for

$$1 \leq i \leq N-1, \text{ and } N = |a| = |b| \text{ or } N = b \text{ or } N = a.$$

The first and the last node of a sequence are called the initium and terminus of the corresponding chain.[10] Let us note that the segment defined by connecting the initium and terminus of a chain containing only elements of one type is of Class I. Then the chain of any non-Class I segment may contain elements of more than one type. It will be shown later that such a chain actually contains elements of two types only.

3.3 Chain Computation by Substitution

Let us consider the effect on C of a rotation of $\ell$, by an angle $\lambda$ with respect to the origin A of the reference frame.

Case 1: $\lambda = \pm 180^\circ$, $C = \underset{i=1}{\overset{N}{C}} \alpha_i$ is changed into $C' = \underset{i=1}{\overset{N}{C}} \alpha_i'$ with $\alpha_i' = \alpha_i \dot{\pm} 4$ (3.2)

where $\dot{+}$ ($\dot{-}$) denotes addition (subtraction) modulo eight.

Case 2: $\lambda = \pm 90^\circ$, $C = \underset{i=1}{\overset{N}{C}} \alpha_i$ is changed into $C' = \underset{i=1}{\overset{N}{C}} \alpha_i'$ with $\alpha_i' = \alpha_i \dot{\pm} 2$. (3.3)

The reader will note that it is always possible to find a segment in the first quadrant of the reference frame such that its relative angle with respect to a given segment is $\pm 90^\circ$ or $\pm 180^\circ$ and its length is equal to that of the given segment. Hence it follows that the chain of any segment can be computed by substituting the elements of the chain of a corresponding segment in the first quadrant.

Let us also note that if $\ell$ is the segment defined by the ordered pair a,b, with $a > b > 0$ and its chain is $C = \mathop{C}_{i=1}^{N} \alpha_i$ and if $C' = \mathop{C}_{i=1}^{N} \alpha_i'$ is the chain of the segment $\ell'$ defined by the ordered pair b,a, then the elements of $C'$ can be computed from those of $C$ by means of the formula $\alpha_i' = 2 \dot{-} \alpha_i$. In other words, the general problem of finding C for a segment $\ell$, given the integers a and b can be reduced to the problem in which $\ell$ belongs to the first octant (i.e., $a>b>0$).

### 3.4 Chains for Segments of Class II

Definition 13: A segment is of Class II if its corresponding segment in the first octant has either $b = \frac{a}{2}$ if a is even or $b = \frac{a-1}{2}$ or $b = \frac{a+1}{2}$ if a is odd.

Statement: The chains of segments of Class II which belong to the first octant are:

1. $C = \mathop{C}_{i=1}^{a} \alpha_i$ with $\alpha_{2j-1} = 0$, $\alpha_{2j} = 1$ or $\alpha_{2j-1} = 1$, $\alpha_{2j} = 0$ for all $1 \leq j \leq \frac{a}{2}$ if $b = \frac{a}{2}$.

2. $C = \mathop{C}_{i=1}^{a} \alpha_i$ with $\alpha_{2j-1} = 0$, $\alpha_{2j} = 1$ for all $1 \leq j \leq \frac{a-1}{2}$ and $\alpha_a = 0$ if $b = \frac{a-1}{2}$

3. $C = \mathop{C}_{i=1}^{a} \alpha_i$ with $\alpha_{2j-1} = 1$, $\alpha_{2j} = 0$ for all $1 \leq j \leq \frac{a-1}{2}$ and $\alpha_a = 1$ if $b = \frac{a+1}{2}$.

Examples of these three cases are shown in Figs. 10, 11 and 12.

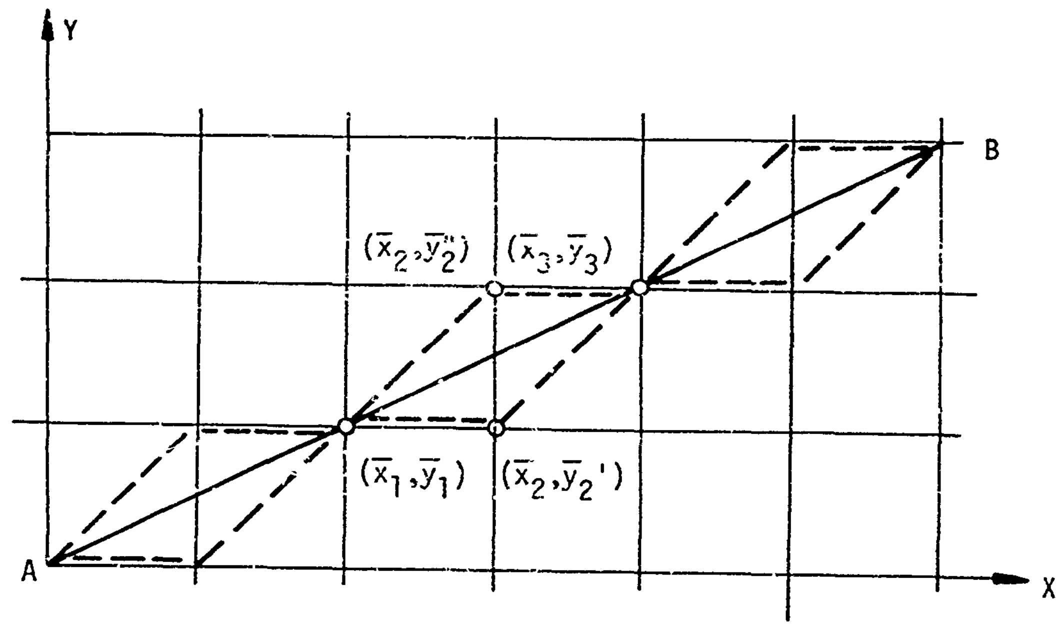


$a = 6$

$b = \frac{a}{2} = 3$

FIG. 10

CHAINS FOR CLASS II SEGMENTS

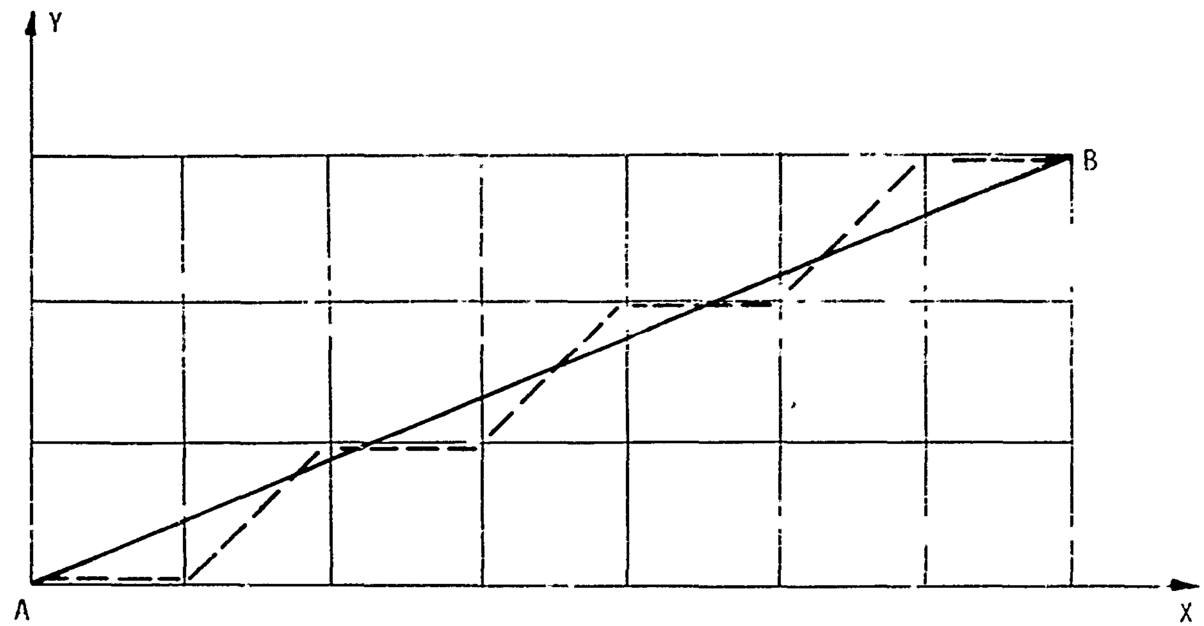


$a = 7$

$b = \frac{a-1}{2} = 3$

FIG. 11

CHAINS FOR CLASS II SEGMENTS

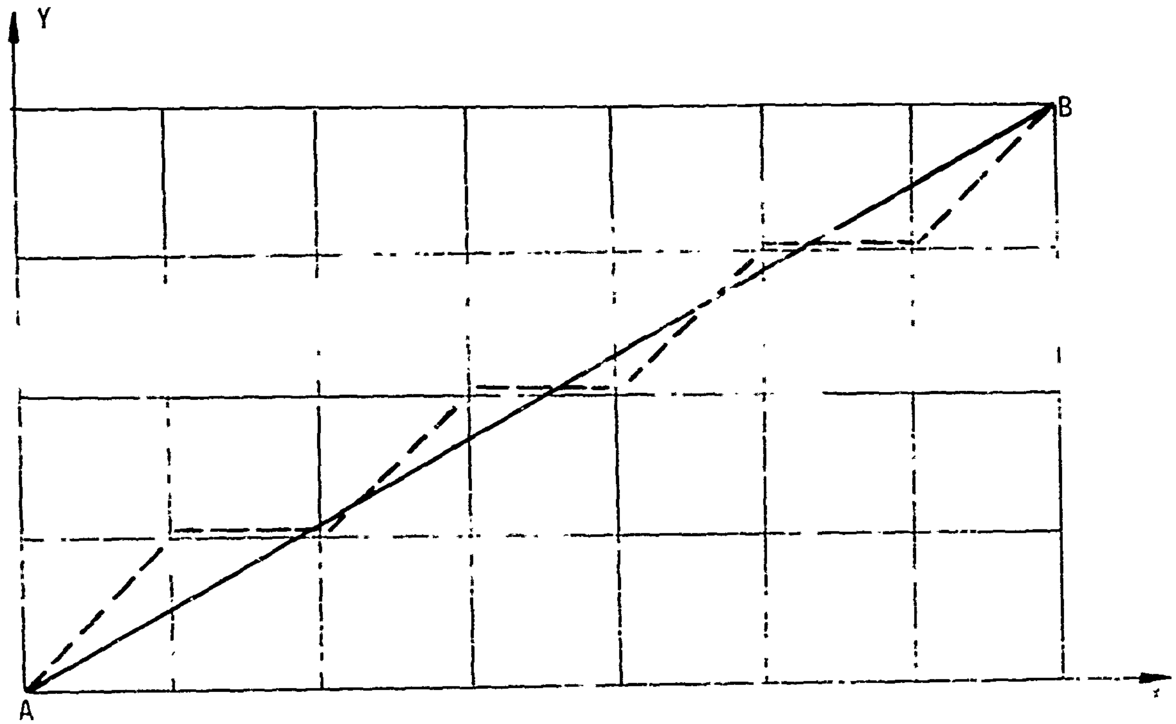


$a = 7$

$$b = \frac{a+1}{2} = 4$$

FIG. 12

CHAINS FOR CLASS II SEGMENTS

## 3.5 Chains for Segments of Class III

Definition 14: A segment is of Class III if its corresponding segment in the first octant is defined by $a > b_o > b > 0$, where $b_o = \frac{a}{2}$ if a is even or $b_o = \frac{a-1}{2}$ if a is odd (i.e. $b_o = \left\lfloor \frac{a}{2} \right\rfloor$, where $\lfloor X \rfloor$ denotes the integer part of X). In the following it will be said that such a corresponding segment is in the first half of the first octant. Let us also note that such a segment is neither of Class I nor of Class II.

Lemma: The chain of a segment of Class III belonging to the first half of the first octant contains only 0's and 1's.

Lemma: The number of 1's, $n_1$, in the chain of a segment of Class III belonging to the first half of the first octant is smaller than the number of 0's, $n_o$. In particular $n_o > b_o > n_1$.

Lemma: Elements of value 1 in the chain of a segment of Class III belonging to the first half of the first octant are separated by at least one element of value 0.

THEOREM 2: The chain $C' = \mathop{C}\limits_{i=1}^{a} \alpha_i'$ of a segment defined by a, a-b with $a > b_o > b > 0$ can be computed by substituting the elements of the chain $C = \mathop{C}\limits_{i=1}^{a} \alpha_i$ of the segment defined by a,b. In particular

$$\alpha_i' = 1 \dot{-} \alpha_i \tag{3.4}$$

Proof: By construction $\alpha_{ix} = \alpha_{ix}' = 1$ and $\alpha_{iy} = \left[\frac{b}{a}(i+1)\right] - \left[\frac{bi}{a}\right]$, Fig. 8, where $[x]$ denotes the integer closest to x; since $b < b_o$, $\frac{b}{a} < 1/2$ and

$$\alpha_{iy}' = [i+1 - b(i+1)/a] - [i-bi/a] = 1 - [b(i+1)/a] + [bi/a] = 1 - \alpha_{iy}$$

Then when $\alpha_{iy} = 0$, $\alpha_{iy}' = 1$ and conversely; therefore when $\alpha_i = 0$, $\alpha_i' = 1$ and conversely. The fact that $\alpha_i$ can only be 0 or 1 is ensured by a previous lemma.

Lemma: A segment is of either Class I or Class II or Class III.

Let us note that because of previous considerations, the chain of a segment can be computed by substituting the elements of the chain of a corresponding segment in the first half of the first octant. This in turn shows that the properties and patterns detectable for such chains are valid in general for the chain of any segment.

It can be stated now that the chain of any segment contains at most elements of two types, whose difference modulo-eight is either 0 or 1, and that in general the two types of elements are present in the chain with a different number of occurrences.[15]

3.6 Chain Patterns

From now on, only chains of segments of Class III belonging to the first half of the first octant will be considered. The results of previous paragraphs guarantee the generality of the results.

By definition the values a and b, specifying the segment $\ell$, satisfy the relation $a > b_o = \lfloor \frac{a}{2} \rfloor \geq b > 0$; moreover the chain C of $\ell$ contains $n_o$ zeros and $n_1$ ones with

$$n_o = a - b > b_o = \left\lfloor \frac{a}{2} \right\rfloor > n_1 = b > 0. \tag{3.5}$$

Let us denote with $I_k$ the position in C of the last zero preceding the k-th one. The number of zeros between the k-th and the (k+1)-th ones is given by $\ell_{k+1} = I_{k+1} - I_k - 1$ which will be referred to as the length of the (k+1)-th sequence of zeros in C.

<u>Lemma</u>: Since $I_k$ is the largest integer such that $\frac{b}{a} I_k - k \leq 1/2$, then

$$I_k = \lfloor (2k+1)a/2b \rfloor \tag{3.6}$$

<u>Proof</u>: Let $i$ and $f_i$ be such that $i$ is an integer, $0 \leq f_i < 1$ and $i + f_i = \frac{ka}{b} + \frac{a}{2b}$. Since $bI_k \leq ka + \frac{a}{2}$ then $I_k = \lfloor I_k \rfloor = i = \lfloor (2k+1) \frac{a}{2b} \rfloor$

THEOREM 3: For all $1 \leq k \leq b-1$, $\ell_{k+1}$ can only have two values, namely $h = \lfloor 1/m \rfloor$ and $h-1$, (3.7) where $m = \frac{b}{a}$ is the rational slope of the segment with respect to the horizontal axis of the frame of reference.

<u>Proof</u>: Let $h$ and $f_h$ be such that $h$ is integer, $0 \leq f_h < 1$ and $h + f_h = \frac{1}{m} = \frac{a}{b}$. Also let $n = 2k+1$ and $i$ and $f_i$ be such that $i$ is integer, $0 \leq f_i < 1$ and $i + f_i = \frac{na}{2b}$ then $h = \lfloor h+f_h \rfloor = \lfloor 1/m \rfloor = \lfloor a/b \rfloor$ and $i = \lfloor na/2b \rfloor$ and

$$\ell_{k+1} = \lfloor (n+2)a/2b \rfloor - \lfloor na/2b \rfloor - 1 = i + h + \lfloor f_i + f_h \rfloor - i - \lfloor f_i \rfloor - 1 = h - 1 + \lfloor f_i + f_h \rfloor$$

and, since by definition both $f_i$ and $f_h$ are positive and less than one,

$$0 \leq f_i + f_h < 2, \quad \lfloor f_i + f_h \rfloor = 0 \quad \text{or} \quad \lfloor f_i + f_h \rfloor = 1 \quad \text{and,}$$

therefore,

$$\ell_{k+1} = h - 1 = \lfloor 1/m \rfloor - 1 \quad \text{or} \quad \ell_{k+1} = h = \lfloor 1/m \rfloor . \tag{3.8}$$

THEOREM 4: If $\ell_1 = \ell_{b+1}$, then $\ell_1 = \lfloor h/2 \rfloor = \lfloor \lfloor 1/m \rfloor /2 \rfloor = \ell_{b+1}$. (3.9)

<u>Proof</u>: Let us note first that the segment $\ell''$ defined by 2a, 2b can be regarded as the concatenation of two segments $\ell$, $\ell'$ each defined by a,b and that the chain C" of $\ell''$ is the concatenation of the chains C, C' of $\ell$, $\ell'$ (C and C' are identical since $\ell$ and $\ell'$ are defined by the same integers). In particular C" has the same value for h as C and C'. However, the

(b+1)-th sequence of zeros in C" is generated by the concatenation of the (b+1)-th sequence of zeros in C and the first sequence of zeros in C'; and this last sequence is identical to the first one in C. Therefore, the following relations hold for C:

$$\ell_1 + \ell_{b+1} = h \quad \text{or} \quad \ell_1 + \ell_{b+1} = h-1 \text{ and } \ell_1 = \ell_{b+1}.$$

Case 1: h is even: $2\ell_1 = h$, $\ell_1 = h/2$ or $\ell_1 = \lfloor h/2 \rfloor$ .

Case 2: h is odd; $2\ell_1 = h-1, \ell_1 = \lfloor \ell_1 + 1/2 \rfloor = \lfloor (h-1)/2 + 1/2 \rfloor = \lfloor h/2 \rfloor$.

Therefore, it is always true that $\ell_1 = \ell_{b+1} = \lfloor h/2 \rfloor$. (3.10)

Let us note that because of geometric symmetries $\ell_1 = \ell_{b+1}$, with the only exceptions being those cases in which there are ambiguities in the chain as will be shown later in considering the effect of certain particular combinations of values for a and b.

THEOREM 5: The number of sequences of zeros with length h, $n_h$, and the number of sequences of zeros with length h-1, $n_{h-1}$, are given by

$$n_{h-1} = b - n_h \tag{3.11}$$

$$n_h = a - bh = (a/b - \lfloor a/b \rfloor)b = bf_h = b|a \tag{3.12}$$

where $b|a$ is the residue of a in base b.

Proof: If one concatenates the first and the last sequence of 0's in C, one obtains b sequences of 0's whose length is either h or h-1. Since the total number of 0's in C is $n_o = a-b$ and also $n_c = (h-1)b + n_h$ then $n_h = a-bh = a-b\lfloor a/b \rfloor = b|a$. The expression giving the total number of 0's can also be rewritten as $n_o = hn_h + (h-1)n_{h-1}$, and, therefore,

$n_{h-1} = b - (a-b\lfloor a/b\rfloor) = b-n_h$.

### 3.7 Algorithm

Advantage is taken here of the fact that the length of a sequence of 0's in C can only assume two values for predicting the position of the next element of type 1 in C. A test is then made for checking the correctness of the predicted position and eventually this position is modified before recycling the algorithm. This occurs when the actual length of the sequence of 0's is h. In the flow chart shown in Fig. 13, array I(k) specifies the position in C of each of the elements of type one; V1(k) and V2(k) are arrays containing the even multiples of b and the odd multiples of a. Let us note that a comparison between the integers V1 and V2 corresponds to a comparison between the ordinates of the intersections of the segment with the grid and the ordinates of the horizontal straight lines passing through the centers of the squares of the grid. In other words, instead of comparing bk/a with i+0.5, one compares 2kb and (2i+1)a.

As can be seen by looking at the flow chart, the branching after the test comparing V1 and V2 corresponds to the two situations in which the length of the k-th sequence of zeros is h-1(yes) or h(no). The constants appearing in the flow chart are

$C_1 = h = \lfloor a/b\rfloor$, $C_2 = 2bC_1$, $C_3 = 2a$, $C_4 = 2b$, $k_{max} = b-1$, $\bar{K} = 1$, $I(1) = \lfloor C_1/2\rfloor+1$, $V1(1) = 2bI(1)$, $V2(1) = a$.

The number of tests and additions required by such an algorithm can be computed since the number of sequences with a given length is known.

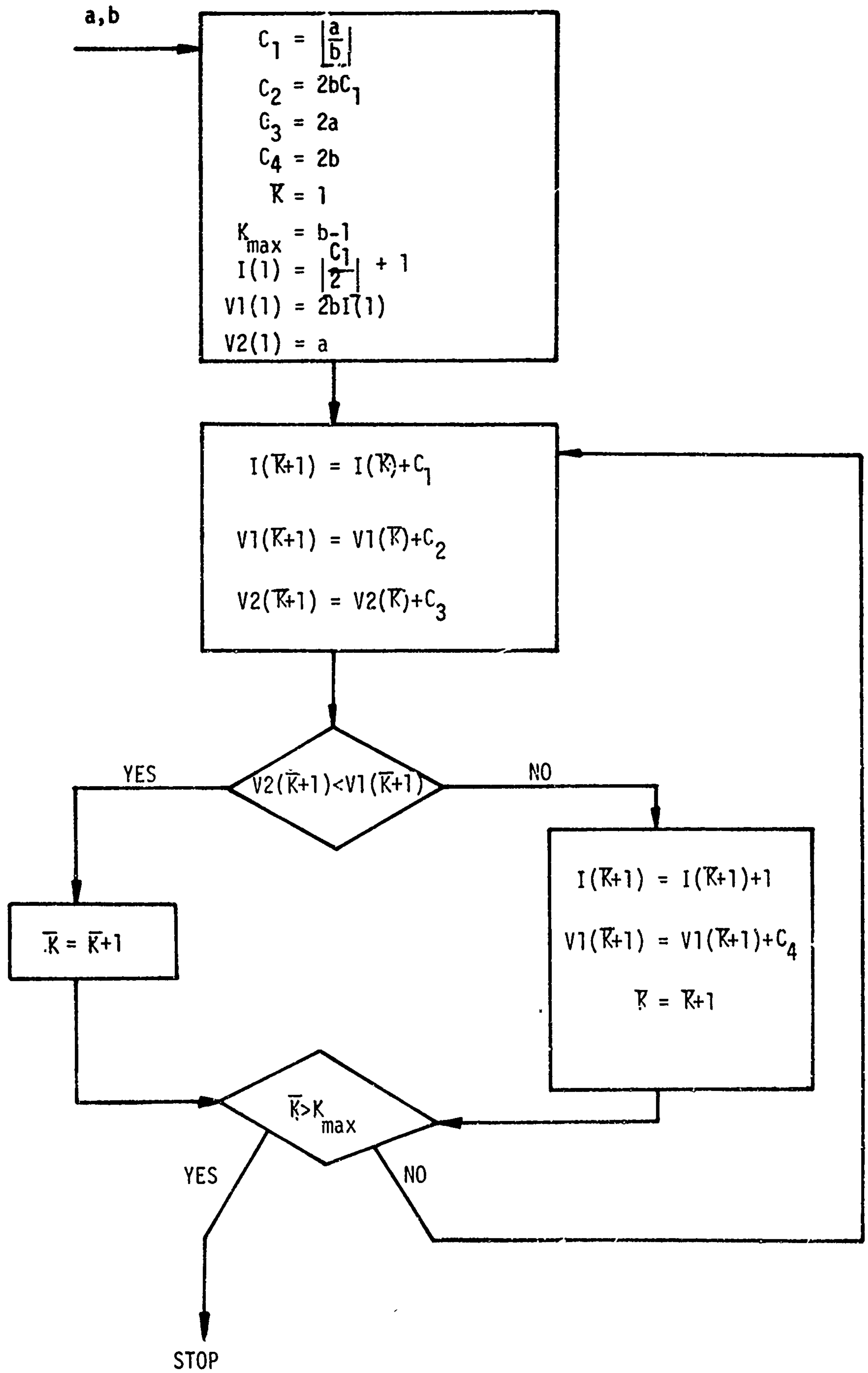


FIG. 13

FLOW CHART

Disregarding the setting of constants and the generation of the chain once the positions of its elements of type 1 are known, the number of additions s and the number of tests t required by this algorithm are $t = (b-n_h)2 + 2n_h = 2b$ and $s = 4(b-n_h) + 6n_h = 2a - 2bh + 4b = 2a + 2b(2-h)$.

The fastest previous algorithm known to the author for generating the chain of a segment is the one described by Bresenham[3], which requires 2(a+1) additions and 2a tests. By hypothesis $\lfloor a/2 \rfloor > b$ and $h = \lfloor a/b \rfloor > 2$, then the proposed algorithm is faster than Bresenham's. In fact we have the following results $2(a+1) - s = 2 + 2b(h-2) > 0$ and $2a - t = 2(a-b) > a > 0$, and, if for example $b = b_o = \lfloor a/2 \rfloor$, $h = 2$, then $2(a+1) - s = 2 > 0$ and $2a - t = a > 0$, which shows the advantage of the proposed algorithm even in the worst case.

### 3.8 Ambiguous Chainlets

Let us recall that a chainlet is a sequence of adjacent chain elements belonging to a given chain.[10]

Definition 15: An ambiguous chainlet in C is one defined by two adjacent chain elements generated by a grid intersection occurring at the midpoint between two adjacent nodes of the grid.

Let us note, as shown in Fig. 14, that if the two nodes, defined by the intersection of the segment with the grid, have $x = k$ and respectively $y = i$ and $y = i + 1$, then the following relation holds $bk/a = i + 1/2$ or $bk = ia + a/2$ with $0 \leq i \leq b - 1$.

Statement: A necessary condition for the existence of ambiguous chainlets in the chain of a segment defined by a,b such that $a > b_o = \lfloor a/2 \rfloor > b > 0$ is that a is even.

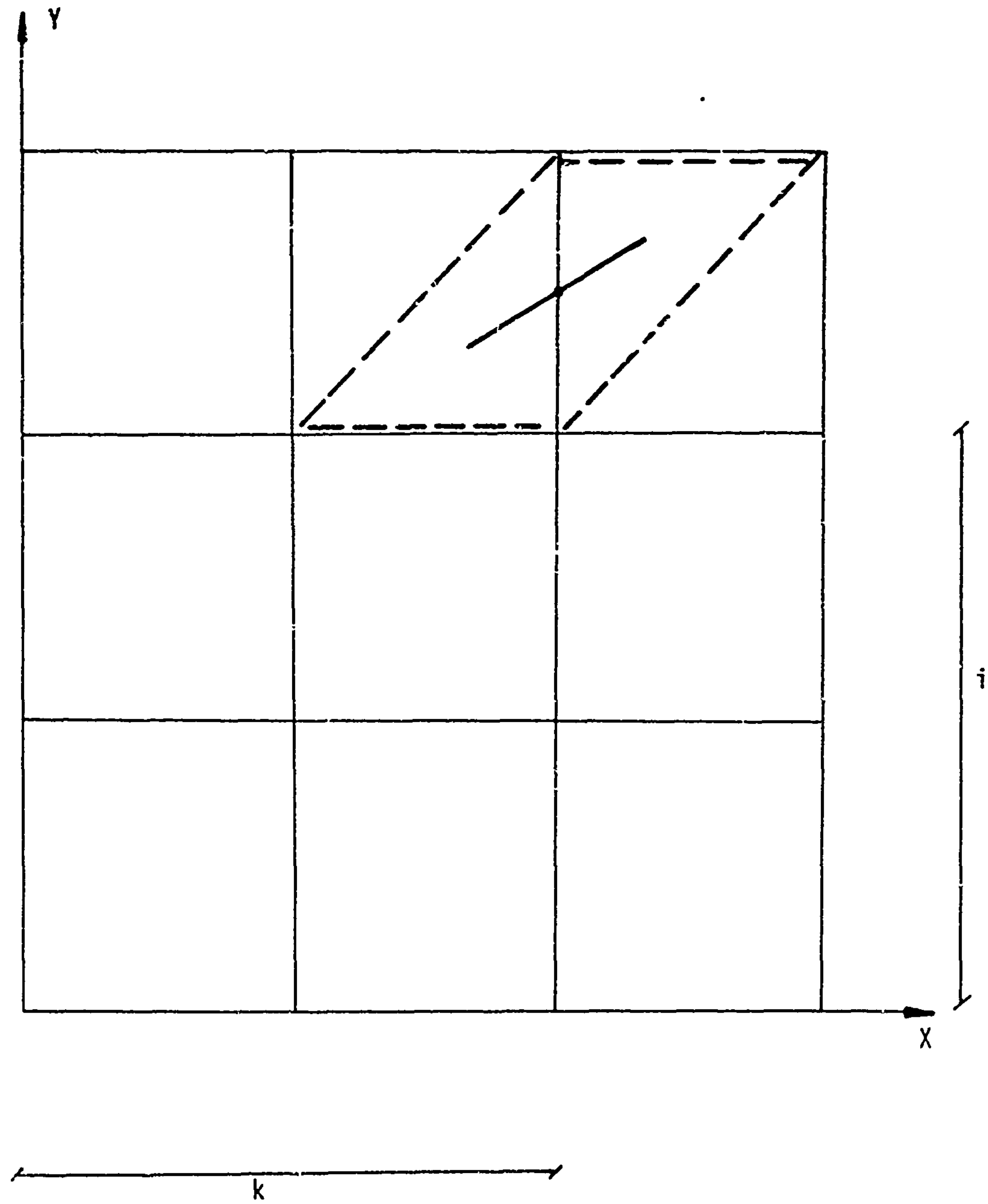


FIG. 14

AMBIGUOUS CHAINLET

In the following it will be assumed that $a = 2n$, $b_o = n$ and $n > b > 0$; ; $bk = (2i+1)n$ with $0 \leq i \leq b - 1$.

Statement: If $a = 2n$ and $b|n = 0$, where $b|n$ is the residue of n in base b, then there are b ambiguous chainlets in C.

Comment: It is sufficient to note that there exists an integer j such that $j = n/b$ and $k = (2i+1)j$ and, therefore, there are as many values for k as i's in the set $\{1,\ldots,b\}$, and hence the number of ambiguous chainlets in C is b.

Statement: If $a = 2n$ but $b|n \neq 0$ and b is even, then there are no ambiguous chainlets in C.

Comment: It is sufficient to note that $n/b$ is not an integer, and $(2i+1)/b$ cannot be integer either, since b is even and $(2i+1)$ is odd. Since by definition k is an integer, $k = (2i+1)n/b$ has no solution for b even.

Statement: If $a = 2n$ and $b|n \neq 0$ and b is odd, then there is just one ambiguous chainlet in C. Such chainlet will occur in the middle of the chain.

Comment: It is sufficient to note that $n/b$ is not an integer, but that $(2i+1)b$ is integer if $i = \frac{b-1}{2}$ (note that $i \leq b - 1$), and, therefore, $k = n = b_o = a/2$ which corresponds to the position of the midpoint of the segment and of its chain. Moreover, since the solution for k is unique, then there is just one ambiguous chainlet in C.

Definition 16: A chain C is called non-ambiguous if either a is odd, or both a and b are even and $b|(a/2) \neq 0$.

Definition 17: A chain C is called one-ambiguous if and only if a is even, b is odd, and $b|(a/2) \neq 0$.

Definition 18: A chain C is called b-ambiguous if and only if a is even, and $b|(a/2) = 0$.

Let us note that a non-, one-, or b- ambiguous chain contains zero, one, or b ambiguous chainlets. Each ambiguous chainlet allows one to build two different chains according to which solution is accepted for the ambiguous chainlet (i.e. the solution 01 or the solution 10).

3.9 Properties of Ambiguous Chains

As indicated in Fig. 15 an area can be associated with a segment and its chain.. An algorithm for computing the area associated with a chain has been derived by Freeman.[10] In the following $a_\ell$ will denote the area associated a segment $\ell$ and $a_c$ the one associated with its chain C. Areas will be measured in terms of $T^2$, where T = 1 is the elementary size of the grid.

Statement: If C is non-ambiguous, then $a_\ell = a_c$ (3.13)

Statement: If C is one-ambiguous, then $|a_\ell - a_c| = 0.5$ (3.14)

Comment: The proof is based on the fact that there is only one ambiguous chainlet in C. According to which solution is chosen for such chainlet, $a_c$ will be either larger or smaller than $a_\ell$ by 0.5.

Statement: If C is b-ambiguous, then $|a_\ell - a_c| \leq b/2$ (3.15)

Comment: If the solution 01 is accepted for all the b-ambiguous chainlets in C, then $a_c$ will assume its minimum value. Because of previous statements, it can be concluded that in such a case $|a_\ell - a_c| = b/2$. The minimum value of $|a_\ell - a_c|$ will occur when $\lfloor b/2 \rfloor$ solutions for the chainlets are of the type 01

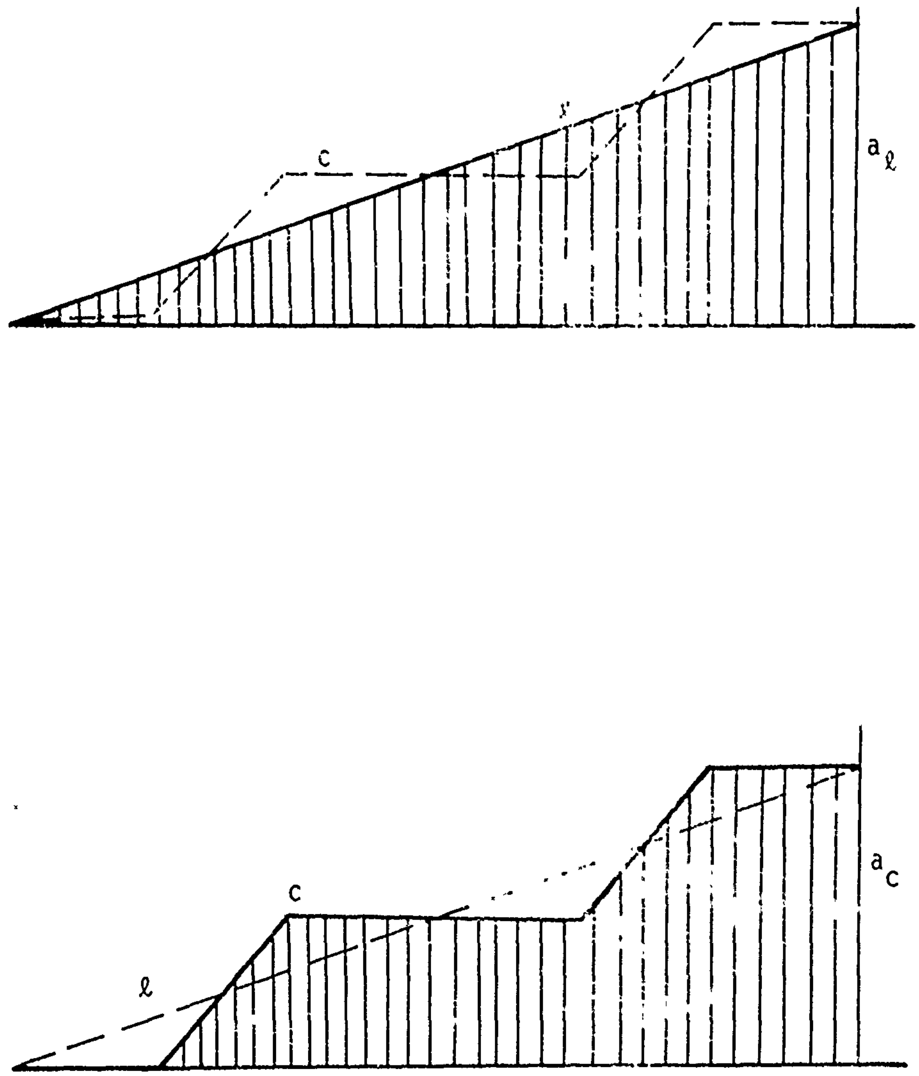


FIG. 15

AREA ASSOCIATED WITH A SEGMENT AND A CHAIN and $\lfloor b/2 \rfloor$ of the type 10. In such a case, if b is even, $a_\ell = a_c$ and, if b is odd, $|a_\ell - a_c| = 0.5$ as in the case of one-ambiguous chains.

We note that the arbitrary rearranging of a b-ambiguous chain, that is the arbitrary selection of the solution 01 or 10 for its ambiguous chainlets, may destroy the chain patterns that are typical of a straight line segment. In particular this rearranging of ambiguous chainlets is responsible for the fact that the first and the last sequence of zeros in C are in general not identical; however, the absolute value of the difference of the lengths of these sequences cannot exceed one; that is,

$$|\ell_1 - \ell_{b+1}| \leq 1 \tag{3.16}$$

3.10 Translational Invariance of Chain Patterns

We will now show the invariance of chain patterns with respect to vertical translations of $\ell$ by an amount c, which without loss of generality is $|c| < 1/2$. Then the invariance with respect to horizontal translations of $\ell$ by an amount $|d| < 1/2$ will be considered. As in the preceding paragraphs, it will be assumed that C is the chain of a segment $\ell$ defined by a,b with $a > b_o = \lfloor a/2 \rfloor > b > 0$. Let i,g,h be integers, and $f, f_g, f_h$ be positive numbers less than one such that the following are true with n = 2k + 1 and k integer

$$i + f_i = na/2b \;, \quad 0 \leq f_i \;\; 11 \;, \quad i = \lfloor na/2b \rfloor \;, \quad n > 1$$

$$\bar{g} + f_g = ca/2b \quad 0 \leq f_g < 1 \;, \quad \bar{g} = \lfloor ca/2b \rfloor \;, \quad |c| < 1/2$$

$$h + f_h = a/b \quad 0 \leq f_h < 1 \;, \quad h = \lfloor a/b \rfloor$$

Let us also note that the following relations hold:

1. $i + f_i > a/2b > ca/2b = \bar{g} + f_g$ , $i \geq \bar{g}$

2. $ca/b < a/2b = (h+f_h)/2$ , $h + f_h > 2\bar{g} + 2f_g$ , $h \geq 2\bar{g}$

3. $n > 1$, $h > 2$

THEOREM 6: For all $1 \leq k \leq b-1$, $\ell_{k+1} = h$ or $\ell_{k+1} = h-1$ for all $c$, $|c|<1/2$.

Proof:

$$\ell_{k+1} = \left\lfloor \frac{na}{2b} + \frac{a}{b} - \frac{ca}{b} \right\rfloor - \left\lfloor \frac{na}{2b} - \frac{ca}{b} \right\rfloor - 1 =$$

$$= \lfloor (i+h-\bar{g}) + (f_i+f_h-f_g) \rfloor - \lfloor (i-\bar{g}) + (f_i-f_g) \rfloor - 1$$

By definition $-1 < f_i - f_g < 1$. Thus there are two possible cases:

Case 1: $0 < f_i - f_g < 1$, $\lfloor f_i - f_g \rfloor = 0$ , $0 \leq f_h + f_i - f_g < 2$

and $\Delta_1 = \lfloor f_i + f_h - f_g \rfloor = \begin{cases} 0 \\ 1 \end{cases}$ , $\ell_{k+1} = h - 1 + \Delta_1 = \begin{cases} h-1 \\ h \end{cases}$

Case 2: $-1 \leq f_i - f_g < 0$ , $0 < 1 + f_i - f_g < 1$

and $0 < 1 + f_i + f_h - f_g < 2$. There are two further possibilities:

Case 2a: $i - \bar{g} - 1 \geq 0$ $i \geq \bar{g} + 1$ and then

$$\ell_{k+1} = i + h - \bar{g} - 1 + \lfloor 1 + f_i + f_h - f_g \rfloor - (i-\bar{g})+1-1 = \begin{cases} h-1 \\ h \end{cases}$$

Case 2b: $i - \bar{g} - 1 < 0$ , $i = \bar{g}$ and then

$$\ell_{k+1} = h - 1 + \lfloor 1 + f_h + f_i - f_g \rfloor + \lceil f_g - f_i \rceil - 1 = \begin{cases} h-1 \\ h \end{cases}$$

THEOREM 7: For all $1 \leq k \leq b - 1$, $\ell_{k+1} = h$ or $\ell_{k+1} = h - 1$ for all $d$, $|d| < 1/2$.

Comment: The proof for this theorem is easier than the one for Theorem 6 since in the expression of $\ell_{k+1}$ the constant d does not appear multiplied by the inverse of the slope of $\ell$.

Let us note that since any translation in the plane can be regarded as a combination of a vertical with a horizontal translation, and since any segment $\ell$ has chain patterns corresponding to those of the chain of a segment of Class III belonging to the first half of the first octant, it can be concluded that such patterns are invariant with respect to any translation of $\ell$ in the plane and for any segment $\ell$. In the case of the first and the last sequence of zeros in C, the translational invariancy is not guaranteed because of the truncation effect caused by the grid-intersect quantization scheme. This truncation effect may cause either $\ell_1$ or $\ell_{b+1}$, or both, to be reduced by one element. Therefore the following relations hold:

1 $\ell_1 + \ell_{b+1}$ is either equal to h or h-1 or h-2 or h-3, and

2. $|\ell_1 - \ell_{b+1}| \leq 2.$ (3.17)

3.11 The Encoding Scheme

In the previous section patterns have been shown to exist in the chain of a straight-line segment. By taking such patterns into account it is now possible further to improve the efficiency of the standard chain code. The new encoding scheme proposed here is essentially a modification of the standard chain code.

The code we propose consists of two different formats, one for the case of straight line segments of Class III and one for the cases of segments of Class I or II.

In the first case, the code begins with a zero followed by a bit specifying whether the segment belongs to the lower part of the octant (0) or not (1). The following three bits specify the octant. Then a number related to the binary value of h-1 is stored. The odd bits of such a number are the corresponding bits of h-1 and the even bits are all zeros except for the one in position two which is a one, and which indicates that the last bit of h-1 is the one following it. For example if h-1 is $5|_{10} = 101|_{2}$ the number to be stored is 01 00 11. Finally the code is completed by what can be referred to as the structure of the chain followed by two bits equal to zero which indicate the end of the code. The structure of the chain is a sequence of strings of zeros separated by ones. Empty strings of zeros are used to encode the information regarding the first, the last and those sequences in C whose length is h-1. Strings containing a single zero are used to encode the information regarding those sequences in C whose length is h. Since no two adjacent zeros appear in this structure of the chain, a code consisting of two zeros can be used to terminate it.

The number of bits required by the proposed code with the presented format is

$$B_{mc_o} = 1+1+3+2[\lfloor \log_2(h-1) \rfloor +1] +b+n_h+2 = 9+2\lfloor \log_2(h-1) \rfloor +a-b(h-1) \qquad (3.18)$$

If the data had been stored by using the standard chain code, then the number of the required bits would have been $B_c = 3a$. Then we have the following:

$$B_c-B_{mc_o} = 3a-9-2\lfloor \log_2(h-1) \rfloor -a+b(h-1) = 2a-9-2\lfloor \log_2(h-1) \rfloor +b(h-1)$$

Since $y = \frac{x}{2} - \log_2 x > 0$ for all $x > 1$, then $x > 2\log_2 x > 2\lfloor \log_2 x \rfloor$ and therefore

$$B_c - B_{mc_o} > 2a-9-(h-1) + b(h-1) = 2a-9+(b-1)(h-1) \tag{3.19}$$

which is always positive for $a \geq 5$, since $b > 0$ and $h > 2$, and which grows linearly with a (see Table I, Chapter II, for relations between precision and segment length).

For example the chain C=4434443444344 which requires 39 bits when the standard chain code is used, will require only 16 bits when the proposed code is used. In fact since $a = 13$, $b = 3$ then $h = 4$, $h - 1 = 3$ and the new code is

0 0 000 01 11 1 0 1 0 1 00

The proposed code requires 23 bits less than those required by the chain code, in this case, and this is a saving which falls short of 60%.

In the case of straight line segments of Class I or II a different format is used. Such format is identified because its first bit is set to one. Then a five bit number identifies the particular case, to which the chain corresponds, among the 32 possible cases; for example

Case 1: $a = 0$, $b > 0$

Case 2: $b = \left\lfloor \frac{a-1}{2} \right\rfloor$, $a > 0$ and a odd

Case 3: $b = \frac{a}{2}$, $a > 0$ and a even

Case 4 $b = \left\lfloor \frac{a+1}{2} \right\rfloor$, $a > 0$ and a odd

Case 5: $b = a > 0$, etc.

Then a number related to the binary value of the length N of the chain is stored. The bits in odd position of this number are the bits of N and the bits in even position are all set to zero except for the one in position two which is set to one and which indicates that the last bit of N is the one following it. For example if $N = 5)_{10} = 101)_2$ it will be encoded as 01 00 11.

The number of bits required by this format of the proposed code is

$$B_{mc_1} = 1+5+2[\lfloor \log_2 N \rfloor +1] = 8+2\lfloor \log_2 N \rfloor \qquad (3.20)$$

The number of bits required by the chain code is

$$B_c = 3N$$

and therefore

$$B_c - B_{mc_1} = 3N-8-2\lfloor \log_2 N \rfloor > 3N-8-N = 2(N-4) \qquad (3.21)$$

which is always positive for $N \geq 5$ (as for the case of previous format) and grows linearly with N (see Table I, Chapter II, for relations between precision and segment length).

For example the chain C = 3434343434343 which requires 39 bits when the standard chain code is used will require only 14 bits when the proposed encoding method is used. In fact since $N = 13)_{10} = 1101)_2$ the new code is

1 0 1 1 0 1 0 1 0 1 0 0 1 1

The proposed code requires then 25 bits less than those required by the chain code, in this case, and this is a saving which is a little above 60%.

Let us note at this point that an efficient code not only has to satisfy the requirement of having the shortest length but it also has to be such to ease the processing of the data. Often the two requirements generate conflicting requests and, therefore, the problem becomes the one of finding an optimal solution.

For example, if the incremental coordinates a,b are the elements of th selected coding scheme, and they are encoded similarly to h-1 in the first format of the proposed code, then the length of the code is given by

$$B_{mc_o} = 2(\lfloor \log_2 a \rfloor + 1) + 2(\lfloor \log_2 b \rfloor + 1) = 2\lfloor \log_2 a \rfloor + 2\lfloor \log_2 b \rfloor + 4 \qquad (3.22)$$

However, if the inverse of the slope of the segment is used together with its related b value and they are encoded similarly to h-1 in the first format of the proposed code, then the length of this code will be given by

$$B_s = 2(\lfloor \log_2 \frac{a}{b} \rfloor + 1) + 2(\lfloor \log_2 b \rfloor + 1) \geq 2\lfloor \log_2 a \rfloor + 2 \qquad (3.23)$$

This last code is probably the shortest, however it does not make it possible to transform the data easily as the chain-structure code proposed here. First of all the actual chain will have to be generated every time the data has to be displayed, and if it is required to rotate the segment from an octant to the next, complicated operations will be involved. If the encoding scheme proposed here is used, then the last problem can be solved by simply changing the first part of the code by applying chain substitution techniques. The same ease of data transforming results in the case in which it is necessary to scale isotropically by an integer factor. In fact, the octant and the value for h-1 are not affected by such a transformation. In both the latter cases the use of the proposed code allows one to simplify the further processing of the data. The proposed code is illustrated in Fig. 16.

## 3.12 Concluding Remarks

An analysis has been presented of patterns in chain-encoded straight line segments. The classification of segments and the properties of their chains have been discussed. The problem of computing the chain of a given

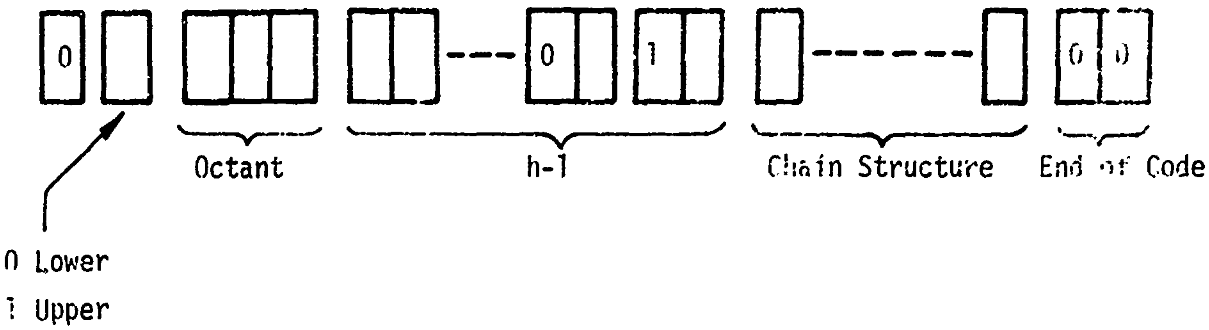


a) First Format (Class III Segments)

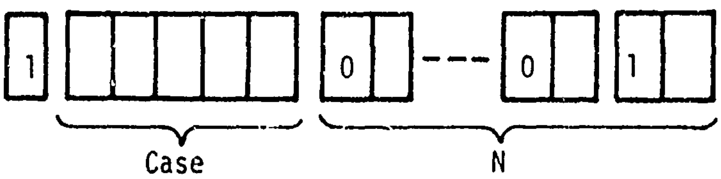


0 $b = 0, \quad a > 0$

1 $b = \left\lfloor \frac{a-1}{2} \right\rfloor, \; a > 0, \quad a \text{ odd}$

.

.

.

31 $-b = \left\lfloor \frac{|a|-1}{2} \right\rfloor, \quad a < 0, \; a \text{ odd}$

b) Second Format (Class I or II Segments)

FIG. 16

PROPOSED CODE

segment has been shown to be equivalent to a simpler one in which the segment is of Class III and belongs to the first half of the first octant. Chain patterns have been found for such segments together with their invariance with respect to translations of the segment in the plane. Special considerations have been dedicated to the case of ambiguous chainlets and their area properties. Moreover an algorithm has been described for the fast generation of the chain of a straight line segment and its efficiency compared with that of a well-known algorithm. Finally a new encoding scheme has been proposed which takes advantage of the so-found patterns for improving the efficiency of the standard chain code. Although for the case of short segments other codes may offer comparable or even better efficiencies, an indication has been given of the advantage of the proposed code for simplifying the further processing of the data whenever such processing is a quantized rotation or an isotropic scaling.

# IV. TRANSFORMATIONS

In this chapter regular transformations (Definition 20, page 60) are considered. It will be shown that any regular transformation can be approximated by a sequence of elementary transformations such as rotations and scalings with any required precision. Relations among transformations and properties of certain transformations will be investigated. The purpose of this chapter is to show that the problem of transforming a quantized drawing is no more complicated than the one of rotating it or of subjecting it to a constant non-isotropic scaling.

In the following chapter the quality of a quantized line drawing is defined in terms of a set of figures of noise. In a later chapter the results of this chapter applied to the so-defined figures of noise will lead to the discovery of the relations between the bounds on the noise figures before and after a transformation. Such relations will constitute a design formula for the precision parameter n which controls the proposed quantization scheme. It will be possible to find with which precision n one must quantize an input irregular line drawing so that, after a given transformation has been applied to it, the quality of its description is still satisfactory in some sense (i.e. the transformed figures of noise do not exceed the prefixed bound).

## 4.1 General Considerations

The kinds of transformations considered here are those that map the points of the plane into themselves. Let us denote with x and y the coordinates of a point with respect to a given frame of reference, and let us denote with u and v the coordinates of the point of the plane corresponding to the one with coordinates x and y through the given transformation M. Then we can write, in general, that $u = f(x,y)$ and $v = g(x,y)$. In the following $M=M(f,g)$ will denote such transformations.

Let us note that something can be said about f and g since the transformations which one might want to apply to irregular line drawings belong to the class of smooth functions and certainly do not include Dirac or Weistrass functions.

<u>Definition 20</u>: A <u>regular</u> transformation $M_r(f,g)$ is one for which f and g are single valued functions whose first partial derivatives exist and are continuous.

Let us note that a regular transformation can be expressed in the following local form:

$$du = f_x dx + f_y dy \tag{4.1}$$

and

$$dv = g_x dx + g_y dy \tag{4.2}$$

where $f_z$ denotes the first partial derivative of f with respect to z . It is now possible to separate regular transformations into three classes.

<u>Definition 21</u>: A regular transformation is of Class I or <u>elementary</u> if $f_x$, $f_y$, $g_x$, $g_y$ are constant and either $f_y = g_x = 0$ and $f_x \neq g_y$ (non-isotropic scaling, $S_{f_x,g_y}$) or $f_y = g_x = 0$ and $f_x = g_y$ (isotropic scaling, $S_{f_x}$) or $f_x^2 + f_y^2 = 1$, $-1 \leq f_x \leq 1$, $g_y = f_x$, $g_x = -f_y$ (rotation, $R_\lambda$ , $\lambda = \cos^{-1} f_x$).

Definition 22: A regular transformation is of Class II or composite, if $f_x$, $f_y$, $g_x$, $g_y$ are constant and the transformation is not of Class I.

Definition 23: A regular transformation is of Class III or general if it is neither Class I nor Class II.

As will be shown in the following paragraphs, a composite transformation can be reduced to a composition of elementary transformations. It will also be shown that a general transformation can be approximated with any required precision by a set of composite transformations and, therefore, by a set of compositions of elementary transformations. Let us also note that non-linear transformations are always of Class III and that linear transformations are either of Class I or Class II.

## 4.2 Approximation of General Transformations

Statement: It is always possible to find a set of composite transformations which will approximate a general transformation with the required precision[37].

Comment: Since the given transformation is regular, it can be expressed in local form. If the infinitesimal dx and dy are replaced by the finite $\Delta x$ and $\Delta y$, then the percentage errors due to the application of the local form of the transformation are:

$$\varepsilon_u = \frac{f(x + \Delta x, y + \Delta y) - f(x,y) - f_x \Delta x - f_y \Delta y}{f(x + \Delta x, y + \Delta y)} \tag{4.3}$$

$$\varepsilon_v = \frac{g(x + \Delta x, y + \Delta y) - g(x,y) - g_x \Delta x - g_y \Delta y}{g(x + \Delta x, y + \Delta y)} \tag{4.4}$$

Then if a bound is required on such errors (required precision) the maximum values for $\Delta x$ and $\Delta y$ can be computed from previous formulas. The quadruplet x, y, $\Delta x$, $\Delta y$ specifies a region of the plane within which the given general transformation can be approximated with the required precision. In fact, as $\Delta x$ and $\Delta y$ tend to zero the associated error tends to zero since a general transformation is regular. In general, it can be said that it is possible to decompose the finite region over which the general transformation is defined (an irregular line drawing is finite in extension) into a set of smaller regions within which the general transformation is approximated with the required precision by a single composite transformation.

The foregoing demonstrates the importance of studying composite transformations. Since a transformation of Class II or Class I is characterized by constant values for $f_x$, $f_y$, $g_x$, $g_y$ the local form of the transformation can be rewritten as follows:

$$u = f_x\, x + f_y\, y \tag{4.5}$$

$$v = g_x\, x + g_y\, y \tag{4.6}$$

or, in matrix notation, as $w' = A\, w$ where $w' = \begin{vmatrix} u \\ v \end{vmatrix}$ , $w = \begin{vmatrix} x \\ y \end{vmatrix}$

and $A = \begin{vmatrix} f_x & f_y \\ g_x & g_y \end{vmatrix}$

In order to simplify the following formulas, the following notation will be used from now on. A Class II transformation will be represented by:

$$L_{a,b,c,d} = \begin{vmatrix} a & b \\ c & d \end{vmatrix}$$

Rotations by an angle $\lambda$ with respect to the center of the reference frame will be denoted by $R_\lambda$. Isotropic scalings by a factor $\alpha$, $S_\alpha$, and non-isotropic scalings by factors $\alpha$ and $\beta$, $S_{\alpha,\beta}$ are given by

$$R_\lambda = \begin{vmatrix} \cos\lambda & -\sin\lambda \\ \sin\lambda & \cos\lambda \end{vmatrix} , \quad S_\alpha = \begin{vmatrix} \alpha & 0 \\ 0 & \alpha \end{vmatrix} , \quad S_{\alpha,\beta} = \begin{vmatrix} \alpha & 0 \\ 0 & \beta \end{vmatrix}$$

4.3 <u>Relations Among Linear Transformations</u>

In this paragraph some interesting relations among linear transformations are shown. Their importance will become clearer later when the problem of decomposing a Class II transformation will be studied. The following relations offer an insight into the transformation problem because they show that in general, the ordering of a composition of transformations (i.e. ordering with which many transformations are applied one after the other ) cannot be disregarded.

<u>Lemma:</u> $$R_{\lambda_1} R_{\lambda_2} = R_{\lambda_2} R_{\lambda_1} \tag{4.7}$$

<u>Comment:</u> It is sufficient to note that since $R_{\lambda_1} R_{\lambda_2} = R_{\lambda_1 + \lambda_2}$ then $R_{\lambda_2} R_{\lambda_1} = R_{\lambda_2 + \lambda_1} = R_{\lambda_1} R_{\lambda_2}$

<u>Lemma:</u> $$S_{\alpha,\beta} S_{\gamma,\delta} = S_{\gamma,\delta} S_{\alpha,\beta} \tag{4.8}$$

<u>Comment:</u> It is sufficient to note that since $S_{\alpha,\beta} S_{\gamma,\beta} = S_{\alpha\gamma,\delta\beta}$ then $S_{\gamma,\delta} S_{\alpha,\beta} = S_{\alpha,\beta} S_{\gamma,\delta}$

<u>Lemma:</u> $$R_\lambda S_\alpha = S_\alpha R_\lambda \tag{4.9}$$

<u>Comment</u>: It is sufficient to note that $S_\alpha = \alpha \begin{vmatrix} 1 & 0 \\ 0 & 1 \end{vmatrix} = \alpha I$

Then $R_\lambda S_\alpha = R_\lambda \alpha I = \alpha R_\lambda I = \alpha R_\lambda = \alpha I R_\lambda = S_\alpha R_\lambda$

<u>Lemma</u>: $$S_{\alpha,\beta} = S_\alpha S_{1,\beta/\alpha} = S_\beta S_{\alpha/\beta,1} \tag{4.10}$$

<u>Comment</u>:

$$S_{\alpha,\beta} = \begin{vmatrix} \alpha & 0 \\ 0 & \beta \end{vmatrix} = \alpha \begin{vmatrix} 1 & 0 \\ 0 & \beta/\alpha \end{vmatrix} = \alpha I \begin{vmatrix} 1 & 0 \\ 0 & \beta/\alpha \end{vmatrix} = S_\alpha S_{1,\beta/\alpha}$$

$$S_{\alpha,\beta} = \begin{vmatrix} \alpha & 0 \\ 0 & \beta \end{vmatrix} = \beta \begin{vmatrix} \alpha/\beta & 0 \\ 0 & 1 \end{vmatrix} = \beta I \begin{vmatrix} \alpha/\beta & 0 \\ 0 & 1 \end{vmatrix} = S_\beta S_{\alpha/\beta,1}$$

Lemma: $$R_\lambda S_{\alpha,\beta} \neq S_{\alpha,\beta} R_\lambda \;,\quad \alpha \neq \beta \;,\quad \lambda \neq 0 \tag{4.11}$$

<u>Comment</u>: It is sufficient to note that

$$R_\lambda S_{\alpha,\beta} = \begin{vmatrix} \alpha \cos \lambda & -\beta \sin \lambda \\ \alpha \sin \lambda & \beta \cos \lambda \end{vmatrix} = \begin{vmatrix} \alpha \cos \lambda & -\alpha \sin \lambda \\ \beta \sin \lambda & \beta \cos \lambda \end{vmatrix} = S_{\alpha,\beta} R_\lambda$$

if either $\alpha = \beta$ or $\lambda = 0$ , but these cases are to be excluded because either $\lambda$ is not positive or $\alpha$ is not different from $\beta$. An intuitive explanation of the apparently strange result of this lemma is offered by Fig. 17. There a rotation with $\lambda = 45^\circ$ followed by a non-isotropic scaling with factors 2 and 1 is applied to a square, which is, therefore, transformed into a rhombus. When the scaling is applied before the rotation the result is a rotated rectangle.

## 4.4 <u>Standard Deccmpositon of Class II Transformations</u>

Let us note that given a Class II transformation L, it is not possible in general, to represent it in one of the following ways:

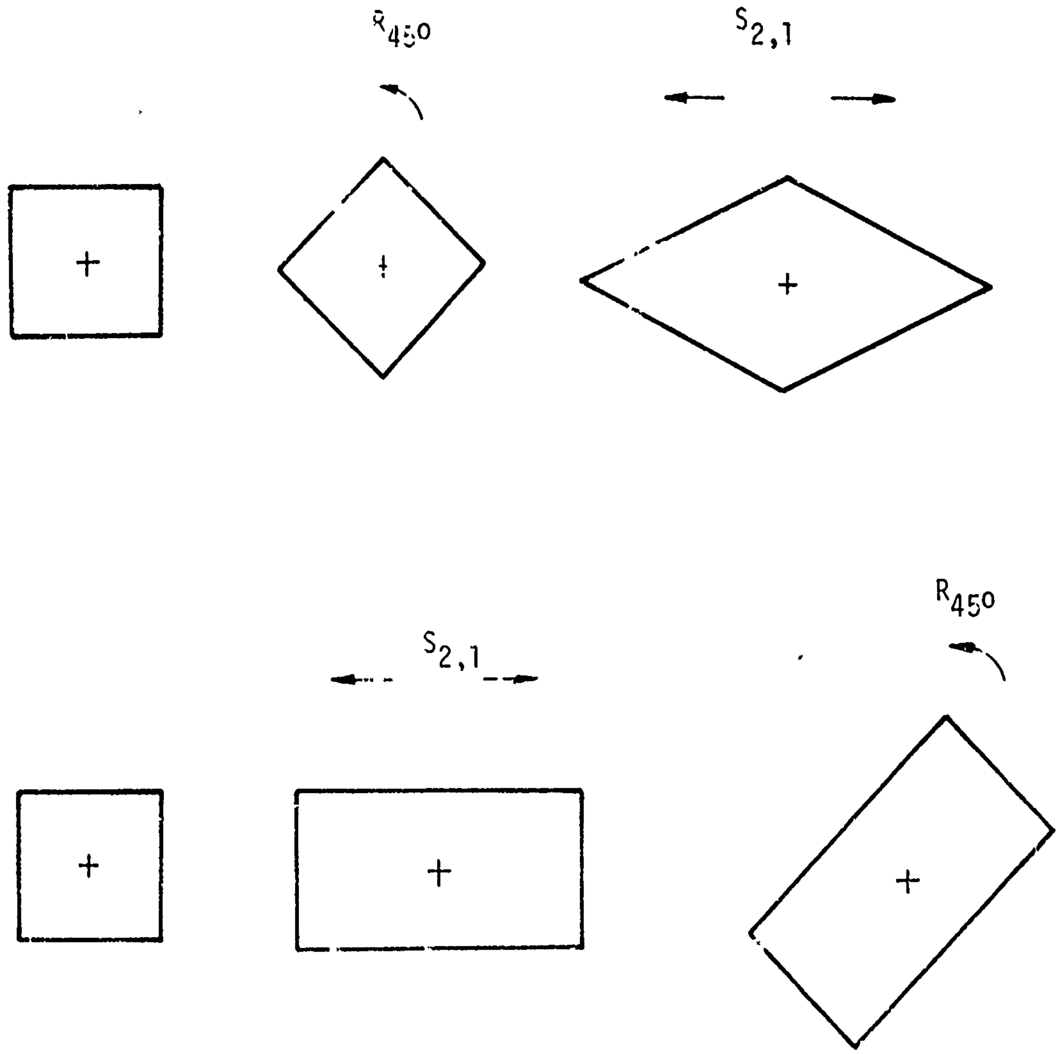


FIG 1/

NON-COMMUTATIVITY OF TRANSFORMATIONS

1) $L_{a,b,c,d} = R_\lambda \, S_{\alpha,\beta}$

2) $L_{a,b,c,d} = S_{\alpha,\beta} \, R_\lambda$

3) $L_{a,b,c,d} = S_{\gamma,\delta} \, R_\lambda \, S_{\alpha,\beta}$

In fact, L is given in terms of four numbers whereas $R_\lambda \, S_{\alpha,\beta}$ and $S_{\alpha,\beta} \, R_\lambda$ are completely specified by three numbers. It is possible to show that if the four numbers specifying L, a,b,c,d are such that ab + cd = 0 then $L_{a,b,c,d} = R_\lambda \, S_{\alpha,\beta}$ and if they are such that ac + bd = 0, then $L_{a,b,c,d} = S_{\alpha,\beta} \, R_\lambda$. $L_{a,b,c,d} \neq S_{\gamma,\delta} \, R_\lambda \, S_{\alpha,\beta}$ because $S_{\gamma,\delta} \, R_\lambda \, S_{\alpha,\beta}$ is a function of five numbers.

THEOREM 8:

$$L_{a,b,c,d} = R_\delta \, S_{\alpha,\beta} R_\lambda \tag{4.12}$$

where, denoting with a,b,c,d the elements of L, we have the following

$$\left\{ \begin{aligned} n_1 &= \frac{a+d}{2} \\ n_2 &= \frac{d-a}{2} \\ n_3 &= \frac{b+c}{2} \\ n_4 &= \frac{c-b}{2} \end{aligned} \right. \qquad \left\{ \begin{aligned} \alpha &= \mp \left(\sqrt{n_2^2+n_3^2} \mp \sqrt{n_1^2+n_4^2}\right) \\ \beta &= \pm \left(\sqrt{n_2^2+n_3^2} \pm \sqrt{n_1^2+n_4^2}\right) \\ \lambda &= \frac{1}{2}\left(\tan^{-1}\frac{n_4}{n_1} + \tan^{-1}\frac{n_3}{n_2}\right) \\ \delta &= \frac{1}{2}\left(\tan^{-1}\frac{n_4}{n_1} - \tan^{-1}\frac{n_3}{n_2}\right) \end{aligned} \right. \tag{4.13}$$

<u>Proof</u>: Let us note that

$$R_\delta \, S_{\alpha,\beta} \, R_\lambda = \begin{bmatrix} \cos\delta & -\sin\delta \\ \sin\delta & \cos\delta \end{bmatrix} \begin{bmatrix} \alpha & 0 \\ 0 & \beta \end{bmatrix} \begin{bmatrix} \cos\chi & -\sin\lambda \\ \sin\lambda & \cos\lambda \end{bmatrix} = L_{a,b,c,d} \begin{bmatrix} a & b \\ c & d \end{bmatrix}$$

and therefore

$$\begin{cases} \alpha \cos\delta \cos\lambda - \beta \sin\delta \sin\lambda = a \\ -\alpha \cos\delta \sin\lambda - \beta \sin\delta \cos\lambda = b \\ \alpha \cos\lambda \sin\delta + \beta \cos\delta \sin\lambda = c \\ -\alpha \sin\delta \sin\lambda + \beta \cos\delta \cos\lambda = d \end{cases}$$

or

$$\begin{cases} (\beta-\alpha) \cos\lambda \cos\delta + (\beta-\alpha) \sin\lambda \sin\delta = (\beta-\alpha) \cos(\lambda-\delta) = d - a \\ (\beta-\alpha) \cos\delta \sin\lambda - (\beta-\alpha) \sin\delta \cos\lambda = (\beta-\alpha) \sin(\lambda-\delta) = c + b \\ (\beta+\alpha) \cos\lambda \cos\delta - (\beta+\alpha) \sin\lambda \sin\delta = (\beta+\alpha) \cos(\lambda+\delta) = d + a \\ (\beta+\alpha) \cos\delta \sin\lambda + (\beta+\alpha) \sin\delta \cos\lambda = (\beta+\alpha) \sin(\lambda+\delta) = c - b \end{cases}$$

or

$$\begin{cases} (\beta-\alpha)^2 = (c+b)^2 + (d-a)^2 \\ (\beta+\alpha)^2 = (a+d)^2 + (c-b)^2 \\ \tan(\lambda-\delta) = \dfrac{c + b}{d - a} \\ \tan(\lambda+\delta) = \dfrac{c - b}{d + a} \end{cases}$$

Then

$$\begin{cases} \lambda = \frac{1}{2}\left(\tan^{-1} \dfrac{c + b}{d - a} + \tan^{-1} \dfrac{c - b}{d + a}\right) \\ \delta = \frac{1}{2}\left(\tan^{-1} \dfrac{c - b}{d + a} - \tan^{-1} \dfrac{c + b}{d - a}\right) \end{cases}$$

and for $\alpha$ and $\beta$ we have

$$\begin{cases} \alpha^2 + \beta^2 = a^2 + b^2 + c^2 + d^2 \\ \alpha \beta = d a - b c \end{cases}$$

Letting $n^2 = a^2 + b^2 + c^2 + d^2$ and $m = da - bc$

The solution is given by $\quad \beta^2 + \dfrac{m^2}{\beta^2} = n^2 \quad$ or $\quad \beta^4 - n^2\beta^2 + m^2 = 0$

and therefore $\beta^2 = \dfrac{n^2 \pm \sqrt{n^4 - 4m^2}}{2}$ and $\beta = \pm \sqrt{\dfrac{n^2 \pm \sqrt{n4 - 4m^2}}{2}}$ .

It can be shown that the following identity is true

$$a \pm \sqrt{b} = \sqrt{\frac{a - \sqrt{a^2 - b}}{2}} \pm \sqrt{\frac{a + \sqrt{a^2 - b}}{2}}$$

Applying the identity to the above expression for $\beta$ , we have:

$$\beta = \pm \frac{1}{\sqrt{2}} \left( \sqrt{\frac{n^2 - \sqrt{n^4 - n^4 + 4m^2}}{2}} \pm \sqrt{\frac{n^2 + \sqrt{n^4 - n^4 + 4m^2}}{2}} \right) =$$

$$\pm \frac{1}{2} \left( \sqrt{n^2 - 2m} \pm \sqrt{n^2 + 2m} \right) =$$

$$\pm \frac{1}{2} \left( \sqrt{(a-d)^2 + (b+c)^2} \pm \sqrt{(a+d)^2 + (b-c)^2} \right.$$

In the case of $\alpha$ we have $\dfrac{m^2}{\alpha^2} + \alpha^2 = n^2$ or $\alpha^4 - n^2\alpha^2 + m^2 = 0$ which leads to a solution analogous to the one found for $\beta$. We have

$$\alpha = \mp \frac{1}{2} \left( \sqrt{(a-d)^2 + (b+c)^2} \mp \sqrt{(a+d)^2 + (c-b)^2} \right) \qquad \text{QED}$$

Let us note that since a general transformation can be approximated with any required precision by a set of composite transformations, then as a consequence of the previous theorem it can be approximated by a set of sequences of elementary transformations.

The importance of having reduced all possible transformations to sets of sequences of elementary transformations will become clearer later when these results will be applied to study the quality of the quantized version of an irregular line drawing after a transformation. This quality will be expressed in terms of a set of figures of noise in the next chapter. In particular, for all the figures of noise which are invariant with respect to rotation and which get worse with scalings proportionally to the largest of the scale factors, the effect of a non-isotropic scaling $S_{\alpha,\beta}$ or of the linear transformation $L_{a,b,c,d} = R_\delta S_{\alpha,\beta} R_\lambda$ or of the non-linear transformation defined by the set $\{R_\delta S_{\gamma,\sigma} R_\lambda\}$ with $\gamma \leq \alpha$ and $\delta \leq \beta$, will be the same.

Since a Class III transformation of particular interest is the Mercator Projection, it will be presented briefly in the next paragraph. It will serve as an example of how to simplify a transformation problem by taking into account the peculiar characteristics of a Class III transformation of known structure.

### 4.5 Mercator Projections

One of the possible applications for the procedures developed here is that of automatically generating geographic maps from preprocessed satellite pictures.

Consider a picture that has been taken from a satellite orbiting the Earth and which has been preprocessed to abstract irregular line drawings from it (continental coastlines). Then the quantization scheme proposed here could be used for quantizing the irregular line drawings, and this will lead to a set of P-structures. Using a digital computer it would then be possible to simulate the projections of these P-structures onto a sphere from a point of projection specified by the position of the satellite relative to the Earth at the time when the picture was taken. Then by applying to the resulting data the required georgraphic transformation (a Mercator Projection, for instance, or, in any case, a Class III transformation) the new data could be obtained and displayed by using a digital plotter.

The input to the digital computer can be obtained by means of a flying spot scanning device from the actual satellite picture, and the output will be a geographic map drawn by a digital plotter.

Among the many types of maps which are of interest, those referred to as Mercator Maps are worth particular consideration. In the following the specific reasons which make Mercator Maps so interesting are given, together with the equations necessary for a clear understanding of the Mercator transformation. Then a proposed method for computing the Mercator Projection of a set of arcs of a circle given on a sphere is presented (the projection on a sphere of a P-structure is a set of arcs of a circle)[18,36].

Definition 24: A Lossodromia (Greek work for curve with constant angle) is a curve on a spherical surface making a constant angle with each intersecting meridian.

Definition 25: A Mercator Projection is a Class III transformation which maps a lossodromia, defined on a given sphere, into a straight line, defined on a given plane.

In order to find the analytical expressions governing a Mercator transformation, the following steps can be followed. First the unit vector tangent to a lossodromia is computed, and then the elementary arc of a lossodromia and the polar coordinate equation of a lossodromia passing through a given point on a sphere are found. This makes it possible to show that meridians are mapped into vertical straight lines that are uniformly spaced in the plane, and that parallels are mapped into horizontal straight lines whose spacing in the plane is symmetrical with respect to a horizontal straight line (the equator) and non-linearly spaced. Any lossodromia can then be plotted by connecting with a straight line the two points of the plane corresponding in the Mercator Projection to the extreme points of a lossodromia on the sphere. The symbols usually used in the literature for representing points in the spherical coordinates are indicated in Fig. 18. The following is to be noted:

1) The unit vector tangent in P to the local meridian and oriented towards the north pole is

$$\vec{t}_1 = -\sin\phi_1 \cos\lambda_1 \vec{i} - \sin\phi_1 \sin\lambda_1 \vec{j} + \cos\phi_1 \vec{k} \tag{4.14}$$

2) The normal at P to the surface of the sphere is:

$$\vec{n}_1 = \cos\phi_1 \cos\lambda_1 \vec{i} + \cos\phi_1 \sin\lambda_1 \vec{j} + \sin\phi_1 \vec{k} \tag{4.15}$$

3) The unit vector at P to the local parallel and oriented towards east is given by:

$$\vec{b}_1 = \sin\lambda_1 \vec{i} - \cos\lambda_1 \vec{j} \tag{4.16}$$

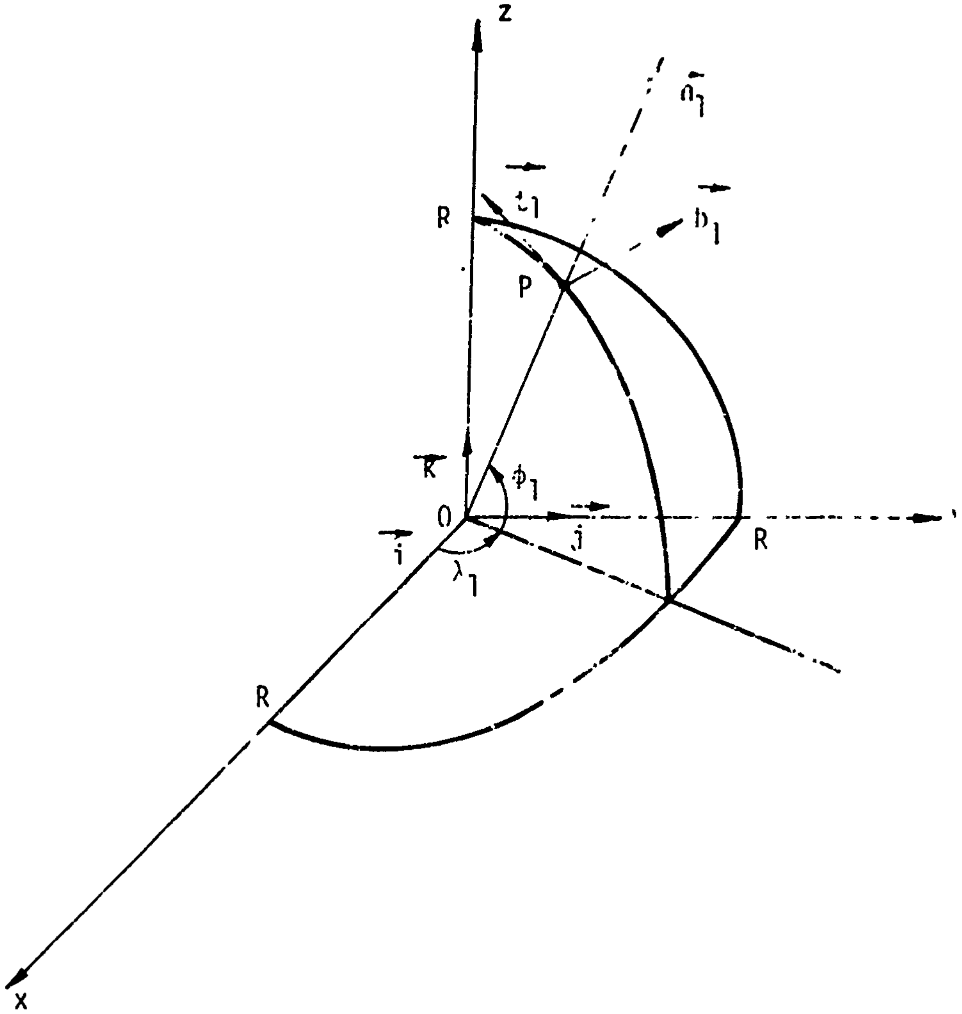


FIG. 18

SPHERICAL REFERENCE FRAME

4) The unit vector tangent to a lossodromia characterized by a constant angle $\bar{\gamma}$ is given by:

$$\vec{\ell}_1 = \cos\bar{\gamma}\,\vec{t}_1 + \sin\bar{\gamma}\vec{b}_1 = \cos\alpha_\ell\vec{i} + \cos\beta_\ell\vec{j} + \cos\gamma_\ell\vec{k} \tag{4.17}$$

where

$$\cos\alpha_\ell = \sin\bar{\gamma}\,\sin\lambda_1 - \cos\bar{\gamma}\,\cos\lambda_1\,\sin\phi_1$$

$$\cos\beta_\ell = -\sin\bar{\gamma}\,\cos\lambda_1 - \cos\bar{\gamma}\,\cos\lambda_1\,\sin\phi_1$$

$$\cos\gamma_\ell = \cos\bar{\gamma}\,\cos\phi_1$$

5) An arc of a lossodromia is given in vector notation by:

$$ds\,\vec{\ell}_1 = dx\,\vec{i} + dy\,\vec{j} + dz\,\vec{k} \tag{4.18}$$

where $dx = ds\cos\alpha_\ell$, $dy = ds\cos\beta_\ell$, $dz = ds\cos\gamma_\ell$

6) The equation of a lossodomia in spherical coordinates is, in local form:

$$\frac{d\phi}{d\lambda} = -\frac{\cos\phi}{\tan\bar{\gamma}} \tag{4.19}$$

7) The equation of a lossodromia passing through a point with spherical coordinates $\lambda_1$ and $\phi_1$ and with constant angle $\bar{\gamma}$

$$\frac{\lambda - \lambda_1}{\tan\bar{\gamma}} = \ell n[\tan\tfrac{1}{2}(\tfrac{\pi}{2} - \phi) / \tan\tfrac{1}{2}(\tfrac{\pi}{2} - \phi_1)] \tag{4.20}$$

8) A Mercator Projection is a Class III transformation defined by the following analytical expressions:

$$x = \lambda,\ y = f(\phi) = \ell n\tan\tfrac{1}{2}(\tfrac{\pi}{2} - \phi) \tag{4.21.}$$

where x and y are the cartesian coordinates of a point in the Mercator plane and $\lambda$ and $\phi$ are the spherical coordinates of the corresponding point on the sphere.

As was mentioned before, in the Mercator plane meridians are represented by vertical, uniformly spaced, straight lines and parallels are represented by horizontal non-uniformly spaced straight lines. The points on the map corresponding to the poles are at infinity in the vertical direction, since $f(\pm \frac{\pi}{2}) = \pm \infty$.

Finally, let us note that in Mercator Projections a single point P with spherical coordinates $(\lambda,\phi)$ is mapped into $\lambda + 2n\pi, f(\phi)$ for all integers n.

By construction any lossodromia corresponds to a straight line in the Mercator plane. The angle characteristic of each lossodromia can then be measured on the map as the one between the straight line corresponding to the given lossodromia and the vertical direction (corresponding to the one of each intersecting meridian). This feature makes the map very useful for navigational purposes when the only available navigational instrumentation consists of a magnetic compass. Fig. 19 shows the basic structure of a Mercator Map as it has been presented here.

For the sake of completeness let us note that since a lossodromia is not an arc of a circle, it does not represent the shortest path between two points on a sphere. A lossodromia is completely specified by three numbers, namely the spherical coordinates of one of its points $(\lambda_1, \phi_1)$ and its characteristic angle $\overline{\gamma}$. The radius of the sphere does not influence

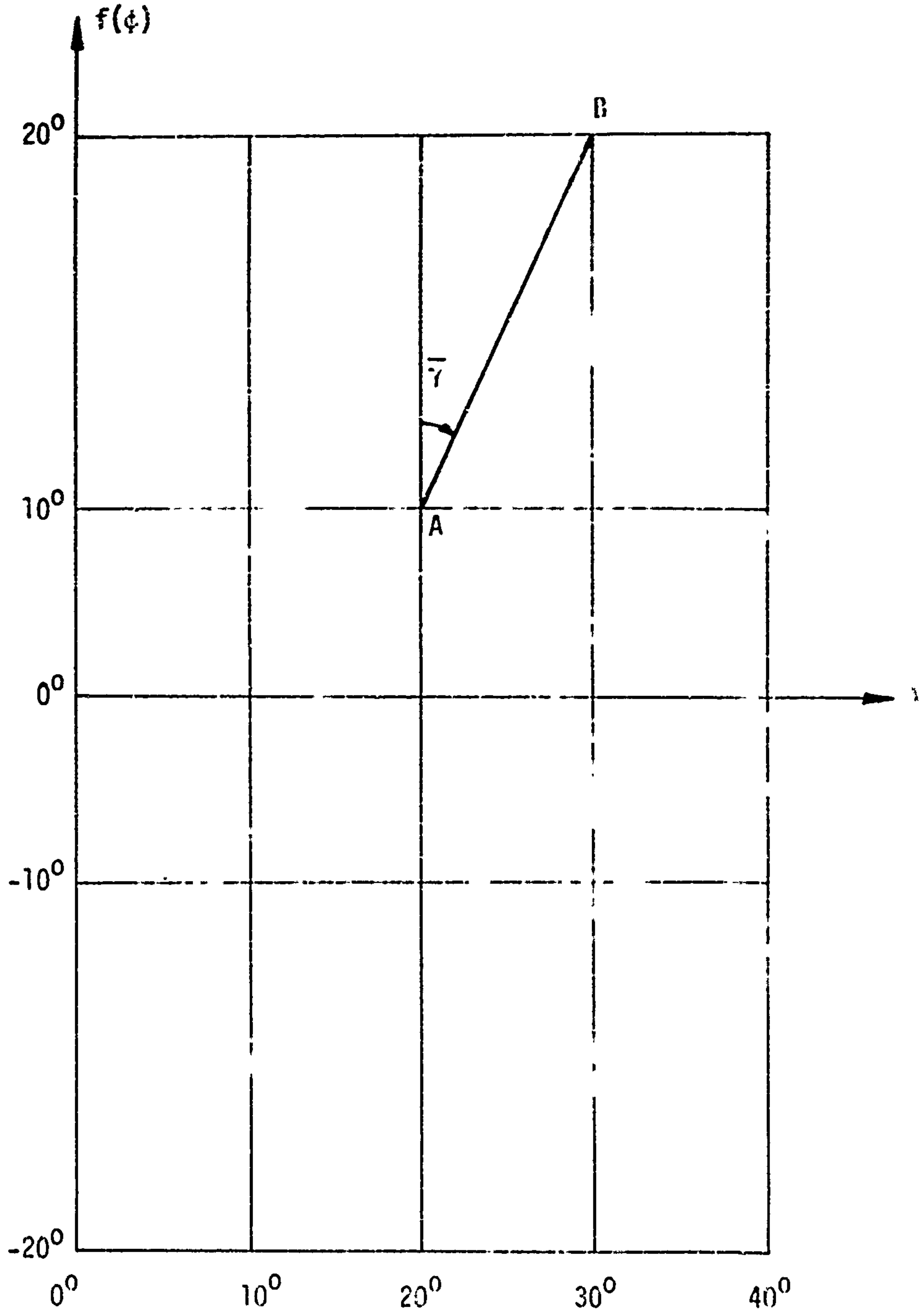


FIG. 19

SCHEMATIC OF MERCATOR MAPS

the lossodromia's equation or position on a Mercator Map but it does effect the length of the path between two points on the same lossodromia. Length can be easily determined, however, by making only one measurement on the map.

Statement: The length of an arc of a lossodomia is given by:

$$\begin{cases} \Delta s = R \cos\phi \, \Delta\lambda & \text{if} \quad \bar{\gamma} = \frac{\pi}{2} \\ \Delta s = \dfrac{R}{\cos\bar{\gamma}} \Delta\phi & \text{otherwise} \end{cases} \tag{4.22}$$

Comment: The proof for the statement involves only routine processing of analytical expressions and is not repeated here.

## 4.6 Mercator Projections of Circular Arcs

A problem of particular interest is the one of Mercator projecting a set of circular arcs defined on a common sphere. Since the required transformation is of Class III, the procedure presented earlier could be applied for reducing the transformation into a set of sequences of elementary transformations.

However, since the Mercator projection has been shown to transform a grid defined on a sphere by uniformly spaced meridians and parallels, into a grid defined on a plane by uniformly distributed vertical lines and non-uniformly distributed horizontal lines, it can be carried out in two steps. First the intersections of the circular arcs with the grid on the sphere are computed and the nodes closer to these intersections selected and connected in a sequence, one after the other, by lossodromias, in a way that is dual of the one with which chain points are selected and connected with straight line segments for the case of grid-intersect quantized straight lines. (Incidentally this approach justifies the use of the chain code for representing a curve on a spherical surface). Let us also note that the precision by which this set of lossodromias approximates the original arcs is a function solely of the elementary size of the grid on the sphere since the features of the given curve (arc of a circle) are already known. Once the arcs of the circles have been approximated by sequences of arcs of lossodomias, each of these lossodromias is mapped into the Mercator plane as a straight line segment. Thus the problem of computing the Mercator projection of a set of circular arcs is reduced to the problem of quantizing with the necessary precision these arcs on a grid defined on the sphere by equally spaced meridians and parallels.

An application of this method, with special attention paid to the achieved precision, will be presented later with a description of a program for automatically obtaining the Mercator Projection.

## 4.7 Concluding Remarks

The transformations which are of interest for applications in computer graphics have been described in terms of a pair of regular functions and subdivided into three Classes. A proof of the decomposability of any regular transformation into a set of sequences of elementary transformations that approximate the given transformation to any required precision has been given. Emphasis has been placed on a special transformation of Class III, involving the mapping of a lossodromia into a Mercator Map. A possible method for Mercator projecting sets of arcs of circles defined on a common sphere has been described to show the usefulness of the scheme.

# V. FIGURES OF NOISE

In this chapter a set of three figures of noise is defined for describing the quality of the proposed quantization scheme. This chapter consists of two main parts.

In the first part of the chapter a detailed description of the figures of noise is given with an explanation of their meaning in the context of the proposed quantization scheme. The relations between the proposed figures of noise and the precision parameter n presented in the second chapter are studied, and some worst-case bounds are derived.

## 5.1 Classical Approach to the Definition of a Figure of Noise

In this paragraph some basic ideas concerning the definition of a figure of noise are presented.

Definition 26: An ideal signal is a deterministic, single-valued function of a variable, called time; the function is continuous together with its derivatives.

Definition 27: Noise is any unwanted signal component.

Definition 28: A real signal is the superposition in time of two components: an ideal signal and noise.

Comment: When signals are transmitted through physical channels, we say that at the input there is an ideal signal, that is, the one which we want to transmit and which we would like to receive at the other end of the channel. However since a physical channel generates by itself spurious signals or receives signals from sources different from the one which is sending the ideal signal, then the signal received at the output of the channel is different from the one transmitted at the input. This unwanted difference is usually random in nature and, therefore, it constitutes the noisy signal component of the real signal received at the output of the transmission channel.

Let us denote with s the ideal signal, with w the noisy signal and with r the real signal. Then it is possible to state that in general r = s+w.

This formula suggests two ways for measuring w:

Method I: By measuring the received signal when no input signal has been sent through the channel. In fact, in this case s = 0 and w = r.

Method II: By measuring the difference between the received signal and the input. In this case

$$w = r-s \tag{5.1}$$

Let us note that since w is random in nature, measures on the function w = w(t) in the interval $0 \leq t \leq T \leq \infty$ are not sufficient for guaranteeing the precision of predictions of the values of w(t) at times outside the interval. However, from a study of the statistical properties of w(t), it is possible to predict the probability of having w(t) above a given threshold at any time t.[33]

Definition 29: The level of a signal is its average power.

Let us note that since s is the signal generated from a physical source it starts at time t = 0 and ends at time $t = T_s$. If the transmission channel is such as to delay a signal by a time $\tau$ , then the levels of s,w and r can be expressed by

$$\ell_s = \frac{1}{T_s} \int_0^{T_s} s^2(t)dt$$

$$\ell_w = \frac{1}{T_s} \int_{\tau}^{T_s+\tau} w^2(t)dt$$

$$\ell_r = \frac{1}{T_s} \int_{\tau}^{T_s+\tau} r^2(t)dt \tag{5.2}$$

A comparison between a real signal and its noisy component can now be made in terms of their levels.

Definition 30: A figure of noise for the real signal $r = s+w$ is the ratio of the levels of the noisy component of the real signal, $\ell_w$, and of the real signal $\ell_r$. Figures of noise will be denoted by $f_w$.

We thus have:

$$f_w = \ell_w/\ell_r \tag{5.3}$$

If the level of noise $\ell_w$ is much smaller than that of the ideal signal contained in r, then $\ell_r \simeq \ell_s$ and $f_w \approx \frac{\ell_w}{\ell_s}$. Then if $f_w \approx 1\%$ it means that the "intensity" of the noise is one hundredth of the one of the signal.

The value of a figure of noise is an indication of the quality of a real signal, or, alternately, of the precision with which a real signal approximates its ideal component.

Finally let us note that because of the way it was defined, a figure of noise must satisfy the following conditions: $f_w > 0$ if $\ell_w \neq 0$ and $f_w = 0$ if and only if $\ell_w = 0$.

## 5.2 Figures of Noise for Quantized Line Drawings

The concepts presented in the previous section can be applied directly to the case of quantized irregular line drawings if the following duality rules are observed:

| Time Domain | Plane Domain |
|---|---|
| Ideal signal s | Irregular line drawing (as a set of features) L |
| Real signal r | Quantized drawings (as a set of quantized features) QL |

| Time Domain | Plane Domain |
|---|---|
| Noisy Signal $w$ | Symbolic difference (as a set of feature differences) $L - QL$ |
| Level of signal $x$ | Level of signal $x$ (as a functional defined |
| $\ell_x$ | on a set of features) $F(x)$ |
| Figure of noise $f_w = \frac{\ell_w}{\ell_r}$ | Figure of noise $f_w = F(L-QL)/F(QL)$ |

Comment: The set of duality rules is probably self-explanatory for the cases of L, QL and the level of signal. In the case of symbolic difference no unique definition can be given. According to the way the difference is defined in each case, a different type of noise will be specified. It is possible and desirable to have this feature of specifying the noise component so that according to the required application, different emphasis can be placed on different disturbing signals.

In the following paragraph three figures of noise oriented towards three different types of applications are defined. The relations between these figures of noise and the precision coefficient n will be given as worst case bounds.

## 5.3 Area-Type Noise

In this paragraph we will associate a set of planar regions with each P-structure of a quantized irregular line drawing. The symbolic difference between L and QL is then the union of all such regions and the functional defining the level of a signal is the area of the region associated with the signal. As is indicated in Fig. 20, the level of noise is $\ell_w = F(L-QL) = \sum_{i=1}^{N} a_i$ where i denotes the i-th segment of a P-structure in QL, $a_i$ is the area defined

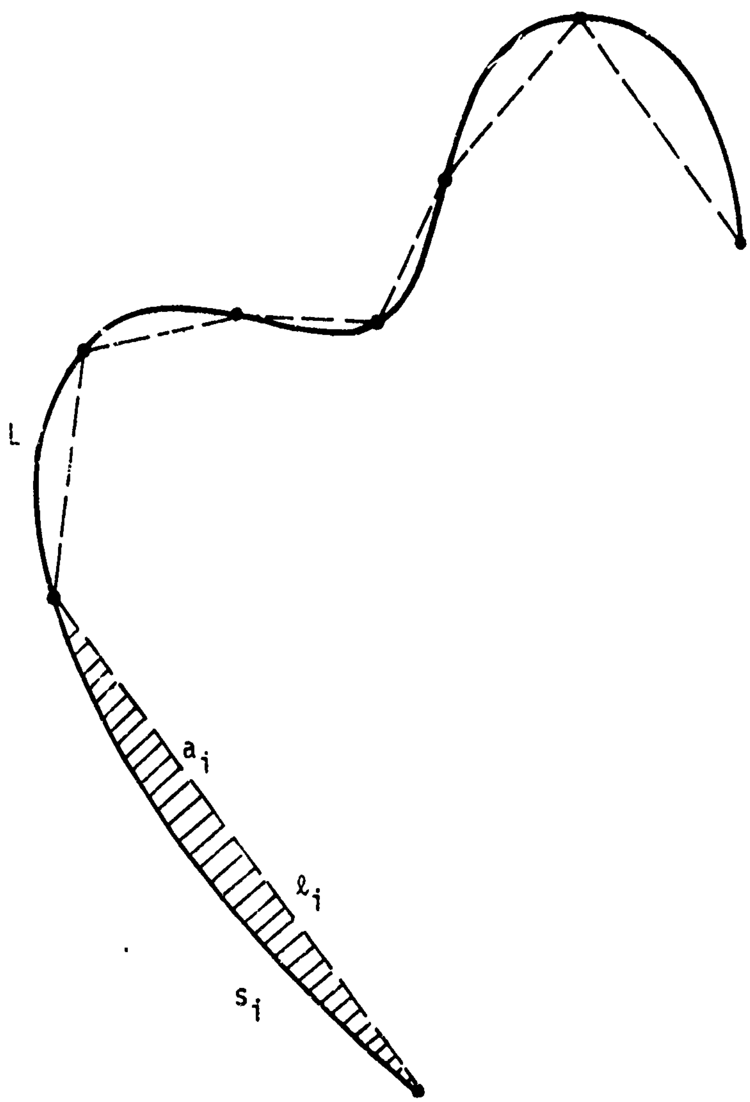


$$\ell(L-QL) = \sum_{i=1}^{N} a_i$$

FIG. 20

by such a segment and L. The level of the signal is $\ell_r = F(QL) = T\sum_{i=1}^{N} \ell_i$ where $\ell_i$ is the length of the i-th segment in QL. The associated figure of noise is then

$$f_{w_a} = \frac{\sum_{i=1}^{N} a_i}{T\sum_{i=1}^{N} \ell_i} \tag{5.4}$$

Let us note that if $\ell_i' = \frac{a_i}{T}$ then

$$f_{w_a} = \frac{\sum_{i=1}^{N} \ell_i'}{\sum_{i=1}^{N} \ell_i} \tag{5.5}$$

which shows that the proposed figure of noise not only has a meaning in evaluating the precision with which QL approximates L ($f_{w_a}$ tends to zero as QL tends to L) but also it gives an indication of the percentage difference between the lengths of L and its quantized version.

The importance of having a figure of noise of the area-type shown here was also stressed in the Proceedings of the Symposium on Map and Chart Digitizing[18] for scientific applications such as those of automatic chart generation from preprocessed satellite pictures.

THEOREM 9: If an irregular line drawing is quantized according to the rules of the quantization scheme proposed here, then $f_{w_a} \leq 1/n$.

Proof: The largest value for $a_i$ can be computed by recalling the rules with which an irregular line drawing is approximated by a set of P-structures.

Letting $x_i = \frac{\delta \bar{i}}{\tan \Delta\alpha_{max}}$ and $\ell_{TOT} = \sum_{i=1}^{N} \ell_i$ (5.6)

and recalling the usual notation in Fig. 21, we have

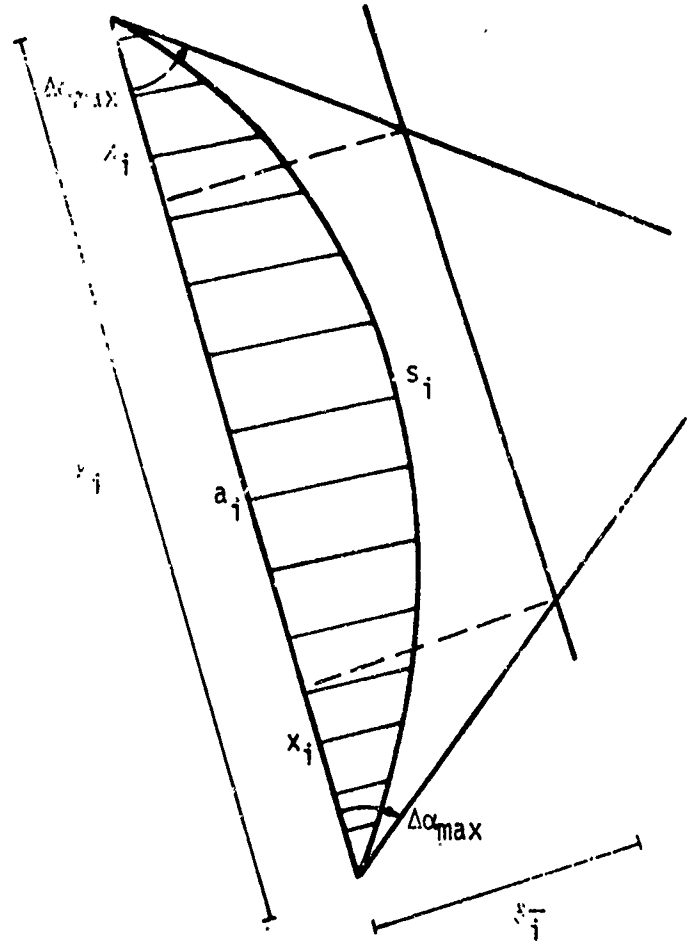


FIG. 21

ARC AND APPROXIMATING CHORD

$$f_{w_a} = \frac{\sum_{i=1}^{N} a_i}{T \sum_{i=1}^{N} \ell_i} < \frac{\sum_{i=1}^{N} \delta_{\bar{i}}(\ell_i - x_i)}{T \sum_{i=1}^{N} \ell_i}$$

$$= \frac{\sum_{i=1}^{N} \delta_{\bar{i}}(\ell_i - \frac{\delta_{\bar{i}}}{\tan \Delta\alpha_{max}})}{T \sum_{i=1}^{N} \ell_i} \leq \frac{k\ell}{T} - \frac{(k\ell)^2}{T} \frac{N}{\tan \Delta\alpha_{max}} \frac{1}{\ell_{TOT}}$$

In the worst case, when all $\delta_{\bar{i}}$ assume their maximum value, we have:

$$f_{w_a} \leq \frac{(\frac{T}{n} \sum_{i=1}^{N} \ell_i - \frac{T^2 N}{n^2 \tan \Delta\alpha_{max}})}{T \sum_{i=1}^{N} \ell_i} = \frac{1}{n} (1 - \frac{TN}{n \tan \Delta\alpha_{max} \ell_{TOT}}) \leq \frac{1}{n}$$

and, therefore,

$$f_{w_a} \leq \frac{1}{n} \qquad (5.7)$$

## 5.4 Displacement-Type Noise

Another type of noise indicator which has been recommended in the Proceedings of the Symposium on Map and Chart Digitizing[18] is the one in which the average distance between a quantized drawing and the original drawing is measured. A figure of noise of this variety will now be proposed and its relation with the precision parameter n investigated.

The symbolic difference L - QL will be interpreted here as being generated by the finite maximum distance between an S-continuous arc and its corresponding segment in the P-structure of the quantized drawing. The level of a signal is then defined as the length of its associated segment. Therefore

$$\ell_w = F(L-QL) = \frac{1}{N} \sum_{i=1}^{N} \delta_i$$

$$\ell_r = F(QL) = T$$

and for the figure of noise we have:

$$f_{w_\ell} = \frac{1}{NT} \sum_{i=1}^{N} \delta_i = \frac{1}{N} \sum_{i=1}^{N} \frac{\delta_i}{T} \tag{5.8}$$

Statement: If an irregular line drawing is quantized according to the rules of the quantization method proposed here, then $f_{w_\ell} \leq \frac{1}{n}$

Comment: It is sufficient to note that in the worst case $\delta_i = \delta_{max} = k\ell$ and therefore

$$f_{w_\ell} = \frac{1}{N} \sum_{i=1}^{N} \frac{\delta_i}{T} \leq \frac{1}{N} \sum_{i=1}^{N} \frac{k\ell}{T} = \frac{1}{N} \sum_{i=1}^{N} \frac{T}{n\ell} \frac{\ell}{T} = \frac{1}{N} \sum_{i=1}^{N} \frac{1}{n} = \frac{1}{n} \tag{5.9}$$

## 5.5 Staircase-Effect-Type Noise

A completely different type of noise is the one which goes under the name of staircase-effect noise. It is due to the fact that the smooth S-continuous arcs of an irregular line drawing are actually represented with non-smooth P-structures. In particular it has been noted by many authors[18] that such an effect is proportional to both the distances between each two consecutive vertices of a P-structure and the angles formed by each two consecutive segments of a P-structure. The majority of authors agree that it is more important to minimize the average staircase effect than the local one.

A figure of noise will now be proposed for measuring such average staircase effect in quantized irregular line drawings. It should be mentioned that although there is much talk on how to describe the staircase effect, no figure of noise for measuring it has been proposed up to date to this author's knowledge.

Denoting with N the number of vertices in the P-structures of QL and letting M = N if QL is closed and otherwise M = N-1, let us define the following entities:

$$r_m = \max_i r_i \qquad ; \qquad \theta_{TOT} = \sum_{i=1}^{N} |\Delta\beta_i| \tag{5.10}$$

$$m_1 = \frac{\sqrt{r_m}}{k\sqrt{n}} \tag{5.11}$$

$$m_2 = \frac{\pi M}{\theta_{TOT}} \tag{5.12}$$

$$\theta_s = \frac{\theta_{TOT}}{M} = \frac{\pi}{m_2} \tag{5.13}$$

$$\begin{aligned} \ell_s &= \ell_{max}\sqrt{n} = \sqrt{r_m}\,\ell\,\sqrt{n} \\ &= m_1\, nk\ell = m_1\, n\, \delta_j = m_1 T \end{aligned} \tag{5.14}$$

and let us recall the following relations which were shown in Chapter II

| | |
|---|---|
| $\Delta\ell = 2r = \sqrt{2}\, T$ | from (2.11), (2.12) |
| $r = \frac{\sqrt{2}}{2} T$ | from (2.11) |
| $\Delta\ell = p\ell$ | from (2.15), (2.16) |
| $\ell < \ell_j < \ell_{max} < \sqrt{r_m}\,\ell$ | from (2.3), (2.4), (2.9) |
| $\ell_j \leq \sqrt{r_j}\,\ell$ | from (2.4) |

Because of the special nature of the staircase-effect noise, a formal definition of the symbolic difference QL-L is omitted here. The levels of noise and real signal are defined as

$$\ell_w = \ell(QL-L) = \frac{1}{M} \sum_{i=1}^{M} \ell_i \, \ell_{i+1} \tan|\Delta\beta_i|$$

$$\ell_r = \ell(QL) = \ell_s^2 \, \theta_s$$

and the staircase-effect-type figure of noise as

$$f_{w_{S.E.}} = \frac{1}{M} \sum_{\substack{i=1 \\ i\epsilon I}}^{M} \frac{\ell_i}{\ell_s} \frac{\ell_{i+1}}{\ell_s} \frac{\tan|\Delta\beta_i|}{\theta_s} \qquad (5.16)$$

Let us note that I is the set of the indices of the vertices of the P-structures of QL which do not correspond to cusps or initium or terminus points of L.

Let us note that $\ell_s$ and $\theta_s$ are essentially user chosen parameters of reference. It could be said that if all $\ell_i < \ell_s$ and $\tan|\Delta\beta_i| < \theta_s$ then there would be little or no staircase-effect at all whereas if $\ell_i \gtrsim \ell_s$ and $\tan|\Delta\beta_i| \gtrsim \theta_s$ then the effect would be larger and $f_{w_{S.E.}} \geq 1$. An example is shown in Fig. 22. These examples clearly manifest the importance of the proposed figure of noise. Fig. 22a shows that the drawing corresponding to a chain encoded quantized irregular line drawing has a small staircase effect if the elementary size of the chosen grid is small, and this in spite of the fact that the angular variations due to the quantization are rather coarse ($\Delta\beta_j = 45^\circ$). For the case of Fig. 22b the staircase effect is much larger than before because long segments are now associated with large angular variations. Fig. 22c shows that a small staircase effect can be achieved even when long segments are present provided that the associated angular variations are very small.

Previous comments show the importance of the figure of noise previously defined for describing the average staircase effect present in quantized irregular line drawings. Also as Fig. 22a has shown, a figure of noise as

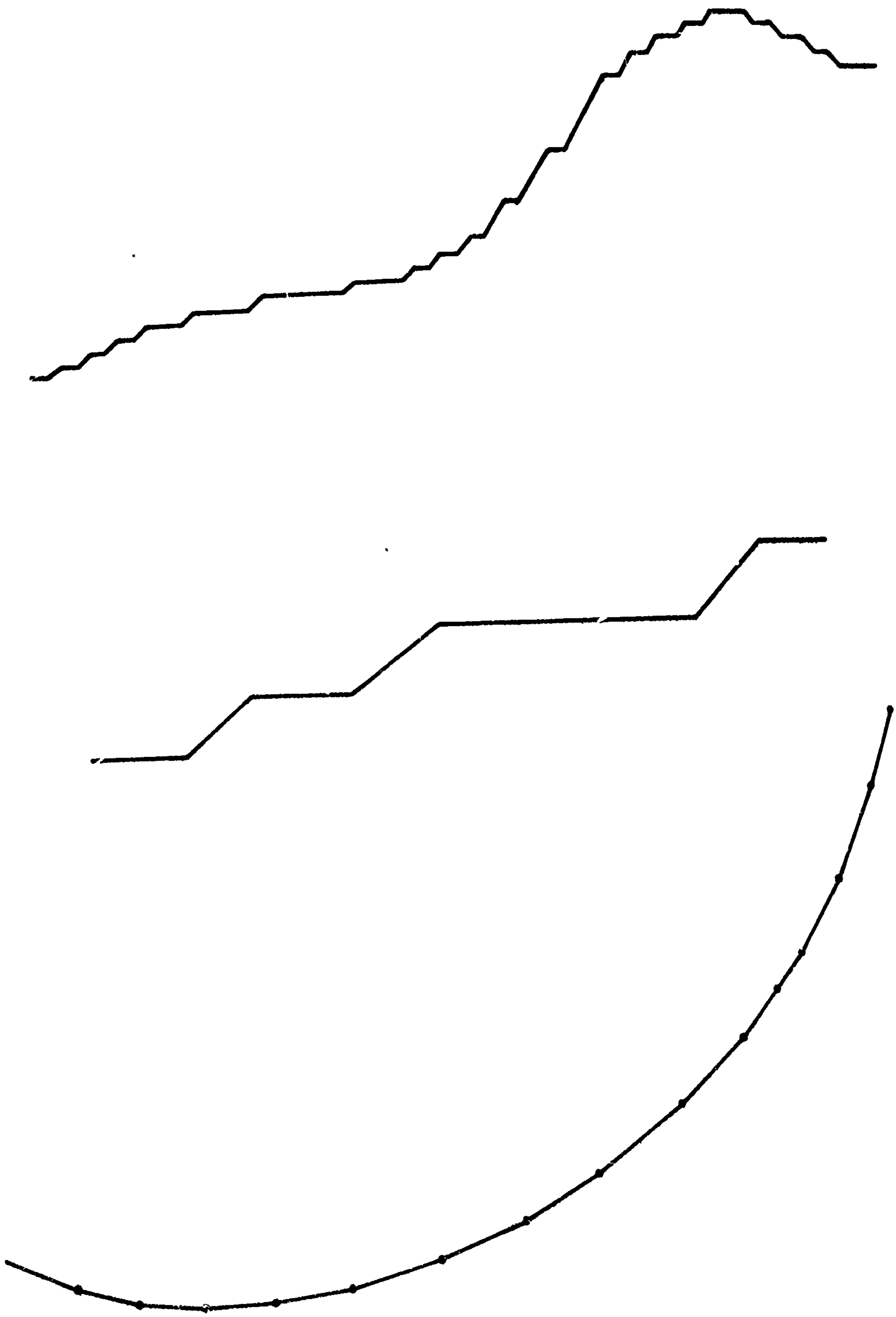

FIG. 22

STAIRCASE-EFFECT IN QUANTIZED DRAWINGS

defined here is not only an original contribution to the solution of the problem of defining the staircase-effect noise but it is also a powerful means of investigation which allows one to obtain insight into the peculiar nature of this type of noise.

The reason for defining $f_{w_{S.E.}}$ in terms of the trigonometric tangent of $\Delta\beta_i$ rather than in terms of the angles themselves will become clear later when the bounds on the transformed figures of noise will be studied. It should be noted, however, that since, in general, the $\Delta\beta_i$ will be small in order to guarantee a minimum level of precision, it follows that for all practical purposes $f_{w_{S.E.}}$ can be regarded as if it were d fined in terms of the angles directly.

THEOREM 10: If an irregular line drawing is quantized according to the rules of the quantization scheme proposed here, then $f_{w_{S.E.}} \leq \frac{1}{n}$ .

<u>Proof</u>: Since we have from (2.4), (2.11), (2.12), (2.16)

$$\ell_j \leq \sqrt{r_m}\, \ell = \sqrt{r_m}\,\frac{\Delta\ell}{p} = \sqrt{r_m}\,\frac{2\sqrt{2}/2\ T}{p} = \sqrt{2r_m}\,\frac{T}{p}$$

it follows that by assuming small $\Delta\beta_i$'s:

$$f_{w_{S.E.}} \leq \frac{1}{M} \sum_{\substack{i=1\\ i\varepsilon I}}^{M} \frac{\sqrt{2r_m}\ T}{p}\,\frac{1}{Tm_1}\,\frac{\sqrt{2r_m}\ T}{p}\,\frac{m_2}{Tm_1}\,\frac{|\Delta\beta_i|}{\pi} =$$

$$f_{w_{S.E.}} \leq \frac{1}{M} \sum_{\substack{i=1\\ i\varepsilon I}}^{M} \left(\frac{\sqrt{2r_m}\ T}{p}\right)^2 \left(\frac{1}{Tm_1}\right)^2 \frac{|\Delta\beta_i|}{\pi}\, m_2 =$$

$$= \frac{1}{M} \sum_{\substack{i=1\\ i\varepsilon I}}^{M} \frac{2r_m m_2 |\Delta\beta_i|}{m_1^2\, p^2\, \pi} = \frac{1}{M}\,\frac{2r_m}{p^2}\,\frac{m_2}{m_1^2}\,\frac{\theta_{TOT}}{\pi} = 2n(\frac{k}{p})^2$$

and since $k = \frac{T}{n\ell}$

then $$f_{w_{S.E.}} \leq 2n\left(\frac{T}{n\ell p}\right)^2 = 2n\left(\frac{T}{n\sqrt{2T}}\right)^2 = \frac{1}{n} \tag{5.17}$$

## 5.6 Concluding Remarks

A solution has been given in terms of the classical approach of the problem of identifying the intensity of the noise component in a real signal and of defining a figure of noise for measuring the relative importance of the noise with respect to the signal. Three types of figures of noise have been presented, justified and studied in relation to the precision parameter n which governs the proposed quantization scheme. This has lead to the interesting result that all three figures of noise have the same worst case bound. This in turn means that when the proposed quantization scheme is used, it is possible at one time to control area-type, displacement-type and staircase-effect-type noise.

In the next chapter we shall study the effect of a transformation on the figures of noise defined here and the relations between the bounds on the figures of noise before and after a regular transformation.

# VI. TRANSFORMATIONS OF FIGURES OF NOISE

## 6.1 General Considerations

In this chapter the effect of a transformation on a figure of noise is studied. In particular, let us note that since it has been shown that any regular transformation can be reduced to a set of triplets of elementary transformations approximating it with any required precision, only elementary transformations need be taken into account here. First, the invariancy of the figures of noise with rotation will be proved. Then the effect of requantization will be studied, both for constant as well as variable elementary grid size. Then the effects of isotropic and non-isotropic scalings will be considered.

The analysis presented here will lead to the discovery of a parameter which is completely defined once the elementary transformation is given. As will be shown, the product of such a parameter with the figure of noise before transformation will give a bound for the figure of noise after transformation.

Since a bound has been established already for the figures of noise before transformation in terms of the precision parameter n, it will become possible to relate a bound on the figures of noise after transformation to the parameter n.

The chapter is concluded with the definition of the figures of cost and merit, associated with each figure of noise. The figure of cost will be shown to be constituted of two factors. The first one expressing the cost of transforming the coordinates of a point and the second one related to the number of points to be transformed. The figure of merit will describe how much has been spent in order to achieve a given quality after a given transformation. Since a particular transformation is the identity transformation which maps a point of the plane into itself, the figures of merit for the identity transformation can be regarded as descriptors of the merit of the given quantization scheme. In this case the cost of transforming one point will be unitary and the figure of merit will become the product of the figure of noise and the number of points in the quantized irregular line drawing. This provides insight into the problem of judging the merit of a quantization scheme since the higher the quality, the lower its figure of noise but the larger the number of points necessary in the quantized version of the drawing.

Finally, let us point out that only the theory of the transformed figures of noise, cost and merit is developed here. Examples with typical values for such figures will be presented in a later chapter with the results of an application program.

## 6.2 Rotations

Let us note that in general there are two contributions to the value of a figure of noise after a transformation. The first one is completely defined in terms of the given transformation. The second one represents the contribution due to requantization on a given grid of the transformed irregular line drawing.

For each transformation these contributions will be computed separately. In the first case the contribution due to requantization, which will be referred to as grid-contribution, will be disregarded. Then the grid-contribution will be studied both for the cases in which the elementary grid size $T_2$ used for requantizing the transformed quantized irregular line drawing is equal or not to the one $T_1$ used for quantizing the input irregular line drawing.

### 6.2.1 Noise After Rotation Without Grid-Contribution

With reference to the symbolism used in Fig. 23, we have the following relations among the following positive entities (the primed symbols refer to values after transformation):

$$a_i' = a_i \quad , \quad \ell_i' = \ell_i \quad , \quad \delta_i' = \delta_i \quad , \quad \Delta\beta_i' = \Delta\beta_i$$

The new values of the three figures of noise after rotation are:

$$f'_{w_a} = \sum_{i=1}^{N} a_i/T_1 \sum_{i=1}^{N} \ell_i' = f_{w_a} \tag{6.1}$$

$$f'_{w_\ell} = \frac{1}{NT_1} \sum_{i=1}^{N} \delta_i' \tag{6.2}$$

$$f'_{w_{S.E.}} = \frac{1}{M} \sum_{\substack{i=1 \\ i\in I}}^{M} \frac{\ell_i'}{\ell_s} \frac{\ell_{i+1}'}{\ell_s} \frac{\tan|\Delta\beta_i'|}{\theta_s} = f_{w_{S.E.}} \tag{6.3}$$

In the following it will be assumed that

$$|\tan\Delta\beta_i| \simeq |\Delta\beta_i| \tag{6.4}$$

### 6.2.2 Noise After Rotation with Grid-Contribution

Let us define the grid-ratio t as $t = \frac{T_2}{T_1}$, where $T_1$ and $T_2$ are, respectively, the elementary grid sizes before and after transformation, and $0 \leq t \leq 1$ since $T_1$ is the largest grid size which allows us to well-quantize $I^*$.

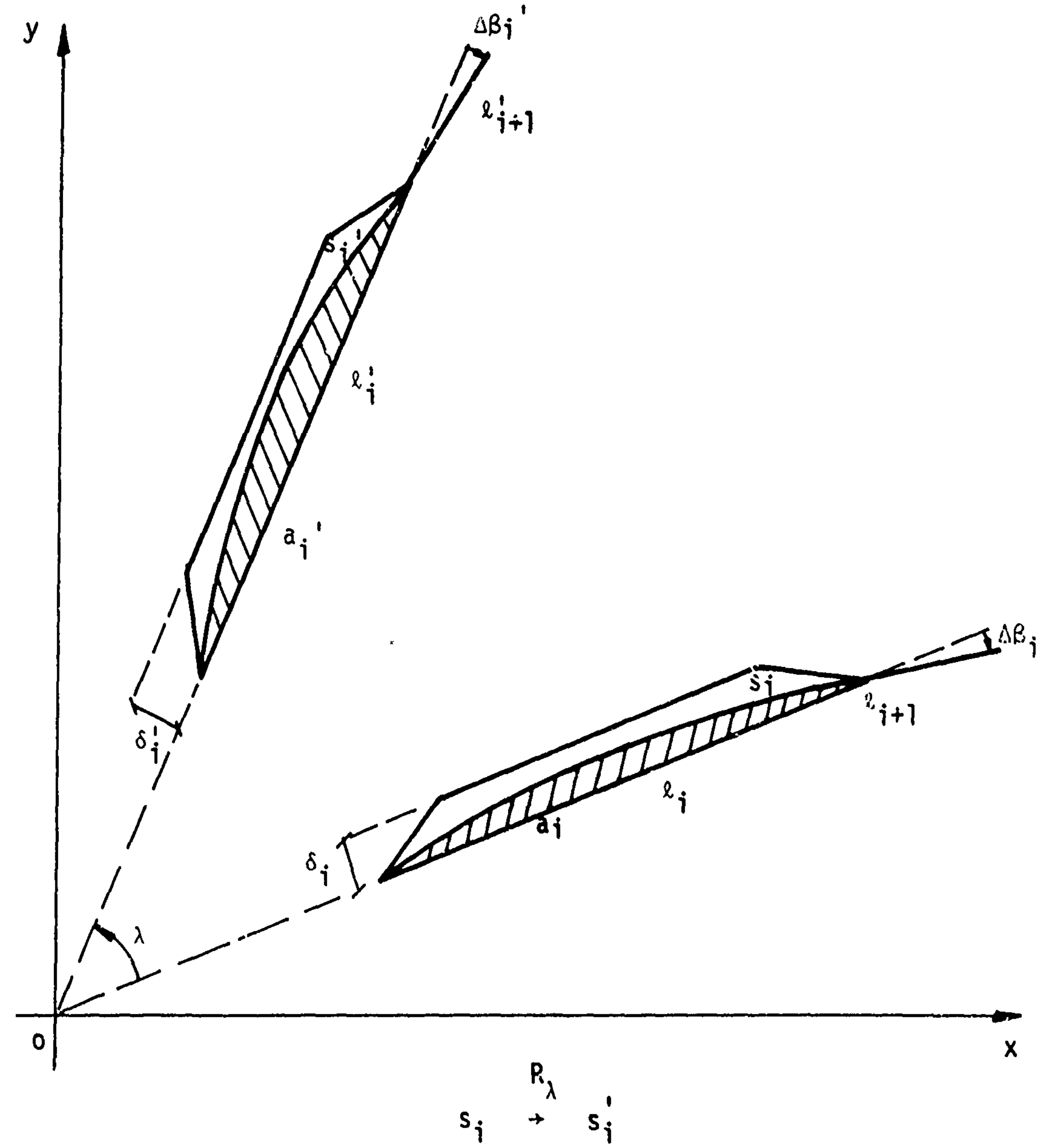


FIG. 23

ARC AND CHORD BEFORE AND AFTER ROTATION

The following relations are easily established:

$$|a_i'-a_i| \leq \frac{\sqrt{2}\, T_2\, \ell_i}{2} = \frac{\sqrt{2}\, T_1\, \ell_i t}{2} \tag{6.5}$$

$$|\delta_i'-\delta_i| \leq \frac{T_2 \sqrt{2}}{2} = \frac{\sqrt{2}}{2} T_1 t \tag{6.6}$$

$$|\ell_i'\ \ell_i| \leq T_2 \sqrt{2} = t\, T_1 \sqrt{2} \tag{6.7}$$

$$|\Delta\beta_i'-\Delta\beta_i| \leq 2 \tan^{-1} \frac{T_2\sqrt{2}}{\ell_i} < 2 \tan^{-1} \frac{t\, T_1\sqrt{2}}{\ell_i} \tag{6.8}$$

Since $L^*$ is well-quantized, $\ell_i \geq \ell >> T_2\sqrt{2} = t\, T_1\sqrt{2}$ (6.9)

In other words, $t\, T_1 \sqrt{2}$ can be disregarded with respect to $\ell_i$ and, therefore, also with respect to $\ell_i'$. Moreover, since $t\, T_1\frac{\sqrt{2}}{2}$ is in general a small number we have $\tan^{-1} t\, T_1 \frac{\sqrt{2}}{2} \simeq t\, T_1 \frac{\sqrt{2}}{2}$

and therefore

$$|\Delta\beta'-\Delta\beta| < \frac{2\sqrt{2}\, T_1 t}{\ell}\ ,\ f_{w_a}' \leq \sum_{i=1}^{N} (a_i + \frac{\sqrt{2}\, T_1 \ell_i t}{2}) \Big/ T_1 \sum_{i=1}^{N} \ell_i = f_{w_a} + \frac{\sqrt{2}}{2} t \tag{6.10}$$

which shows, as expected, that the influence of the grid-contribution decreases with the grid size $T_2$. In particular, if $T_2 = T_1$, then

$$f_{w_a}' \leq f_{w_a} + \frac{\sqrt{2}}{2} \tag{6.11}$$

It can be concluded that a rotation followed by requantization on the same grid leads to a constant increment in the noise figure, in the worst case. Similar relations hold for the two other types of figures of noise. We have

$$f'_{w_\ell} = \sum_{i=1}^{N} \delta'_i/NT_1 \leq \sum_{i=1}^{N} (\delta_i+T_1\sqrt{2}\,t/2)/T_1N = f_{w_\ell} + \frac{\sqrt{2}}{2}\,t \tag{6.12}$$

Again the grid-contribution decreases with $T_2$. In particular if $T_2 = T_1$ then

$$f'_{w_\ell} \leq f_{w_\ell} \frac{\sqrt{2}}{2} \tag{6.13}$$

As before it can be concluded that a rotation followed by requantization on the same grid leads, in the worst case, to a constant increment in the figure of noise.

In the case of the staircase-effect-type figure of noise we have

$$f'_{w_{S.E.}} = \frac{1}{M} \sum_{\substack{i=1 \\ i\epsilon I}}^{M} \frac{\ell'_i}{\ell_s} \frac{\ell'_{i+1}}{\ell_s} \frac{|\Delta\beta_i|}{\sigma_s}$$

and since by hypothesis the variations of $\ell_i$, $\ell_{i+1}$, $\Delta\beta_i$ due to rotation and requantization are small, this can be written as

$$\Delta(\ell_i\ \ell_{i+1}|\Delta\beta_i|) = \ell_i\ \ell_{i+1}|\Delta\beta_i|\left(\frac{\Delta\ell_i}{\ell_i} + \frac{\Delta\ell_{i+1}}{\ell_{i+1}} + \frac{\Delta|\Delta\beta_i|}{|\Delta\beta_i|}\right) \tag{6.14}$$

$$f'_{w_{S.E.}} = \frac{1}{M} \sum_{\substack{i=1 \\ i\epsilon I}}^{M} \frac{\ell_i}{\ell_s} \frac{\ell_{i+1}}{\ell_s} \frac{|\Delta\beta_i|}{\theta_s} \left(1+\frac{\Delta\ell_i}{\ell_i} + \frac{\Delta\ell_{i+1}}{\ell_{i+1}} + \frac{\Delta|\Delta\beta_i|}{|\Delta\beta_i|}\right) \tag{6.15}$$

and since

$$\frac{\Delta\ell_i}{\ell_i} < \frac{\Delta\ell}{\ell} \leq \frac{\sqrt{2}\,T_2}{\ell} = \frac{\sqrt{2}\,T_1 t}{\ell}, \quad \frac{\Delta|\Delta\beta_i|}{|\Delta\beta_i|} = \frac{\Delta\theta}{\Delta\beta_i} \leq \frac{2\sqrt{2}\,T_2}{\ell\theta} = \frac{2\sqrt{2}\,T_1 t}{\ell\theta} \tag{6.16}$$

Then

$$f'_{w_{S.E.}} \leq f_{w_{S.E.}}\left(1+\frac{2\sqrt{2}\,T_1 t}{\ell}+\frac{2\sqrt{2}\,T_1 t}{\ell\theta}\right) = f_{w_{S.E.}}\left(1+2\frac{\theta+1}{\theta}\frac{\sqrt{2}\,T_1 t}{\ell}\right) \tag{6.17}$$

This result shows that also in this case the grid-contribution decreases with t. In particular if $T_2 = T_1$ we have the following worst-case bound

$$f'_{w_{S.E.}} \leq f_{w_{S.E.}}\left(1+\frac{\theta+1}{\theta}\frac{2\sqrt{2}\,T_1}{\ell}\right) \tag{6.18}$$

Comment: It has been shown that the effect of the grid-contribution to the transformed figure of noise is a function of the size of the grid on which the transformed data are requantized. In particular this contribution can be kept as low as necessary by choosing a suitable grid size $T_2$.

In the case of linear and non-linear transformations which can be decomposed into a set of triplets of elementary transformations, containing two rotations each, the grid-contributions for the two rotations can be considered exactly zero since the quantized drawing is requantized only once after transformation and not after each of the elementary transformations of the given triplet. Such unique requantization will have an effect which can be taken into account either at the end or when applying the non-isotropic scaling to the triplet. Let us also note that if $t>1$, that is $T_2>T_1$, the grid-contribution to rotation increases, as expected. This can be understood by considering the case of zero rotation and change of grid size. Finally let us note that the grid-contribution has been evaluated in terms of a worst-case bound which is likely to be much higher than the actual value.

## 6.3 Isotropic Scalings

As in the case of rotation, two cases will be considered; in the first one the grid contribution will be disregarded, and in the second one the effect of a new grid will be studied.

### 6.3.1 Noise After Isotropic Scaling Without Grid-Contribution

With reference to Fig. 24 let us note the following relations:

$$\ell_i' = |\alpha|\ell_i \tag{6.19}$$

$$\delta_i' = |\alpha|\delta_i \tag{6.20}$$

$$a_i' = \alpha^2 a_i \tag{6.21}$$

$$|\Delta\beta_i'| = |\Delta\beta_i| \tag{6.22}$$

The new values of the three figures of noise after an isotropic scaling are:

$$f'_{w_a} = \sum_{i=1}^{N} a_i'/T_1 \sum_{i=1}^{N} \ell_i' = \sum_{i=1}^{N} \alpha^2 a_i/T_1|\alpha| \sum_{i=1}^{N} \ell_i = |\alpha| f_{w_a} \tag{6.23}$$

$$f'_{w_\ell} = \frac{1}{NT_1} \sum_{i=1}^{N} \delta_i' = |\alpha| \frac{1}{NT_1} \sum_{i=1}^{N} \delta_i = |\alpha| f_{w_\ell} \tag{6.24}$$

$$f'_{w_{S.E.}} = \frac{1}{M} \sum_{\substack{i=1 \\ i\epsilon I}}^{M} \frac{\ell_i|\alpha|}{\ell_s} \frac{\ell_{i+1}|\alpha|}{\ell_s} \frac{|\Delta\beta_i|}{\theta_s} = \alpha^2 f_{w_{S.E.}} \tag{6.25}$$

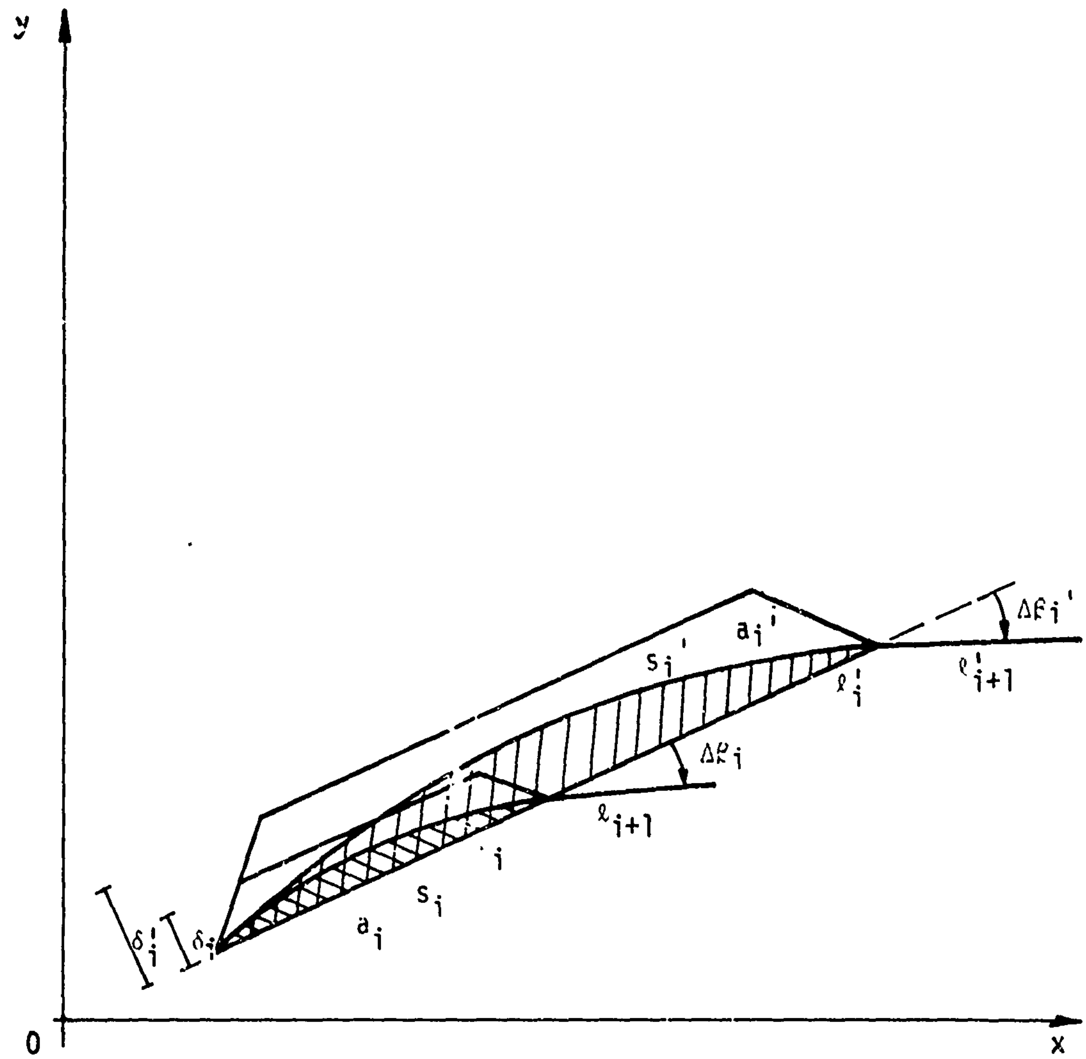


$S_\alpha$

$s_i \rightarrow s_i'$

$|\alpha| \cdot 1$

FIG. 24

ARC AND CHORD BEFORE AND AFTER AN ISOTROPIC SCALING

### 6.3.2 Noise After Isotropic Scaling with Grid-Contribution

Two cases will be considered. In the first one the case of expansions, that is isotropic scalings with $|\alpha|\geq 1$, will be considered; then the case of contractions, that is isotropic scalings with $|\alpha|<1$, will be studied.

#### 6.3.2.1 Expansions

Since by hypothesis $|\alpha|\geq 1$, we have $\ell_i'>>\sqrt{2}\, tT_1$ and, therefore, $\ell_i' \approx |\alpha|\ell_i$

$$f'_{w_a} \leq \Delta\sum_{i=1}^{N}\left(|\alpha|^2 a_i + |\alpha|\,\frac{\sqrt{2}\,T_1}{2}\,\ell_i\, t\right)/T_1 \sum_{i=1}^{N}|\alpha|\ell_i = |\alpha| f_{w_a} + \frac{\sqrt{2}}{2}\,t \qquad (6.26)$$

Let us note that this result is similar to the one obtained in the case of rotation in the sense that the grid contribution decreases with $T_2$. Similarly we have the following relations for the other two figures of noise:

$$f'_{w_\ell} \leq \frac{1}{NT_1}\sum_{i=1}^{N}\left(|\alpha|\delta_i + \frac{\sqrt{2}}{2}\,T_1 t\right) = f_{w_\ell}|\alpha| + \frac{\sqrt{2}}{2}\,t \qquad (6.27)$$

$$f'_{w_{S.E.}} \leq \frac{1}{M}\sum_{\substack{i=1\\ i\in I}}^{M}\frac{\ell_i|\alpha|}{\ell_s}\,\frac{\ell_{i+1}|\alpha|}{\ell_s}\,\frac{|\Delta\beta_i|}{\theta_s}\left(1+\frac{\Delta\ell_i}{\ell_i}+\frac{\Delta\ell_{i+1}}{\ell_{i+1}}+\frac{\Delta|\Delta\beta_i|}{|\Delta\beta_i|}\right) \leq \alpha^2 f_{w_{S.E.}}\left(1+\frac{\theta+1}{\theta}\,\frac{2\sqrt{2}\,T_1 t}{\ell}\right) \qquad (6.28)$$

As in the case of rotation the grid-contributions decrease with the grid size $T_2$. If $T_2 = T_1$ the three worst-case bounds computed here are the same as those found for the case of rotation with the only obvious difference that here $|\alpha|\geq 1$.

6.3.2.2. Contractions

By hypothesis $|\alpha|<1$. In general the output will no longer be a well quantized irregular line drawing. However, if we assume that the size of the grid on which the output will be quantized is specified by $t < \frac{|\alpha|\ell}{\sqrt{2}\,T_1}$ then $|\alpha|\ell > \sqrt{2}\,T_1\,t$ and since $\ell_i > \ell$, it follows that

$|\alpha|\ell_i + \sqrt{2}\,T_1\,t \simeq |\alpha|\ell_i$ and then

$$f'_{w_a} \leq \sum_{i=1}^{N} (\alpha^2 a_i + \sqrt{2}\,T_1\,t\,\ell_i|\alpha|/2)/T_1 \sum_{i=1}^{N} \ell_i|\alpha| = |\alpha| f_{w_a} + \frac{\sqrt{2}}{2} t \qquad (6.29)$$

Similar considerations hold for the other two types of figures of noise. If for example $t < |\alpha|\ 2 \min_i \delta_i/\sqrt{2}\,T_1$ then

$$|\alpha|\ \delta_i + \frac{\sqrt{2}}{2} T_1\ t > |\alpha| \min_i \delta_i + \frac{\sqrt{2}\,T_1\ t}{2} \simeq |\alpha| \min_i \delta_i$$

$$|\alpha|\ \delta_i + \frac{\sqrt{2}}{2} T_1\ t \simeq |\alpha|\ \delta_i$$

$$f'_{w_\ell} = \frac{1}{NT_1} \sum_{i=1}^{N} |\alpha|\ \delta_i = |\alpha|\ f_{w_\ell} \qquad (6.30)$$

while if $t < |\alpha|\ \ell\sqrt{2}\,T_1$, $\quad |\alpha|\ \ell_i + \sqrt{2}\,T_1\ t \simeq |\alpha|\ \ell_i$

and since $\ell_i > \ell$ then as before we have

$$f'_{w_{S.E.}} = |\alpha|^2\ f_{w_{S.E.}} \left(1 + \frac{2\sqrt{2}\,T_1}{\ell}\ \frac{\theta+1}{\theta}\ t\right) \qquad (6.31)$$

Finally let us note that if $T = |\alpha|$, then the noise after a contraction is equal to the one before this transformation only if the grid-contribution is not taken into account.

Let us note that from the theory developed so far there are identical bounds for the figures of noise when the grid-contributions are taken into account, both for the case of expansion and for the one of contraction. In the case of contractions the grid-contributions may tend to dominate over those due to other types of noise. This is an obvious consequence of the fact that the original grid size $T_1$ is the largest possible for well-quantizing the given irregular line drawing. To contract such an input is equivalent to requantizing it on a coarser grid, and in this case the output cannot be considered a well-quantized line drawing any more. If the grid size for the input was chosen so to minimize the noise after contraction, then it means that the input irregular line drawing was quantized on a grid much finer than the one strictly necessary for well-quantizing it. In this case contractions defined by an $|\alpha|$ such that in the worst case the irregular line drawings will be requantized on a grid smaller or equal to the one with the largest elementary size will still lead to well-quantized line drawings and to reduced values for the figures of noise. This can be clearly understood by referring to the following example in which an expansion is followed by a contraction and the grid-contribution is disregarded. Let $L_1$ with figure of noise $f_{w_1}$ be an irregular line drawing which has been well-quantized on a given grid. If $L_1$ is expanded than $L_2$ is obtained with noise $f_{w_2} > f_{w_1}$ ; if $L_3 = L_2$ with noise $f_{w_3} = f_{w_2}$ is now contracted so that $L_4 = L_1$ is obtained, then the value of the output figure of noise will be $f_{w_4} = f_{w_1} < f_{w_3}$. This process in which noise has been reduced is, of course, a theoretical one since in practice the grid-contribution will always prevent $f_{w_4}$ to equal $f_{w_1}$. Still it is possible that $f_{w_4} \approx f_{w_1}$ for very small grid-contributions. This apparently strange result can be justified by saying that the previous transformation has generated the non-redundant $L_4$ from the redundant $L_3$. This example also points out the different nature of the two components of a transformed figure of noise: the one associated with the given transformation which is reversible and the one associated with the size of the grid on which the output is requantized, which is not reversible.

## 6.4 Non-Isotropic Scalings

The grid-contributions for the case of non-isotropic scaling will not be explored in detail since it has already been shown in previous paragraphs that a figure of noise always increases with the scale factor $\alpha$. Bounds for the figures of noise can be found for $S_{\alpha,\beta}$ by studying the case of $S_\gamma$ where $\gamma=\max(|\alpha|,|\beta|)$.

Using the symbolism of Fig. 25 we have:

$$a_i = |\frac{1}{2} x_1y_1 + (x_2-x_1)y_1 + (x_2-x_1)(y_2-y_1)\frac{1}{2} +$$

$$+ (y_2-y_3)(x_3-x_2) \frac{1}{2} + y_3(x_3-x_2) - y_3x3 \frac{1}{2} | =$$

$$= | - \frac{1}{2} x_1y_1 + \frac{1}{2} x_2y_1 + \frac{x_2y_2}{2} - \frac{x_1y_2}{2} + \frac{x_1y_1}{2} + \frac{x_3y_2}{2} - \frac{x_3y_3}{2}$$

$$- \frac{x_2y_2}{2} + \frac{x_2y_3}{2} + y_3x_3 - y_3x_2 - y_3 \frac{x_3}{2} | =$$

$$a_i = | \frac{1}{2} [(y_1x_2 + x_3y_2) - (x_1y_2 + x_2y_3)] |$$

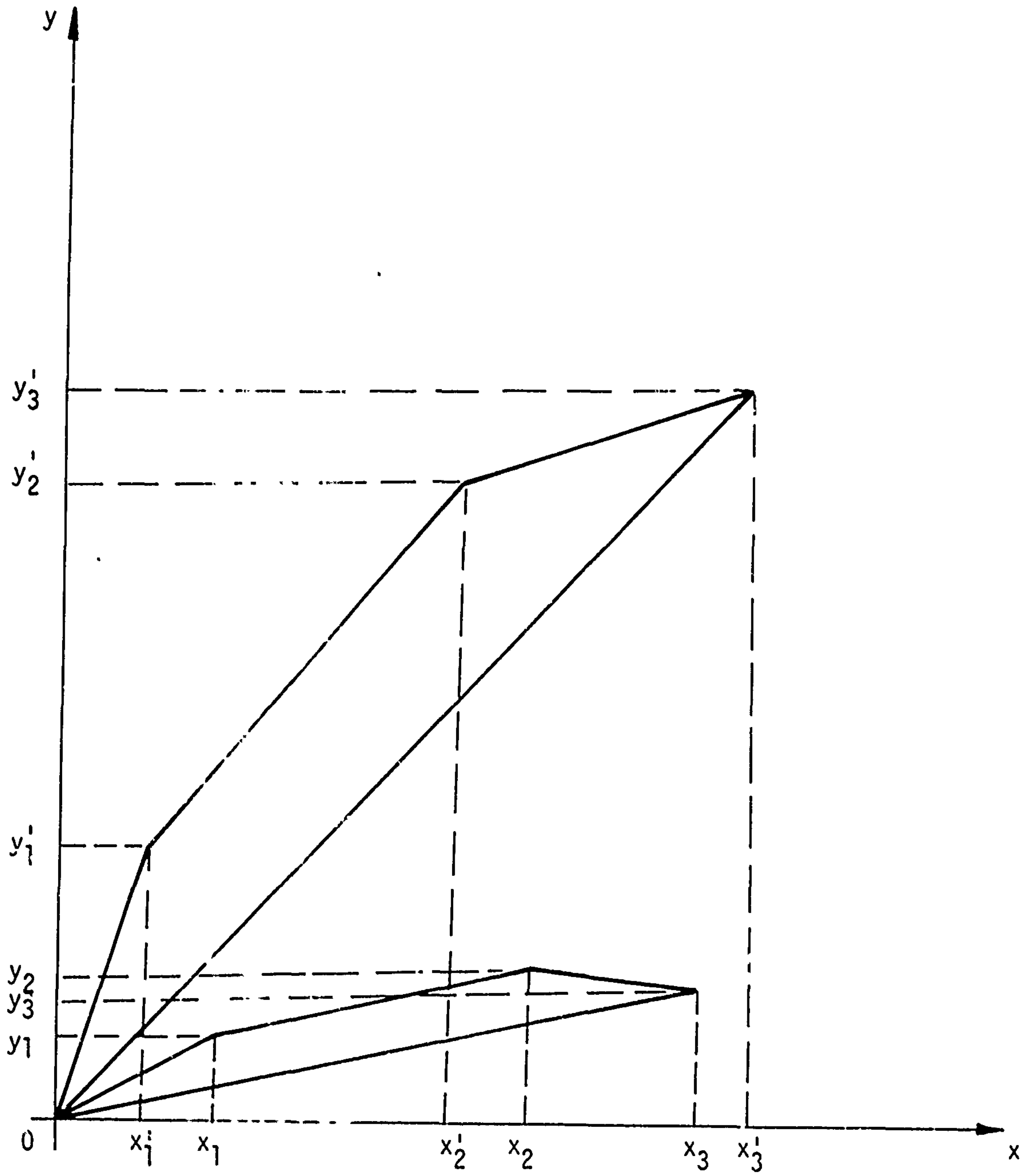


$y_i' = \beta\, y_i$

$x_i' = \alpha\, x_i$

FIG. 25

ARC AND CHORD BEFORE AND AFTER A NON-ISOTROPIC SCALING

And since $y_i' = \beta\, y_i$ and $x_i' = \alpha\, x_i$ we have the following result

$$a_i' = \left|\, \frac{1}{2}\, [\alpha\,\beta\, y_1 x_2 + \alpha\,\beta\, x_3 y_2 - \alpha\,\beta\, x_1\, y_2 - \alpha\,\beta\, x_2\, y_3] \right| = |\alpha\beta|\; a_i \qquad (6.32)$$

Using the symbolism of Fig. 26 we obtain:

$$\ell_i = \sqrt{\Delta x_i^2 + \Delta y_i^2}$$

$$\ell_i' = \sqrt{\alpha^2 \Delta x_i^2 + \beta^2 \Delta y_i^2}$$

$$\tan \Delta\beta_i = (y_2/x_2 - y_1/x_1)/(1 + y_1 y_2/x_1 x_2)$$

$$\tan \Delta\beta_i' = \alpha\beta(x_1 y_2 - x_2 y_1)/(\alpha^2 x_1 x_2 + \beta^2 y_1 y_2)$$

Let us now introduce the following constants:

$$\gamma = \max(|\alpha|, |\beta|) \qquad (6.33)$$

$$\delta = \min(|\alpha|, |\beta|) \qquad (6.34)$$

Then the following relations hold

$$\left(\frac{\delta}{\gamma}\right)^2 \tan \Delta\beta_i = \left|\delta^2 \frac{x_1 y_2 - x_2 y_1}{\gamma^2 (x_1 x_2 + y_1 y_2)}\right| \leq \tan \Delta\beta_i' \leq \left|\gamma^2 \frac{x_1 y_2 - x_2 y_1}{\delta^2 (x_1 x_2 + y_1 y_2)}\right| = \left(\frac{\gamma}{\delta}\right)^2 \tan \Delta\beta_i \qquad (6.35)$$

$$\delta \ell_i = \sqrt{\delta^2 (\Delta x_i^2 + \Delta y_i^2)} \leq \ell_i' \leq \sqrt{\gamma^2 (\Delta x_i^2 + \Delta y_i^2)} = \gamma \ell_i \qquad (6.36)$$

As a consequence of the relations established so far, we have:

$$f_{w_a}' = |\alpha\beta| \sum_{i=1}^{N} a_i / T_1 \sum_{i=1}^{N} \ell_i'$$

$$\frac{|\alpha\beta| \sum_{i=1}^{N} a_i}{\gamma T_1 \sum_{i=1}^{N} \ell_i} \leq f_{w_a}' \leq |\alpha\beta| \sum_{i=1}^{N} a_i / T_1\, \delta \sum_{i=1}^{N} \ell_i$$

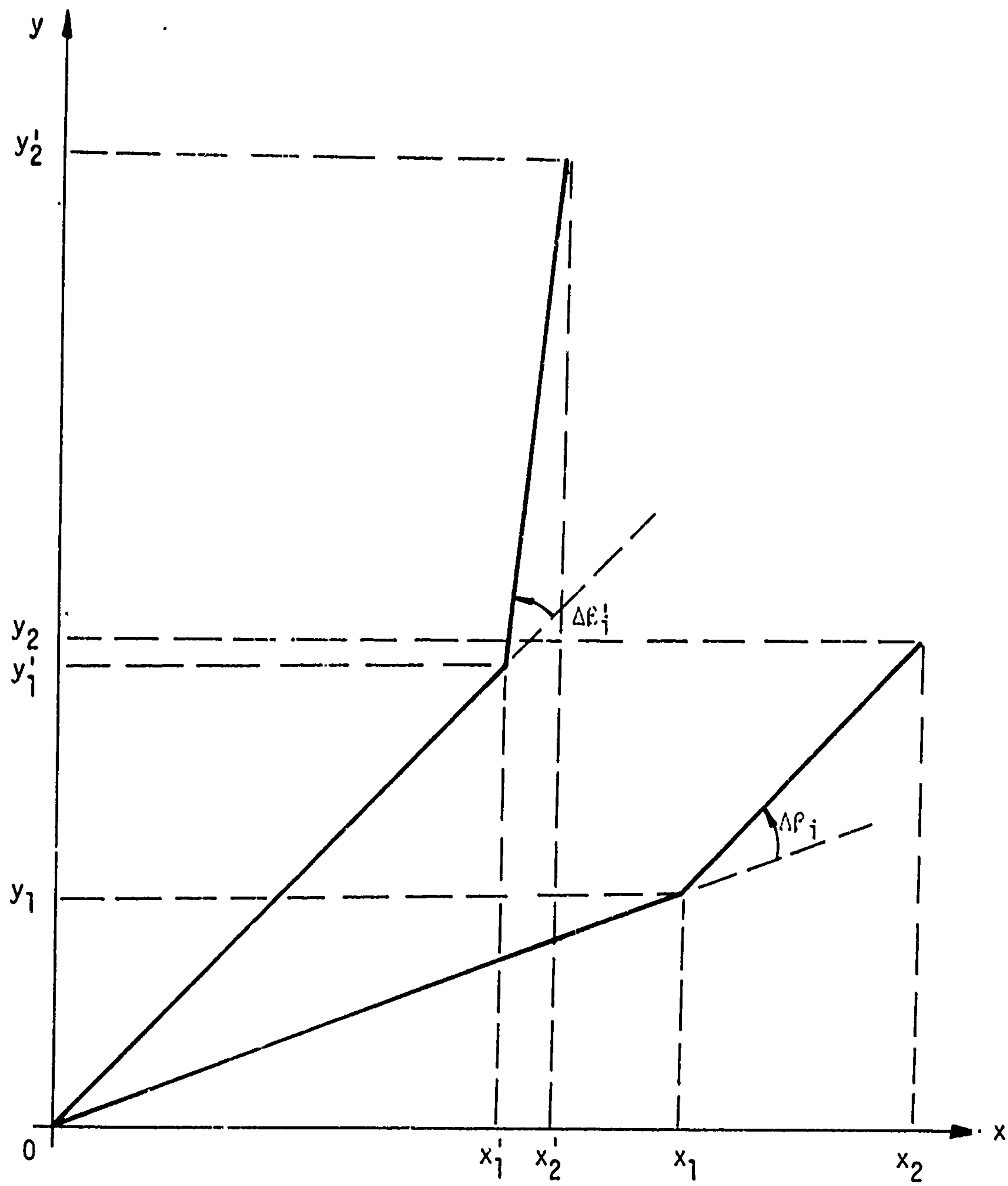


$$y_i' = \beta\, y_i$$

$$x_i' = \alpha\, x_i$$

FIG. 26

ANGULAR VARIATIONS DUE TO NON-ISOTROPIC SCALINGS

Since $|\alpha\beta| / \delta = \gamma$ and $|\alpha\beta| / \gamma = \delta$ then

$$\delta f_{w_a} = \frac{|\alpha\beta|}{\gamma} f_{w_a} \leq f'_{w_a} \leq \frac{|\alpha\beta|}{\delta} f_{w_a} = \gamma f_{w_a} = \frac{|\alpha\beta|}{\gamma} \tag{6.37}$$

Also we have $\delta\, \delta_i \leq \delta'_i \leq \gamma\, \delta_i$

Then

$$\delta f_{w_\ell} \leq f'_{w_\ell} \leq \gamma f_{w_\ell} \tag{6.38}$$

In the case of the staircase-effect figure of noise, we have

$$f'_{w_{S.E.}} = \frac{1}{M} \sum_{\substack{i=1 \\ i\varepsilon I}}^{M} \frac{\ell_i}{\ell_s} \frac{\ell_{i+1}}{\ell_s} \frac{\tan|\Delta\beta'_i|}{\theta_s}$$

and since it was shown that

$$\delta\ell_i \leq \ell'_i < \gamma\ell_i \,; \; (\frac{\delta}{\gamma})^2 \tan|\Delta\beta_i| \leq \tan|\Delta\beta'_i| \leq (\frac{\gamma}{\delta})^2 \tan|\Delta\beta_i|$$

then

$$\delta^2(\frac{\delta}{\gamma})^2 f_{w_{S.E.}} \leq f'_{w_{S.E.}} \leq \gamma^2(\frac{\gamma}{\delta})^2 f_{w_{S.E.}} \tag{6.39}$$

## 6.5 Summary of Noise Transformations

In previous paragraphs the effects of transformations on figures of noise have been presented. In particular the cases of absence and presence of grid-contributions have been studied. Since in most practical applications these grid-contributions will be small with respect to the actual values of the figures of noise, only the cases of absence of grid-contributions will be summarized here. Let us first define the following constants:

$$B_1 = \frac{\delta^2}{\gamma} \;, \quad B_2 = \frac{\gamma^2}{\delta}$$

and let us note that they depend only on the particular transformation under consideration. In fact

1) Rotation $R_\lambda$ , $B_1 = B_2 = 1$

2) Isotropic scaling $S_\alpha$ , $B_1 = B_2 = |\alpha|$

3) Non-isotropic scaling $S_{\alpha,\beta}$ , $B_1 = \frac{\delta^2}{\gamma}$ , $B_2 = \frac{\gamma^2}{\delta}$

where as usual $\gamma = \max(|\alpha|,|\beta|)$ , $\delta = \min(|\alpha|,|\beta|)$

Then when grid contributions are disregarded we have

$$0 \leq B_1 \, f_{w_a} \leq f'_{w_a} \leq B_2 \, f_{w_a} \leq \frac{B_2}{n} \qquad (6.40)$$

$$0 \leq B_1 \, f_{w_\ell} \leq f'_{w_\ell} \leq B_2 \, f_{w_\ell} \leq \frac{B_2}{n} \qquad (6.41)$$

$$0 \leq B_1^2 \, f_{w_{S.E.}} \leq f'_{w_{S.E.}} \leq B_2^2 \, f_{w_{S.E.}} \leq \frac{B_2^2}{n} \qquad (6.42)$$

As can be seen from these relations the value of a figure of noise after a transformation is bounded by the product of a constant which is dependent on the transformation only and of the value of the figure of noise before transformation. Since there is an upper bound relating the figure of noise before transformation and the precision parameter n, then is also possible to establish such a relation between the value of the figure of noise after transformation and the precision parameter n. Of course, this relation is true in general only if the grid-contributions are neglected. As was shown in studying such grid-contributions to the figures of noise the following condition has to be fulfilled:

$$2\sqrt{2}\,\frac{T}{\ell}\;\frac{\theta+1}{\theta} << 1 \qquad (6.17), (6.28), (6.31)$$

If this is the case and for example bound B is imposed on the staircase effect figure of noise after a transformation characterized by $B_2$, it will be sufficient to let: $n > B_2^2/B$.

Finally let us note that since $B_1$ and $B_2$ are functions of $\alpha$ and $\beta$, in the case of a non-linear transformation it will be sufficient to study the values of $\alpha$ and $\beta$ for each of the non-isotropic scalings in the triplet approximating it. Since a figure of noise increases with the larger of $\alpha$ and $\beta$ it will be important to search the region of existence of the given irregular line drawing for finding the largest values of $\alpha$ and $\beta$. A worst case bound on the transformed figures of noise will then be a function of such maximum value.

For example since a Mercator projection can be regarded as a transformation mapping the polar coordinates $(\lambda,\phi)$ into $(\lambda, f(\phi) = \ln \tan\frac{1}{2}(\frac{\pi}{2}-\phi))$ then such a transformation can be regarded as one mapping a grid, defined on a sphere by uniformly spaced meridians and parallels, into a non-linear rectangular grid in the Mercator plane. This concept is shown in Fig. 27. Using the symbolism presented there it can be seen that the highest non-isotropic scale coefficient in the piecewise linear approximation of the Mercator projection is a function of the larger of the two values $\phi_1$, $\phi_2$.

## 6.6 Figures of Cost and Merit

As was mentioned before, an important aspect of the problem of efficiently quantizing irregular line drawings is the one of defining the cost of the achieved precision (figure of noise). In particular since the proposed quantization scheme is oriented towards the problem of transforming quantized irregular line drawings it is important to define a figure of cost related to a given transformation.

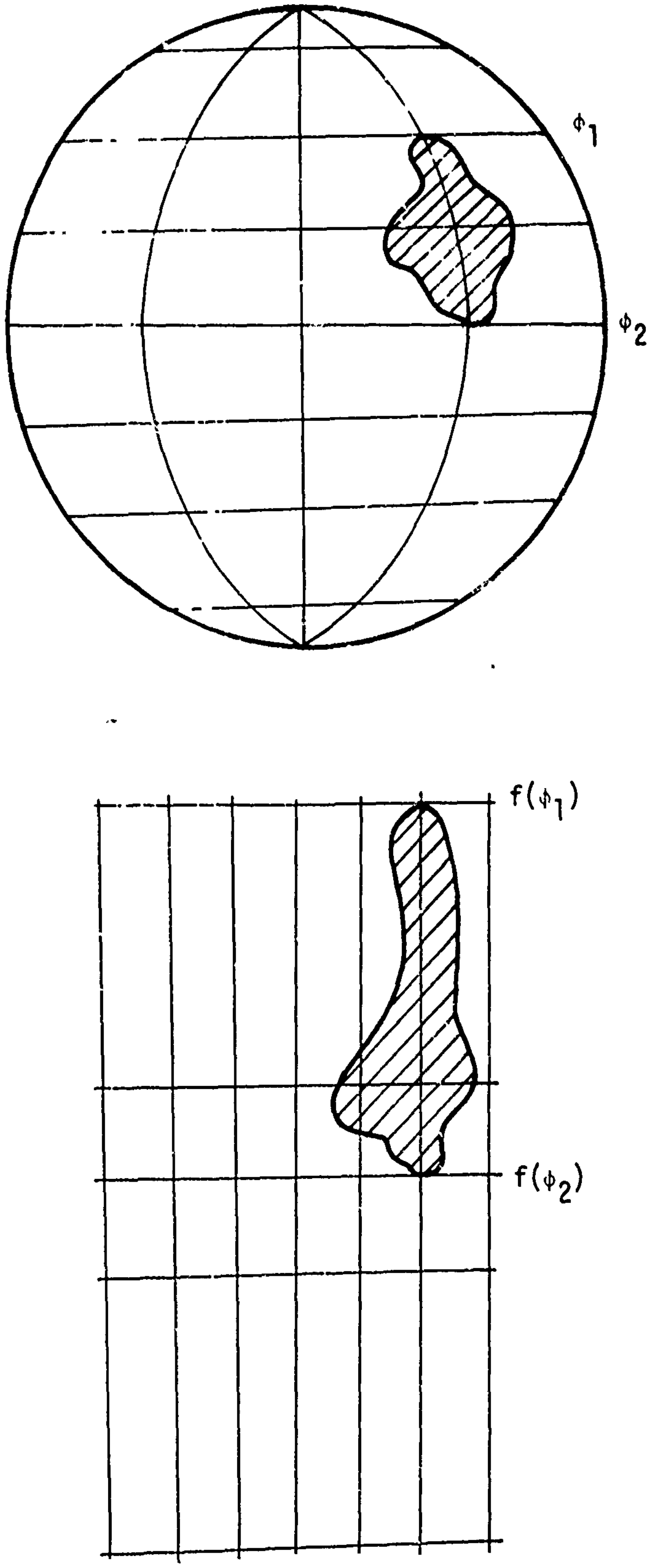


FIG. 27

EXAMPLE OF NON-LINEAR TRANSFORMATION
(MERCATOR PROJECTION)

Since a quantized irregular line drawing can be regarded as an ordered set of points and a tranformation as a mapping of the points of the plane into themselves, a figure of cost for describing the cost of transforming a quantized irregular line drawing consisting of N points is

$$f_c = K_p N \tag{6.43}$$

where $K_p$ defines the cost of transforming one point and N is the number of points in the drawing.

A figure of merit $f_m$ associated with a given figure of noise $f_w$ can now be defined as:

$$f_m = f_w \cdot f_c \tag{6.44}$$

Such a figure of merit tells us that for a constant merit a higher quality (lower figure of noise) is achieved with a higher cost, while if the quality is poorer (higher figure of noise) then there will be in general fewer points in the quantized irregular line drawing and the figure of cost will be lower.

Since each figure of merit is associated with a figure of noise, the following relations hold

$$0 \le f'_{m_a} \le K_p B_2 \frac{N}{n} \tag{6.45}$$

$$0 \le f'_{m_\ell} \le K_p B_2 \frac{N}{n} \tag{6.46}$$

$$0 \le f'_{m_{S.E.}} \le K_p B_2^2 \frac{N}{n} \tag{6.47}$$

Since $K_p B_2$ and $K_p B_2^2$ depend only on the transformation, it follows that the value of a figure of merit after the given transformation is bounded by N/n where N is the number of points in the quantized drawing and n is the precision parameter for the proposed quantization scheme.

# VII. COMPARISONS WITH OTHER METHODS

## 7.1 General

We shall consider the effect of requantization on a square grid of a rotated straight line segment for various types of quantization schemes. The scheme which on the average case will lead to the least distortion of the segment will be chosen as the best. Scalings are not considered here since the length of the segment is chosen equal to the smallest possible value within the frame of the given quantization scheme; in this case the largest possible distortion due to requantization occurs after a rotation of the segment with respect to an arbitrary point of the plane.

In the case of quantization schemes defined in reference to a square grid the problem can be stated as the one of exploring how an element with length 1 and another with length $\sqrt{2}$ are changed after a rotation followed by requantization.

In the following figures, P and $Q_i$ are the initium and a possible terminus node (the actual terminus node being defined once the value of the rotation angle is given) of the new element generated by requantizing the old one after rotation. A(P) will denote the region centered in P and within which the rotated element is contained. It should be noted that whereas $P \epsilon A(P)$, it is not true in general that $Q_i \epsilon A(P)$. R(S) will denote a region of the plane associated with a grid node S. In particular for the grid intersect quantization method, R(S) is a cross centered in S and containing all the points, on the grid lines, whose distance from S is less or equal to 1/2. For the square box and the rounding of coordinates methods, R(S) is a square box with size equal to the elementary grid size T=1 and centered in S and parallel to the grid lines. For the diamond box and circular box methods, R(S) is, respectively, a rhombus centered in S and with axes directed along the grid lines and with lengths equal to the elementary grid size T=1 and a circle centered in S and with radius half the elementary grid size T=1.

Case 1: Grid Intersect Method

In Figs. 28a and 28b the regions A(P) and R(S) for elements with length 1 and $\sqrt{2}$ are shown, and the possible $Q_i$'s are encircled. In both cases there are four $Q_i$'s outside A(P). If one of them or the degenerate case $Q_i$=P is selected as terminus point, then a length distortion of the original element will occur by a factor $\sqrt{2}$ or 0, for the case of Fig. 28a and of $1/\sqrt{2}$ or $2/\sqrt{2} = \sqrt{2}$ or 0 for the case of Fig. 28b.

In the case of Fig. 28a to each input element there corresponds no more then one output element while for the case in Fig. 28b the output may consist of either one or two elements, or zero elements in the degenerate case. When two elements are generated, however, they are identical, as easily verified by looking at A(P) in Fig. 28b. As indicated in Fig. 28a the maximum angular distortion for a single element is $\pm 45^{\circ}$. The situation is the same for Fig. 28b when a unique element is generated in the output. When two elements are generated, no angular distortion can exist; by construction when this happens the original

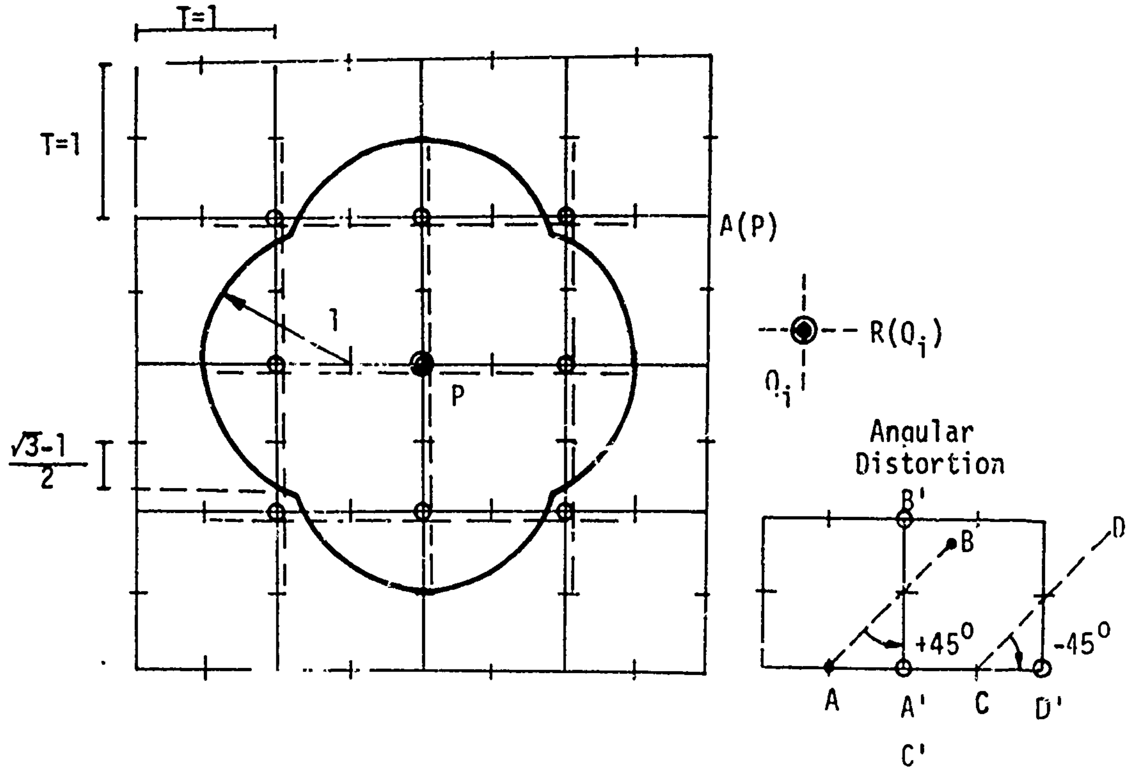


A) Element Length is 1

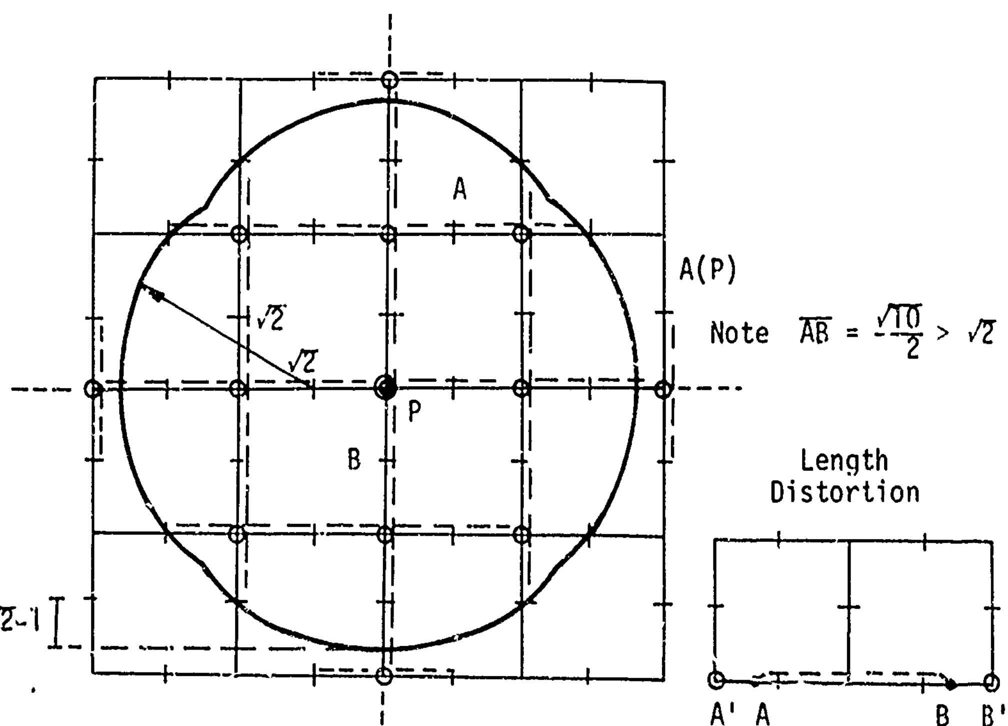


B) Element Length is $\sqrt{2}$

FIG. 28

DISTORTIONS DUE TO GRID INTERSECT REQUANTIZATION element must be coincident with a segment of a grid line (as shown in Fig. 28b) and in this case its slope is not altered.

Angles between adjacent elements are not conserved during the quantization process because they depend on the positions of the elements within the regions A(P) associated with them. Even in the case of parallel and equal-length elements, the extreme point Q may be a point within A(P) and then for the next element it may be outside A(Q) and, therefore, an angle of $\pm 45^{\circ}$ is introduced as shown in Fig. 29.

This is, however, the maximum angular distortion for two equal elements because, as we have already shown, the maximum change for a single element is $\pm 45^{\circ}$, and from geometric considerations, it is not possible that one element be distorted by $+45^{\circ}$ and the other by $-45^{\circ}$.

In the case of two different adjacent elements, angular distortion has maximum values which change according to the types of the two elements; moreover a single element may be generated from a couple of input elements as shown in Fig. 30, for the case of two orthogonal unit elements. This disappearance of an element however, is really important only for the case of the last element of an open sequence of elements because for an intermediate one the intersection of the next element with the grid will provide the new element which was not generated previously.

As shown in Fig. 31a, the angular distortion for a couple of orthogonal unit length elements may be $\pm 45^{\circ}$ or $-90^{\circ}$.

The unlikely case of two opposite unit-length elements is shown in Fig. 28b; they may give rise to a couple of inverse elements or dis-

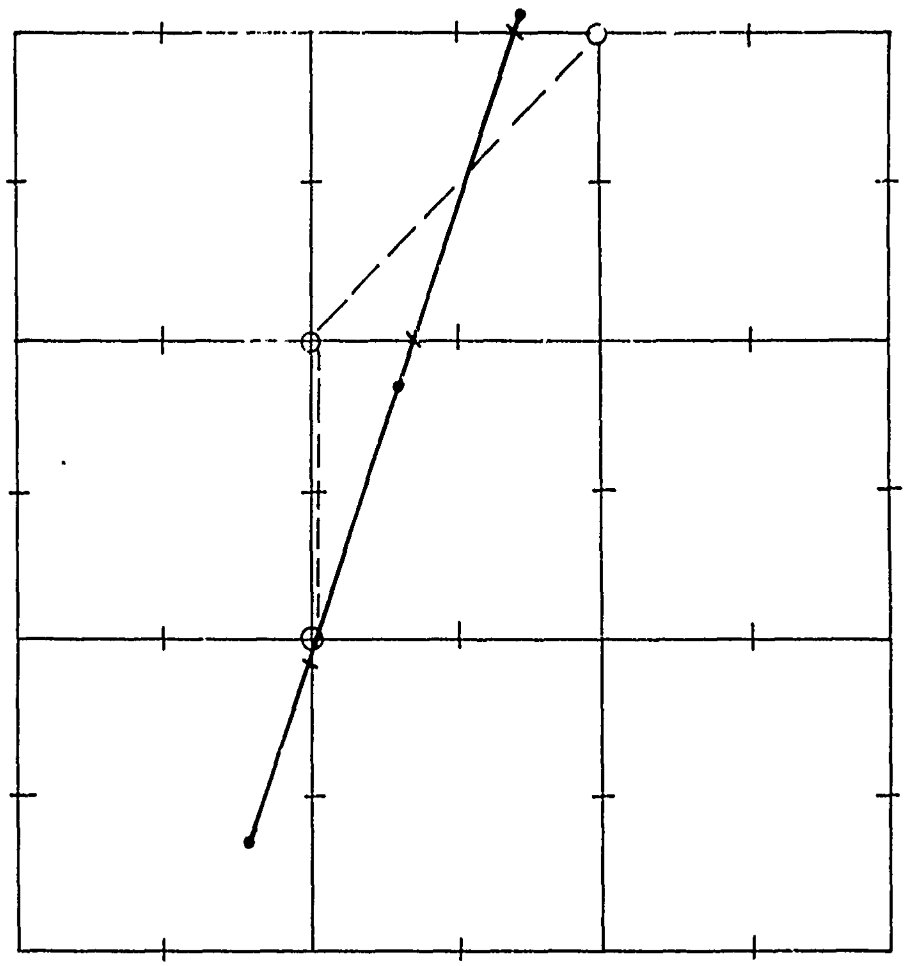

FIG. 29

ANGULAR DISTORTION

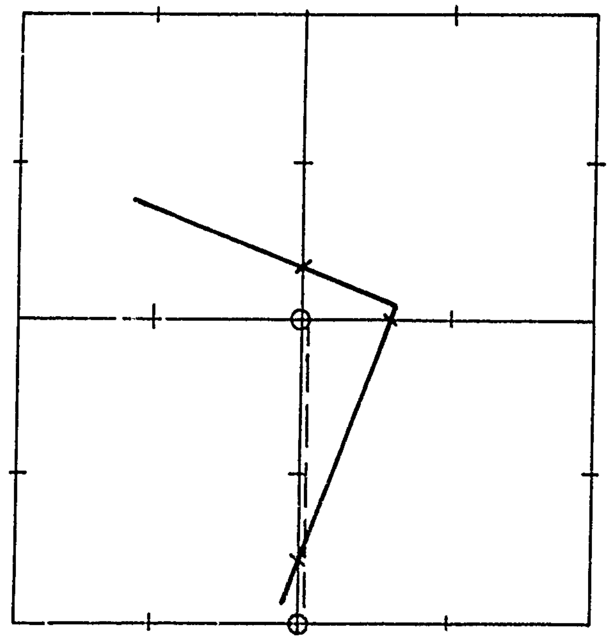

FIG. 30

LENGTH DISTORTION

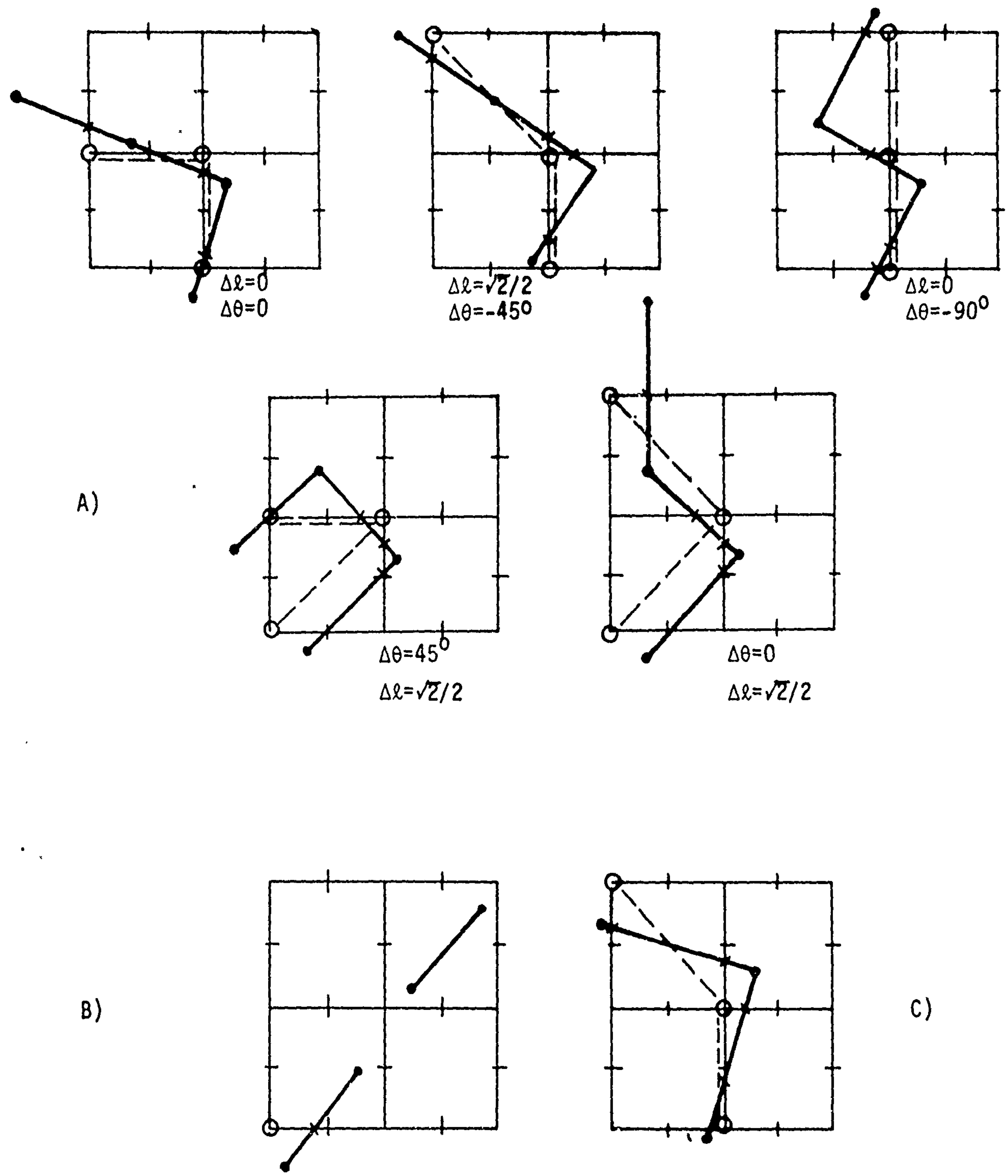


FIG. 31

LENGTH AND ANGULAR DISTORTION FOR A PAIR OF ORTHOGONAL ELEMENTS appear, possibly generating a point as shown in Fig. 31b.

For the case of two $\sqrt{2}$ length orthogonal elements, the output may have an angular distortion of $-45^{\circ}$ as shown in Fig. 31c, and even for the case in which no angular distortion occurs, there might be a length distortion because at least one of the two elements may change its length from $\sqrt{2}$ to 0 or from 1 to 2. In the case of two $\sqrt{2}$ length inverse elements the output may be either equal to the input or it may present length distortion from $\sqrt{2}$ to 0 or from 1 to 2 for both elements.

Finally we have to explore the cases in which the two adjacent elements have different lengths. If the first has a unit length and the second $\sqrt{2}$ and their angle is $\pm 45^{\circ}$ then when the first element generates one element in the output the result may present no angular distortion or no length distortion or both of them as shown in Fig. 32a.

When the first element does not generate an element in the output, then the angular distortion is a function of the type of element preceding the unit element in the input, and, therefore, as shown in Fig. 32b, there may be length distortion together with angular distortion.

When previous elements form an angle of $\pm 135^{\circ}$, this pattern is preserved with the exception of special cases, as shown in Fig. 33a, where the couple of elements may degenerate into one point or one element immediately before and after the original pair. The situation is a little different when the first element of the pair has $\sqrt{2}$ length and the second unit length. If they form an angle equal to $\pm 45^{\circ}$, either this situation is unchanged in the output or a length and angle distortion are introduced

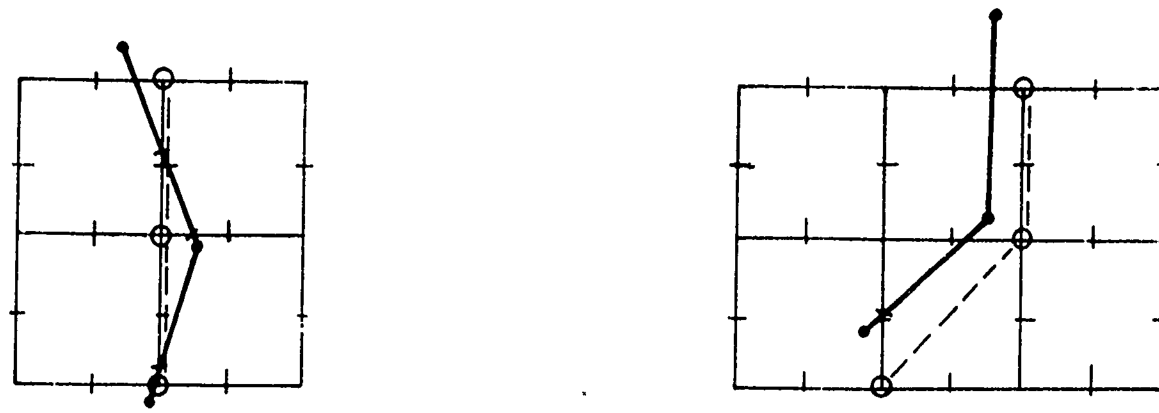

A)

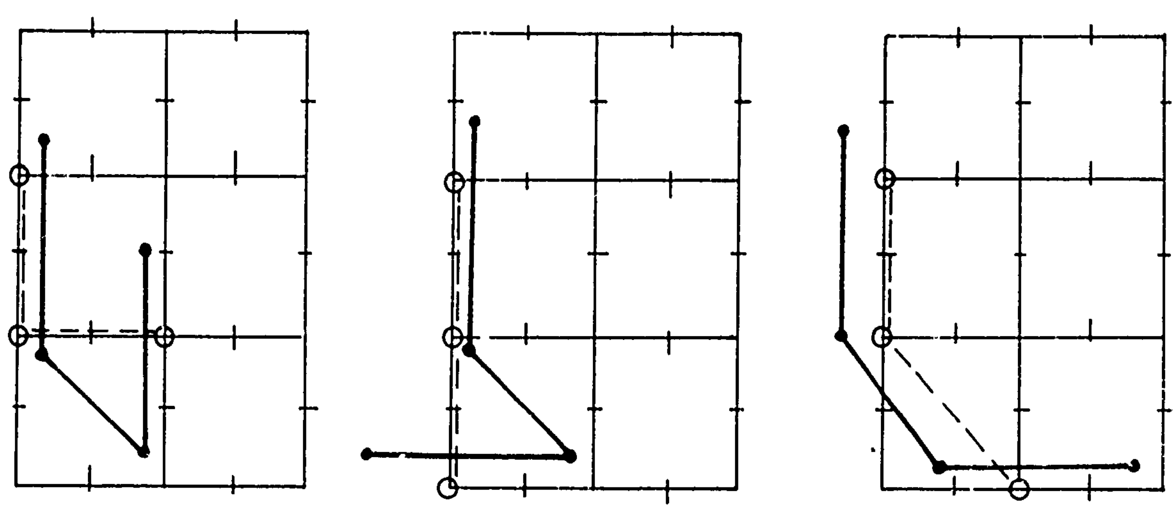

B)

FIG. 32

DISTORTIONS FOR PAIR OF ELEMENTS WITH DIFFERENT LENGTH

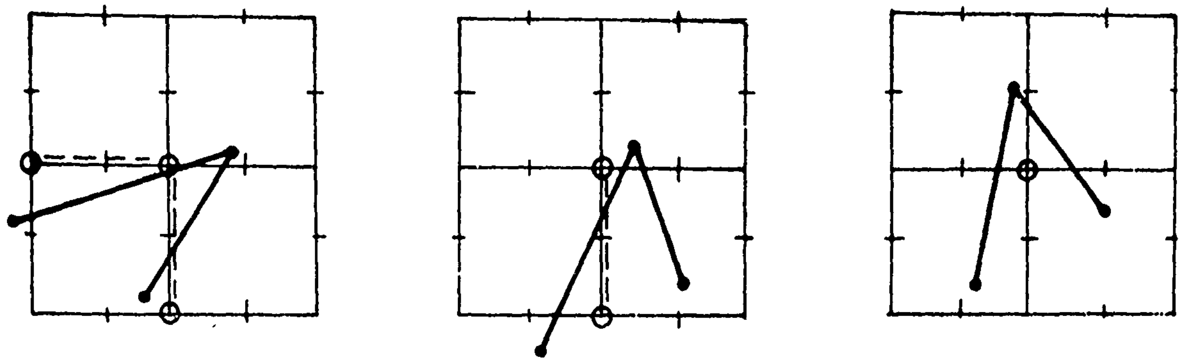

FIG. 33a

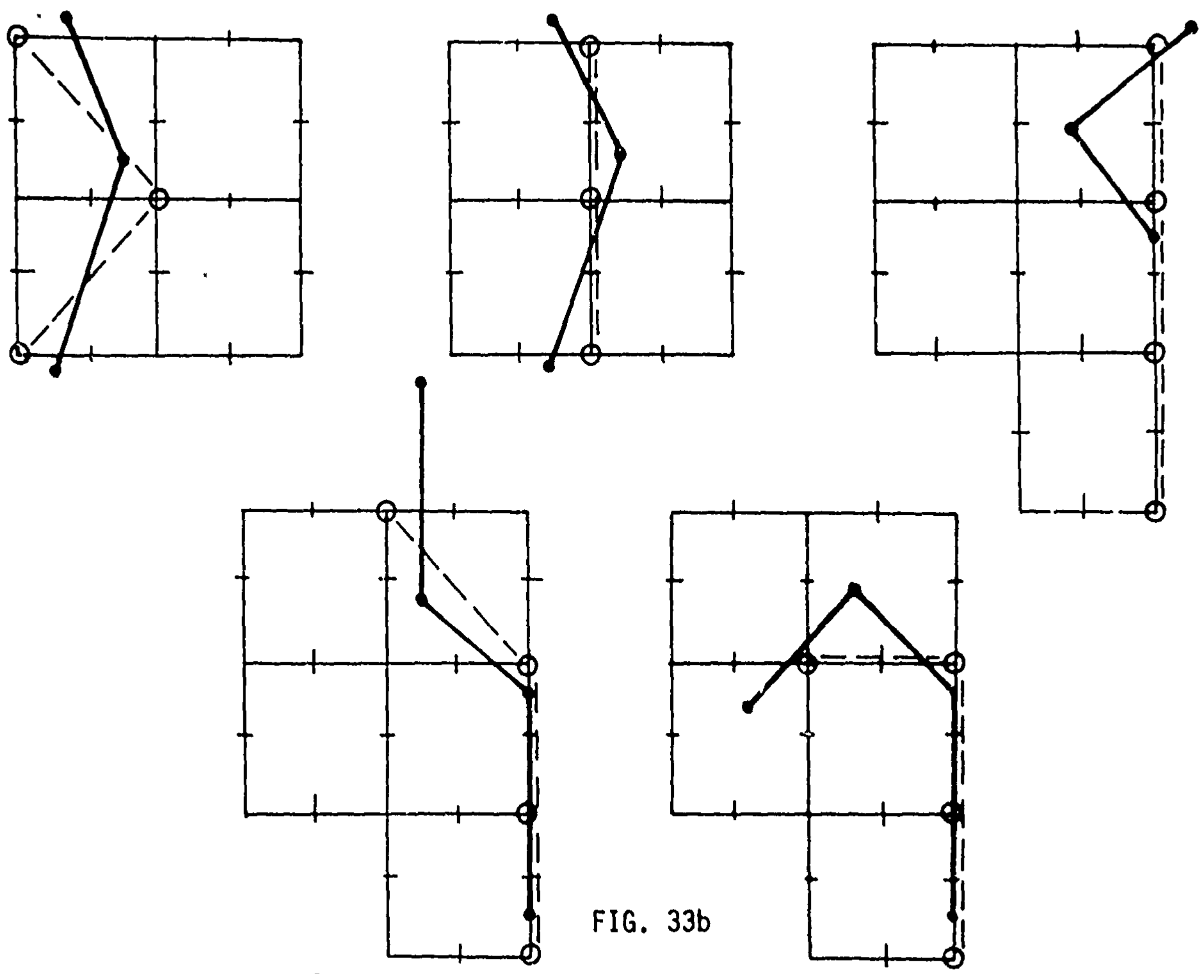

FIG. 33b

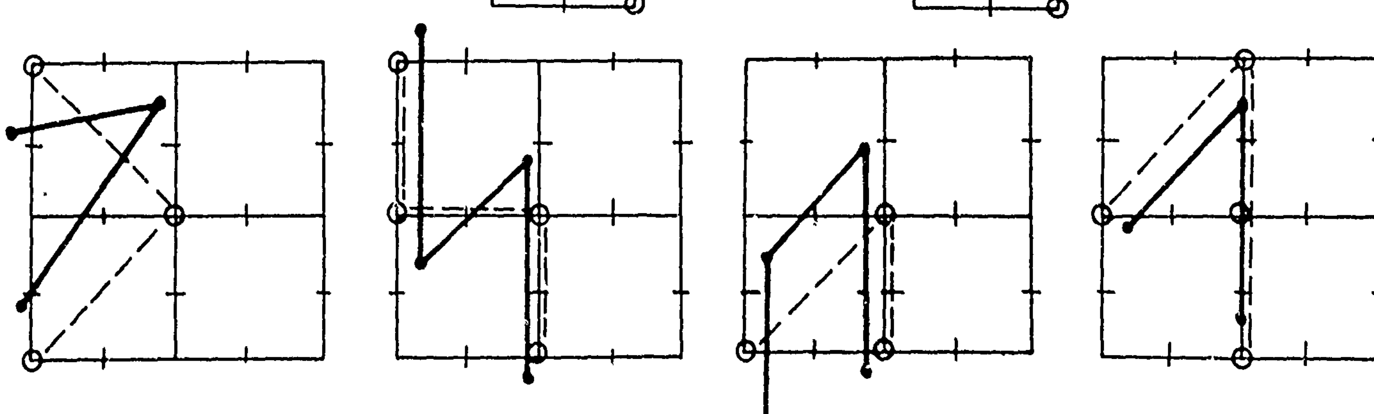

FIG. 33c

DISTORTIONS FOR A PAIR OF ELEMENTS FORMING AN ANGLE LARGER THAN $90^{\circ}$

as illustrated by the pictures in Fig. 33b.

When the input pair form an angle equal to $\pm 135^{\circ}$ this pattern may be preserved in the output or be altered as shown in Fig. 33c.

Previous analysis of distortions due to requantization of segments by applying the grid intersect quantization scheme can be summarized by saying that such a scheme may lead to length distortions with ratios: 0, $\sqrt{2}$, $1/\sqrt{2}$, for single elements and angular distortions up to $\pm 90^{\circ}$ for a pair of adjacent elements. Also elements with unit length may disappear or degenerate into one point. In general given an angle of rotation $\theta$ and a sequence of four adjacent elements, it is possible to specify the type of the worst output which the second and the third element of the sequence will generate after rotation and requantization.

Finally let us note that in previous analysis the case of elements which after rotation are in ambiguous positions like those in Fig. 34 were not included since a solution can always be found by looking at the elements preceding or following them or by sorting a solution arbitrarily (for example in the case of a horizontal straight line segment passing through the midpoints of the grid, as shown in Fig. 34).

Case 2: Square Box Method

Figs. 35a and 35b show the regions A(P) for the case of an element with unit length and $\sqrt{2}$ length respectively. In the case of Fig. 35a, no point exists outside A(P), whereas for Fig. 35b there are more points outside A(P) than inside. Length distortion may occur in both cases. For the one of Fig. 35a in terms of the ratios 0 (when the element is entirely in-

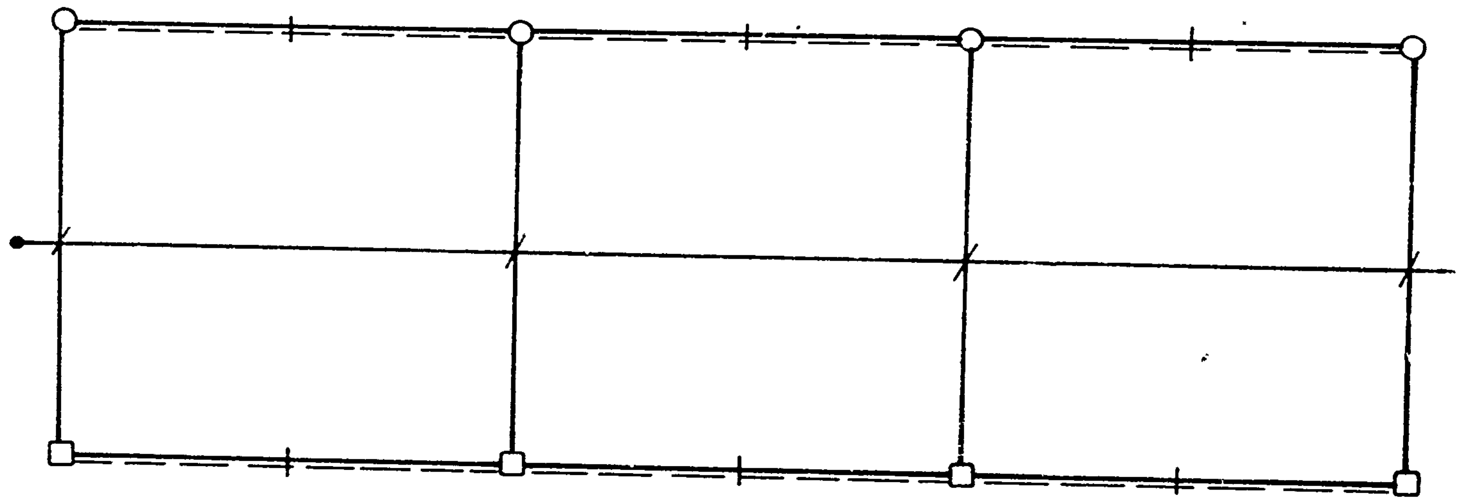

N $\geq$ 2 Equal Elements Crossings the Midpoints of the Grid, Two Solutions

FIG 34

AMBIGUOUS CASE

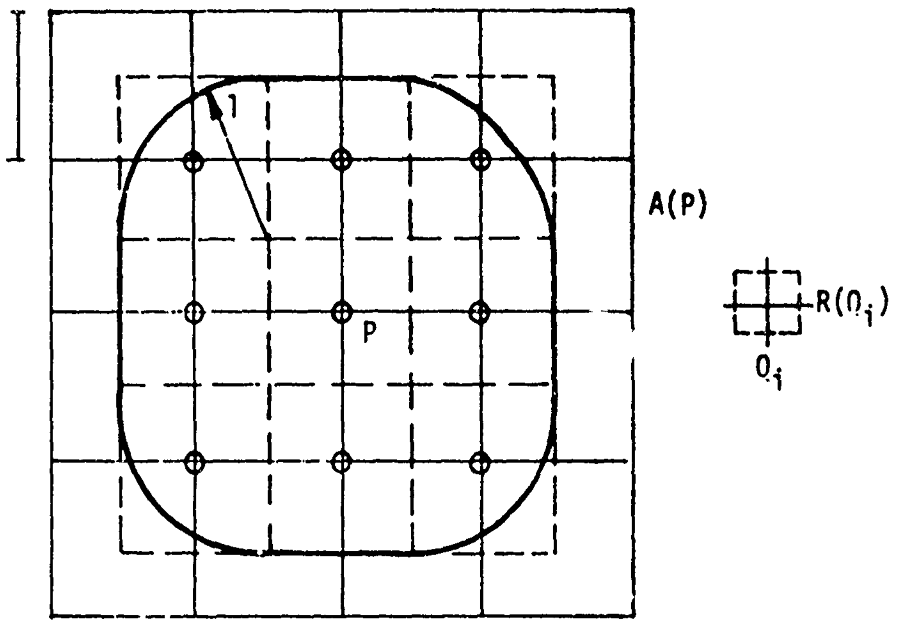


A) Element Length is 1

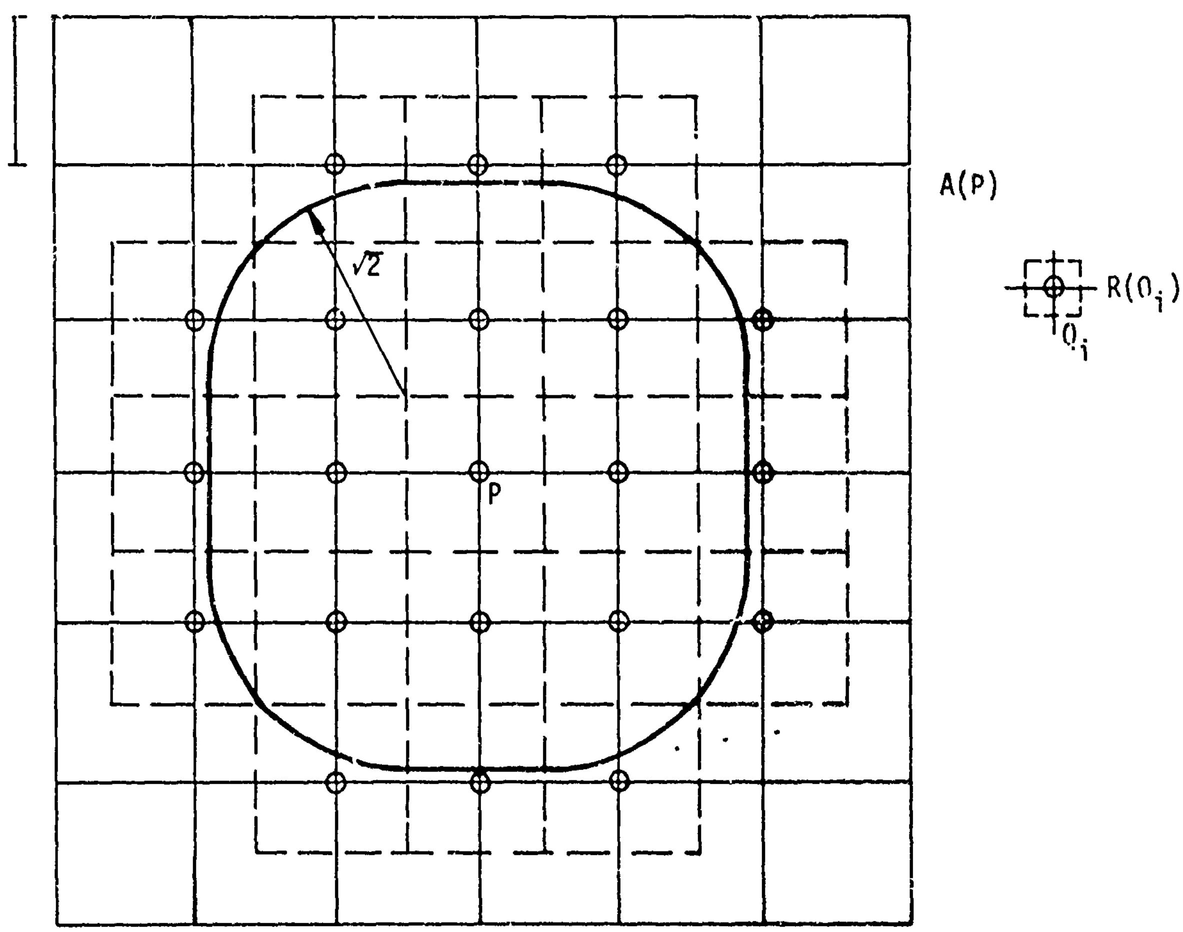


B) Element Length is $\sqrt{2}$

FIG. 35
DISTORTIONS DUE TO SQUARE BOX METHOD

side R(P), or $\sqrt{2}$, and for the case in Fig. 35b in terms of the ratios: 0 or $1\sqrt{2}$ or 2 or $\sqrt{5}/\sqrt{2}$. With this method a point P is assigned as the extreme of an element of the new sequence when there is an arc of input which after rotation passes through the square box centered at point P.

Let us note that the region A(P) of Fig. 35a leads to the same number of selectable points as the one in Fig. 28a, whereas the one in Fig. 35b allows a much wider possibility in terms of selectable points around P than the one in Fig. 28b. Again it is not claimed that each element in the input sequence will generate at least one element in the output because even an element with length equal to $\sqrt{2}$ may be completely inside R(P) after rotation.

Both in the case of Figs. 35a and 35b, no diagonal element can be generated unless after rotation the input element passes precisely through the center of a square of the grid. If this possibility is excluded either on the basis of its low probability of occurrence or because an assignment is given in such situations either on the basis of the positions of other elements, or aribtrarily when no choice can be made uniquely (for example in the case of a straight line segment with unit slope passing through the nodes of the grid), then in both cases of Figs. 35a and 35b an element is either unchanged or it generates zero to two elements (and with an angle of $90^{\circ}$ between them in the last case). This last situation may occur when the input element has a length equal to $\sqrt{2}$; these situations are shown in Fig. 36. Moreover with the assumption of no generation of diagonal elements, the output sequence will consist entirely of elements of unit length.

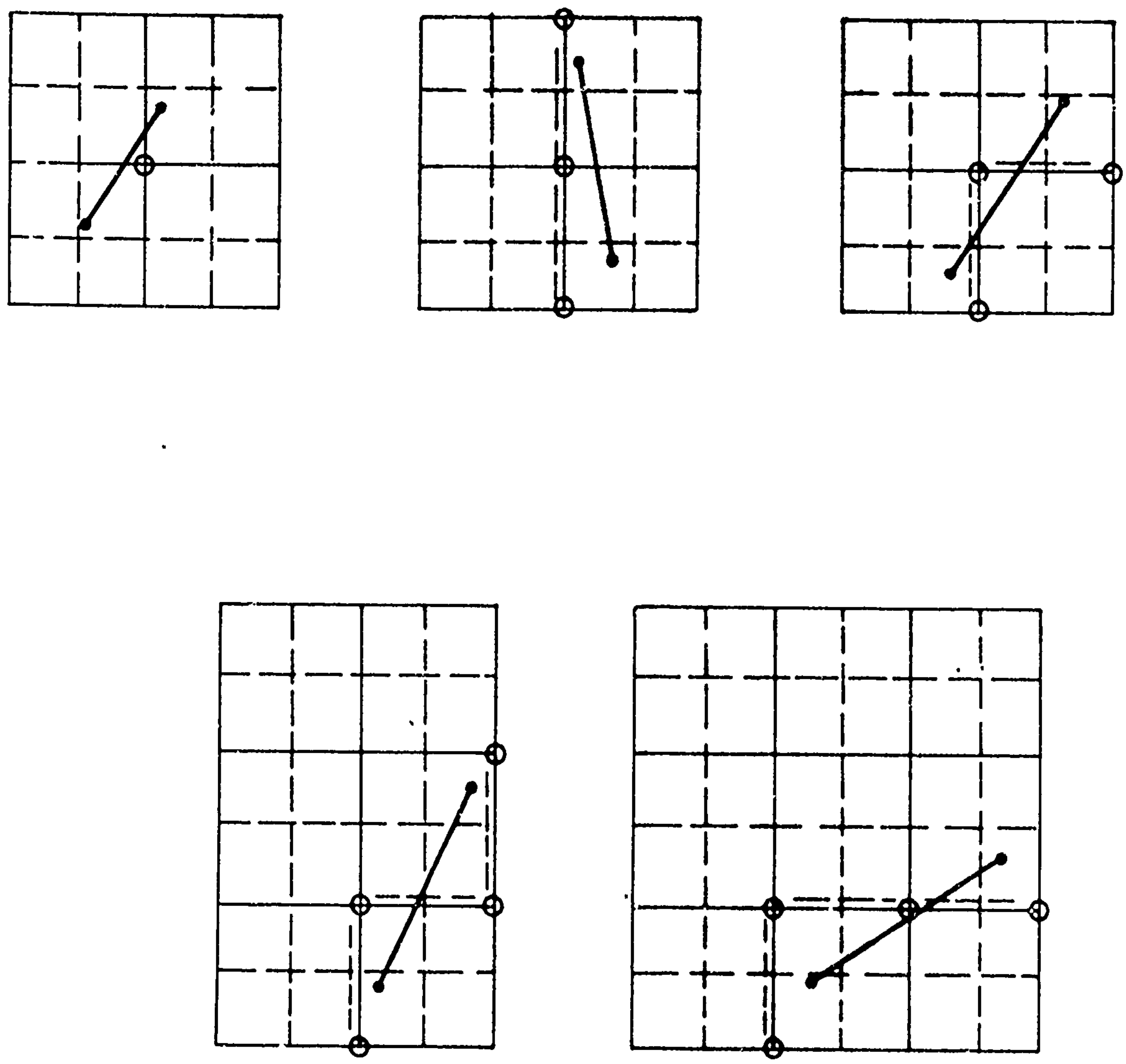

FIG. 36

LENGTH DISTORTIONS

The method described in this section, when compared to that of grid intersection, is subject to more extensive shape distortion in length, angle and number of elements and, moreover, it involves complicated computations for testing which box has sensed the input sequence after rotation. A way for improving this method is to modify it into the one described in the next paragraph.

Case 3: Rounded Coordinates Method

Consider a scheme in which the coordinates of the extreme points of each element after rotation are rounded off and the resulting values used to define the grid points for generating the output. Domains A(P) of Figs. 35a and 35b are still valid, but now diagonal elements can be generated in the output; the ambiguity of an element in a position such as the one described by Fig. 34 leads now to four possible points which can represent each center of a grid square. We will suppose here that such ambiguous situations will never occur. However, they may be resolved by giving simple decision rules as hinted before.

A different kind of ambiguity arises for the case of Fig. 35b when a $\sqrt{2}$ length element generates two elements in the output. In this case one may assume that a choice is made by rounding the coordinates of the midpoint of the input element. When one element in the input generates one element in the output, length distortion may be specified by factors like 0 or $\sqrt{2}$ for the case of Fig. 35a, and 0, $1/\sqrt{2}$ or $\sqrt{2}$ for the case of Fig. 35b; when a $\sqrt{2}$-length element generates two elements in the output, there is both the generation of a corner of $45^{\circ}$ and a length distortion of $\sqrt{5}/\sqrt{2}$. Angular distortion is $\pm 45^\circ$ for the case of Fig. 35a, which corresponds to the one described in Fig. 28a, and the same is true for the case of Fig. 35b, where one element is generated; when two elements are generated their angle may be either 0 with length distortion equal to $\sqrt{2}$, or $45^\circ$ with length distortion equal to $\sqrt{5}/\sqrt{2}$. In the case of pairs of elements, the many possible configurations are similar to the ones studied before for the case of the grid-intersect quantization method.

Case 4: Diamond and Circular Boxes Methods

Regions A(P) for the cases of diamond and circular-box methods are shown in Figs. 37a and 37b and in Fig. 38a and 38b respectively. Since they do not offer any significant advantages over the previous methods but do require more involved computations, these two methods will not be studied in further detail.

Case 5: Modified Grid-Intersect Method

A modified grid-intersect method can be defined for which each input element generates only one output element. Such a method, for example, will exclude from A(P) of Fig. 28b the four points lying outside of A(P), and when an element in a non-ambiguous position disappears, then the rounded coordinates method will be used if it leads to an output; otherwise the length of the element is changed in such a way as to allow the generation of an output (for example the length can be changed from 1 to 2).

It is easy to check that this scheme does not interrupt the continuity of adjacent elements in the output. Also note that it generates

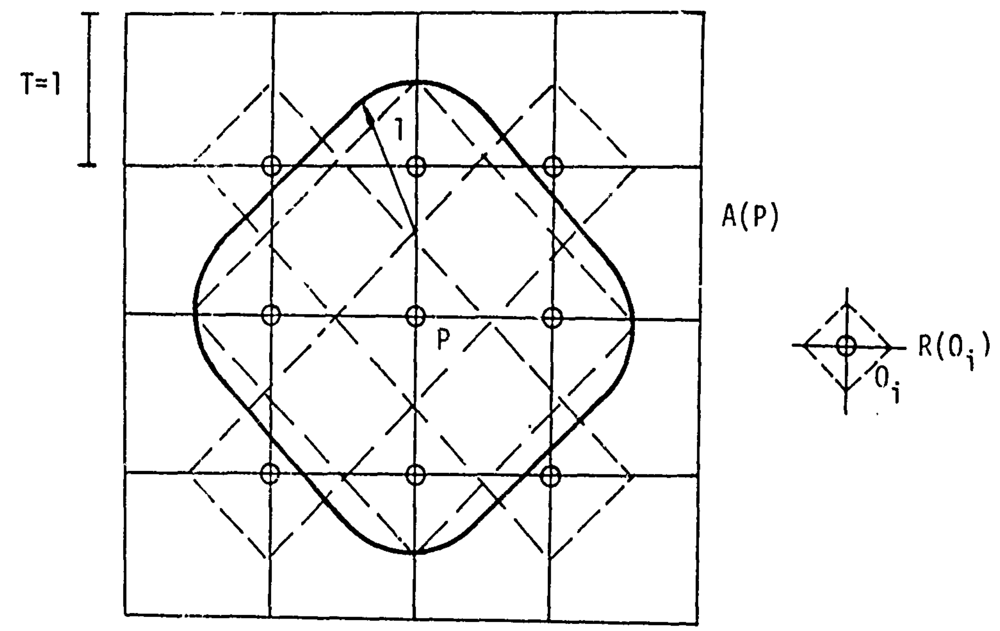


A) Element Length is 1

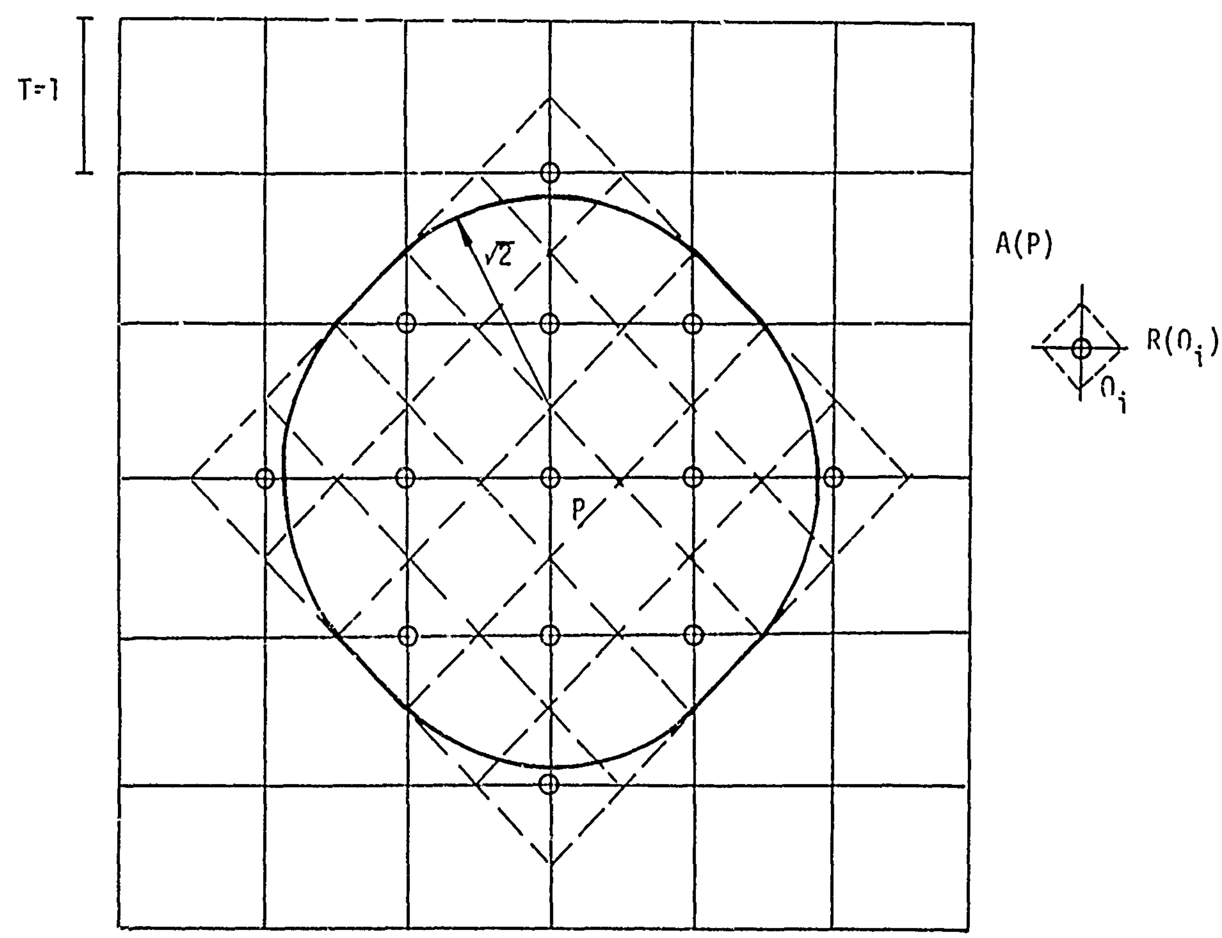


B) Element Length is $\sqrt{2}$

FIG. 37
DISTORTIONS DUE TO DIAMOND BOX METHOD

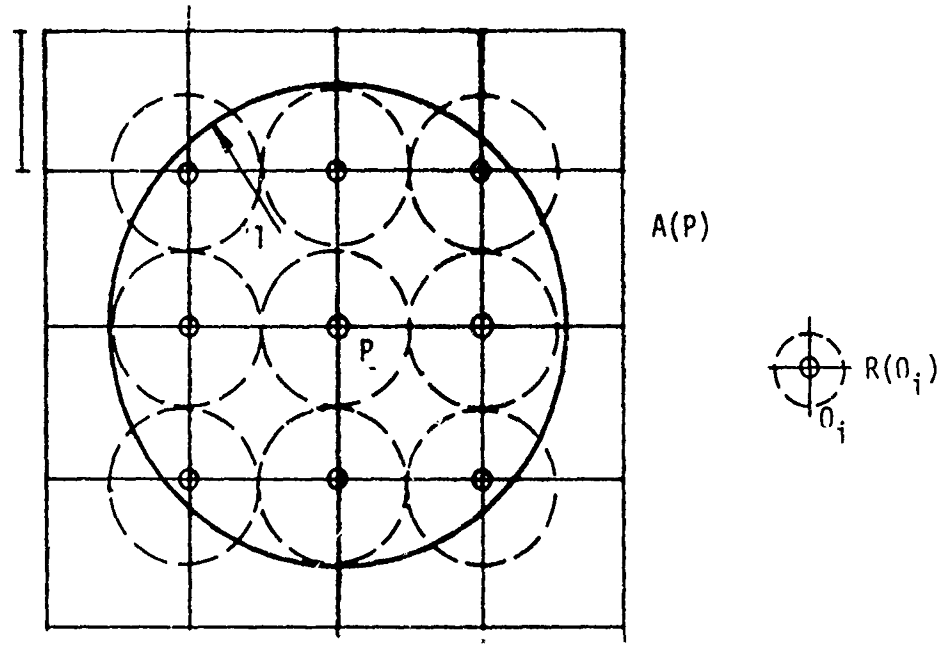


A) Element Length is 1

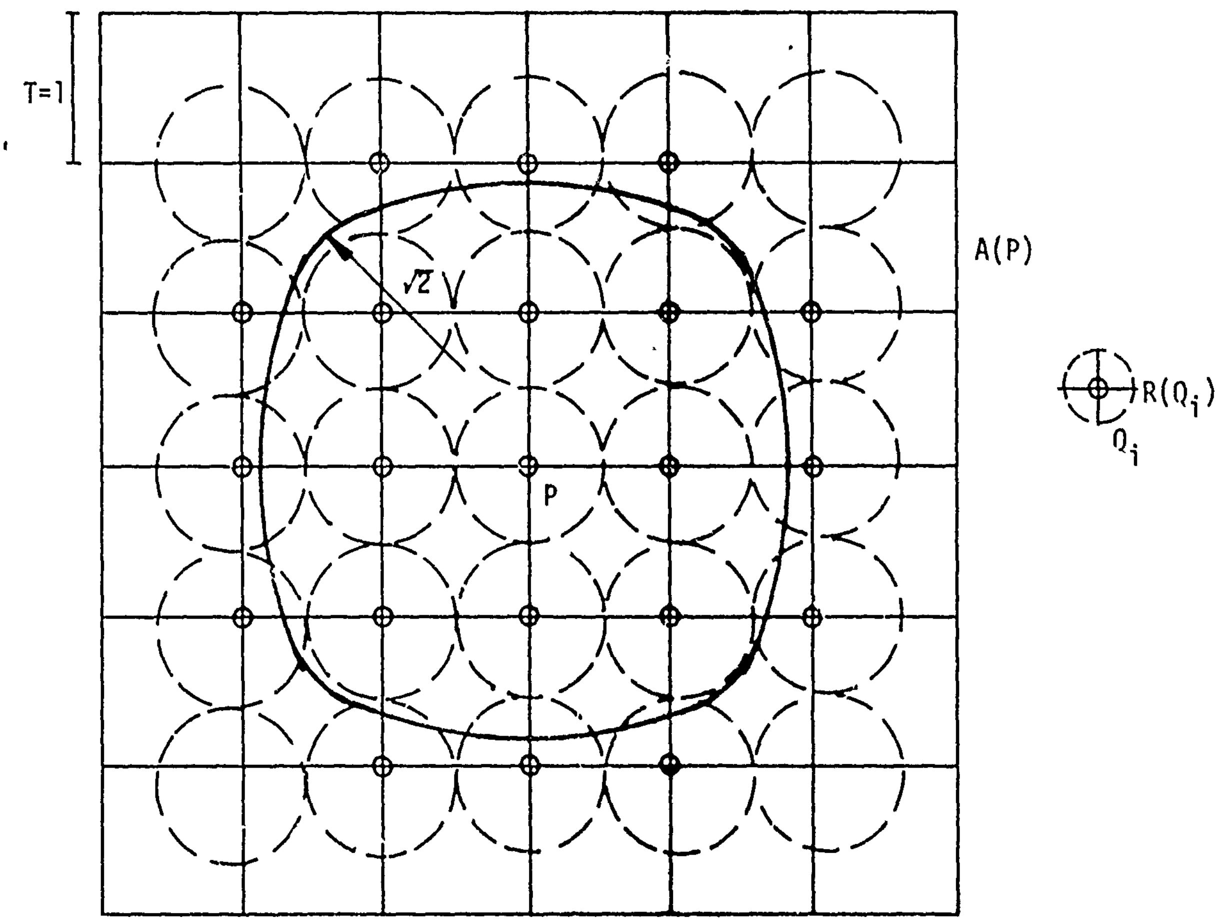


B) Element Length is $\sqrt{2}$

FIG. 38

DISTORTIONS DUE TO CIRCULAR BOX METHOD

length distortions which are at most given by factors $1/\sqrt{2}$ or $\sqrt{2}$, and angular distortions of at most $\pm 45^{\circ}$ for a single element.

An analysis has been presented of the noise generated by requantizing rotated data in terms of a variety of quantization schemes. Emphasis has been placed on the grid-intersect method which offers a lower length and angular distortion with respect to any other standard quantization scheme. It has been shown, however, that such a method leads to more complicated computations than the rounded coordinates method, which can be easily simulated on a digital computer by simply truncating numbers. When the quality of the output is more important than computational cost, then one should use the grid-intersect method rather than the one of rounded coordinates. Finally, a modified grid-intersect method, which combines the advantages of both the grid-intersect method and the one of rounded coordinates, has been proposed.

In the next section the modified grid-intersect quantization scheme will be compared with the one proposed in this thesis. Such comparison will be based on the values of the figures of merit for the two quantization methods. As will be shown, the quantization scheme described in Chapter II tends to have a smaller figure of merit and, therefore, to give better results on average.

## 7.2 Comparison Between Modified Grid-Intersect Scheme and Proposed New Scheme

A comparison will now be made between the proposed scheme and the modified grid intersect quantization scheme in terms of their figures of merit, as these are defined in this thesis. In carrying out this comparison it will be supposed that in both cases the original line drawing has been finely quantized, that is, its local behavior around any grid node is essentially that of a straight line segment. The assumption is then made that in its quantized version such a drawing consists of $N_2$ chain-encoded straight line segments with an average of $N_1$ chain elements each.

Case 1: Area-Type Figure of Merit

From (5.4), (6.45), (6.46)

$$f_{m_a} = N \sum_{i=1}^{N} a_i/T \sum_{i=1}^{N} \ell_i$$

For the proposed quantization scheme we have:

$$f_{m_{a_1}} = \frac{T}{2} N_2 \sum_{i=1}^{N_2} \ell_i/T \sum_{i=1}^{N_2} \ell_i = \frac{N_2}{2} \qquad (7.1)$$

and for the modified grid intersect quantization scheme, we have:

$$f_{m_{a_2}} = \frac{T}{2} TN_1N_2 N_1N_2/T TN_1N_2 = N_1 \frac{N_2}{2} \qquad (7.2)$$

clearly,

$$f_{m_{a_2}} > f_{m_{a_1}} \quad \text{for } N_1 > 2 \qquad (7.3)$$

Case 2: Displacement-Type Figure of Merit

From (5.8), (6.45), (6.46)

$$f_{m_\ell} = N \sum_{i=1}^{N} \delta_i/TN$$

For the proposed quantization scheme we have:

$$f_{m_{\ell_1}} = \frac{\sqrt{2}}{2}\, N_2 \quad TN_2/TN_2 = \frac{\sqrt{2}}{2}\, N_2 \tag{7.4}$$

and for the modified grid intersect quantization scheme we have:

$$f_{m_{\ell_2}} = \frac{T}{2}\, N_1 N_2 \; N_1 N_2/TN_1 N_2 = N_1 \frac{N_2}{2} \tag{7.5}$$

Again,

$$f_{m_{\ell_2}} > f_{m_{\ell_1}} \quad \text{if} \quad N_1 > 2 \tag{7.6}$$

<u>Case 3: Staircase-Effect-Type Figure of Merit</u>

From (5.16), (6.45), (6.46)

$$f_{m_{S.E.}} = \frac{1}{M} \sum_{i=1, i\varepsilon I}^{M} \frac{\ell_i}{\ell_s} \; \frac{\ell_{i+1}}{\ell_s} \; \frac{\tan|\Delta\beta_i|}{\theta_s}\, M$$

For the proposed quantization scheme we have:

$$f_{m_{S.E._1}} = \frac{1}{N_2} \; \frac{N_1^{\,2}\, T^2 \tan\Delta\theta}{\ell_s^{\,2}\;\theta_s}\; N_2^2$$

$$= N_2 N_1 \frac{T^2 \sqrt{2}}{\ell_s^{\,2}\;\theta_s} \; \frac{\tan\Delta\theta}{\sqrt{2}}\; N_1 \tag{7.7}$$

and for the modified grid intersect quantization scheme we have:

$$f_{m_{S.E._2}} = \frac{1}{N_1 N_2} \; \frac{T^2 \sqrt{2}}{\ell_s^{\,2}\;\theta_s} \; N_1 N_2 \; N_1 N_2$$

$$= N_1 N_2 \frac{T^2 \sqrt{2}}{\ell_s^{\,2}\;\theta_s} \tag{7.8}$$

Therefore, we can write

$$f_{m_{S.E._1}} = f_{m_{S.E._2}} \frac{\tan \Delta\theta}{\sqrt{2}} N_1 \tag{7.9}$$

as shown in Table II (which has been derived directly from Table I by assuming an average number of chain elements $N_1 = \frac{N_{min} + N_{max}}{2}$) it is always true that

$$\bar{N}_1 \tan \Delta\theta << \sqrt{2} \tag{7.10}$$

for $N_1 > 2$. Hence it can be concluded that, as in the previous two cases,

$$f_{m_{S.E._1}} > f_{m_{S.E._2}} \quad \text{if} \quad N_1 > 2 \tag{7.11}$$

Since the higher the figure of merit, the higher the cost for the same quality, or the lower the quality for the same cost, we can conclude that, in terms of their average figures of merit, the proposed quantization scheme tends to give a more satisfactory performance in terms of quality of description and transformation cost.

| $N_1$ | $\tan \Delta\theta$ | $N_1 \tan \Delta\theta$ |
|---|---|---|
| 1 | 1 | 1 |
| 10 | 0.03 | 0.3 |
| 100 | 0.002 | 0.2 |
| 1,000 | 0.0003 | 0.3 |
| 2,000 | 0.00015 | 0.3 |
| 20,000 | 0.000005 | 0.01 |

TABLE II

# VIII. APPLICATION PROGRAM AND RESULTS

## 8.1 General

In this chapter after a brief outline describing an application program in terms of its input and output data and type of computations executable by it, the results of such a program will be shown and explained. A copy of the listings of the program may be obtained from Professor H. Freeman of New York University.

### A) Input Data

A set of connected straight line segments represents the drawing, as an abstraction of an image, as a digital computer sees it through an input flying spot scanning unit. The proposed quantization scheme is then applied to it and a quantized version is obtained. By comparing the input with the quantized version, the input values for the figures of noise are obtained.

### B) Output Data

Consists of two transformed data: the first for the input drawing and the second for the quantized version. Again noise figures are evaluated by comparing the transformed input with the transformed quantized version of it. Checks are then made to verify the predictions of the theory presented in this thesis, like for example the relations between input and output noise and their dependence on the particular transformation. Also the figures of cost and merit are evaluated and the bounds predicted by the theory here developed checked.

c) General Comments

The program executes rotations, isotropic and non-isotropic scalings, linear transformations and Mercator projections of quantized data (with the restrictions on the dynamic range of the input data imposed by the Basic Fortran formats for single precision operations). The program also evaluates the figures of noise, cost and merit by computing areas and lengths and by plugging these values in the formulas presented in this thesis. Also the program allows one to select the precision of the input quantization so that a given bound on the output noise can be satisfied.

## 8.2 Results of the Program

In order to give a complete presentation of the options offered by the proposed quantization scheme, three types of examples are shown in the following pages.

The first example refers to a direct approach in quantizing the data to be transformed. The transformation M, the drawing L and the precision parameters $k$, $k_\alpha$, $k_\ell$, $\bar{\alpha}_{max}$, $p_\ell$, $p_\theta$ are given. (Note that because of the relations shown at the end of Chapter II only four of previous parameters are independent from the others). Then the quantized drawing $L^*$ can be generated and $\ell$, $\theta$, T, n can be evaluated. The transformed $L^*$, $TL^*$, the input and output figures of noise, cost and merit are computed by making measures on $L^*$ and $TL^*$. Fig. 39 shows the block structure of the system. When the direct approach is taken the loop in the system is open and no bound on the output is applied at the input (SW1 and SW2 are

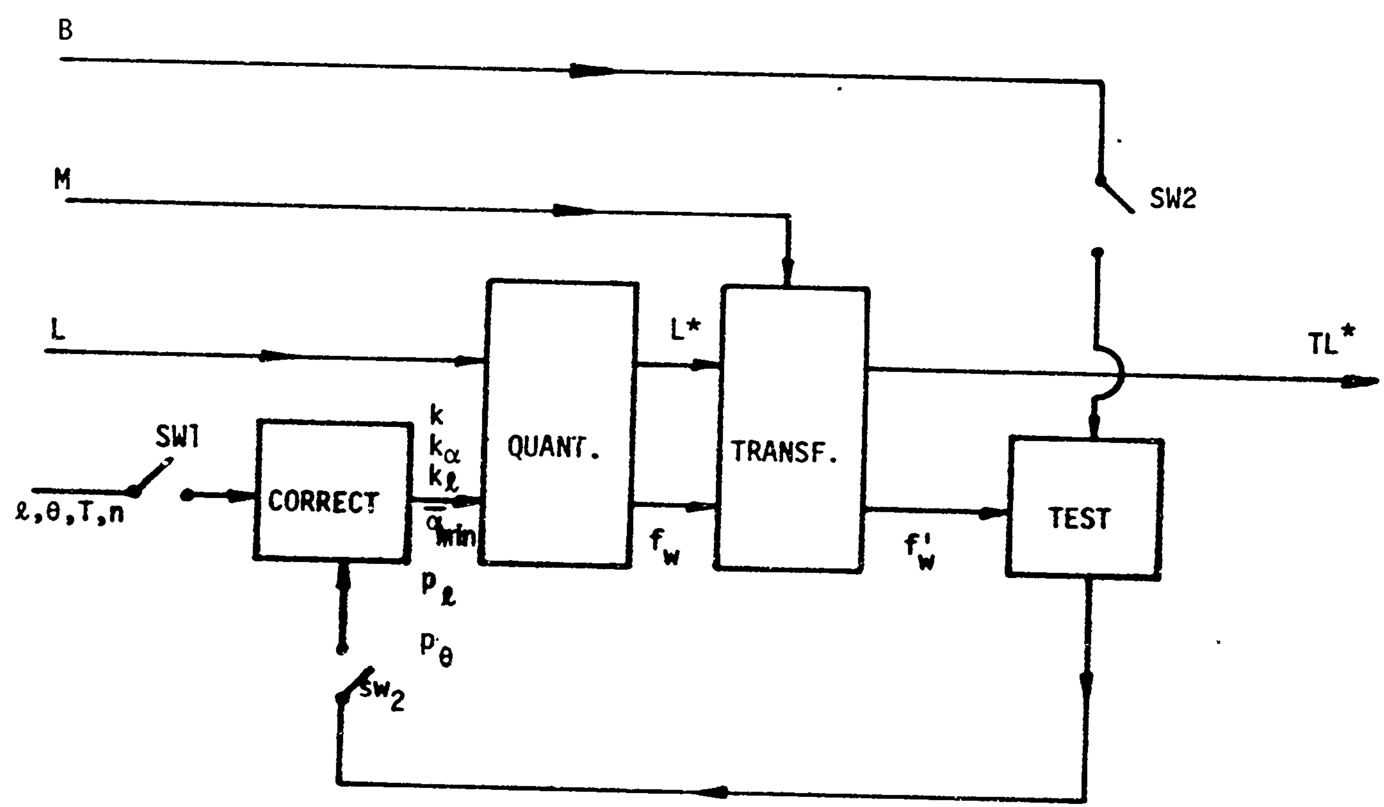


FIG. 39
BLOCK DIAGRAM

open).

The second example refers to an indirect approach because the precision parameters are not given directly but through $\ell$, $\theta$, T, n by applying (with the equal sign) the inequalities shown at the end of Chapter II. Such relations are $k=T/n\ell$, $k_\alpha=1+4/\theta \tan^{-1}\frac{T/\sqrt{2}}{2\ell}$, $k_\ell=1+\sqrt{2}\,\frac{T}{\ell}$, $\bar{\alpha}_{min}=\theta+4\tan^{-1}\frac{T/\sqrt{2}}{2\ell}$, $p_\ell=T\,\frac{\sqrt{2}}{2\ell}$, and $p_\theta=\frac{2}{\theta}\tan^{-1}(\frac{T\sqrt{2}}{2\ell})$. Again the loop in the system is open (SW1 is closed and SW2 is open) and $L^*$ is generated by finding first $k$, $k_\alpha$, $k_\ell$, $\bar{\alpha}_{min}$, $p_\ell$, $p_\theta$ and by applying the algorithm presented in Chapter II.

The third example refers to an inverse approach. In this case a bound B on the output figures of noise is the only given input value instead of the four parameters $\ell$, $\theta$, T, n. However n can be computed from B as was shown at the end of Chapter VI by assuming that the grid contribution to the figures of noise is negligible, that is that the following relation is fulfilled

$$\frac{2\sqrt{2}\,T}{\ell}\quad\frac{\theta+1}{\theta} << 1$$

This relation defines T once $\ell$ and $\theta$ are given. On the other hand $\ell$ and $\theta$ are the minimum detail parameters of $L^*$, that is the already quantized drawing. In order to find them their values are predicted and $L^*$ generated. Then the new values for $\ell$ and $\theta$ are measured on $L^*$ and a new value for T is computed from previous formula. (n is still the same since it only depends on B). Then the new values are used to requantize L and generate a new $L^*$ and the process is repeated. This procedure halts once the old and the new values of $\ell$ and $\theta$ coincide (or differ, say, by less than 10% as in the example). In this example SW1 is open and SW2 is closed and stays closed up to when the condition on $\ell$ and $\theta$ is verified.

A) Direct Approach

In Fig. 40a, 40b, 40c, 40d are shown, respectively, the input drawing L, its quantized version $L^*$, and the transformed L and $L^*$. The transformation is a rotation by $60^\circ$. The following precision parameters have been used:

$$k = 0.36$$
$$k_\alpha = 1.84$$
$$k_\ell = 1.072$$
$$\bar{\alpha}_{min} = 18^\circ (0.33 \text{ rad})$$
$$p_\ell = 0.036$$
$$p_\theta = 0.42$$

They define $\ell$, $\theta$, T, and n as follows

$$\ell = 19.1$$
$$\theta = 10^\circ \ (0.17 \text{ rad})$$
$$T = 1$$
$$n = 0.15$$

Input and output figures of noise were computed by comparing L with $L^*$ and TL with $TL^*$ (i.e., the transformed L and $L^*$). All the constraints predicted by the theory are satisfied both for the figures of noise and those of merit. The figures of merit, their bounds as well as the figure of cost have been normalized by assuming $K_r = 1$. We have:

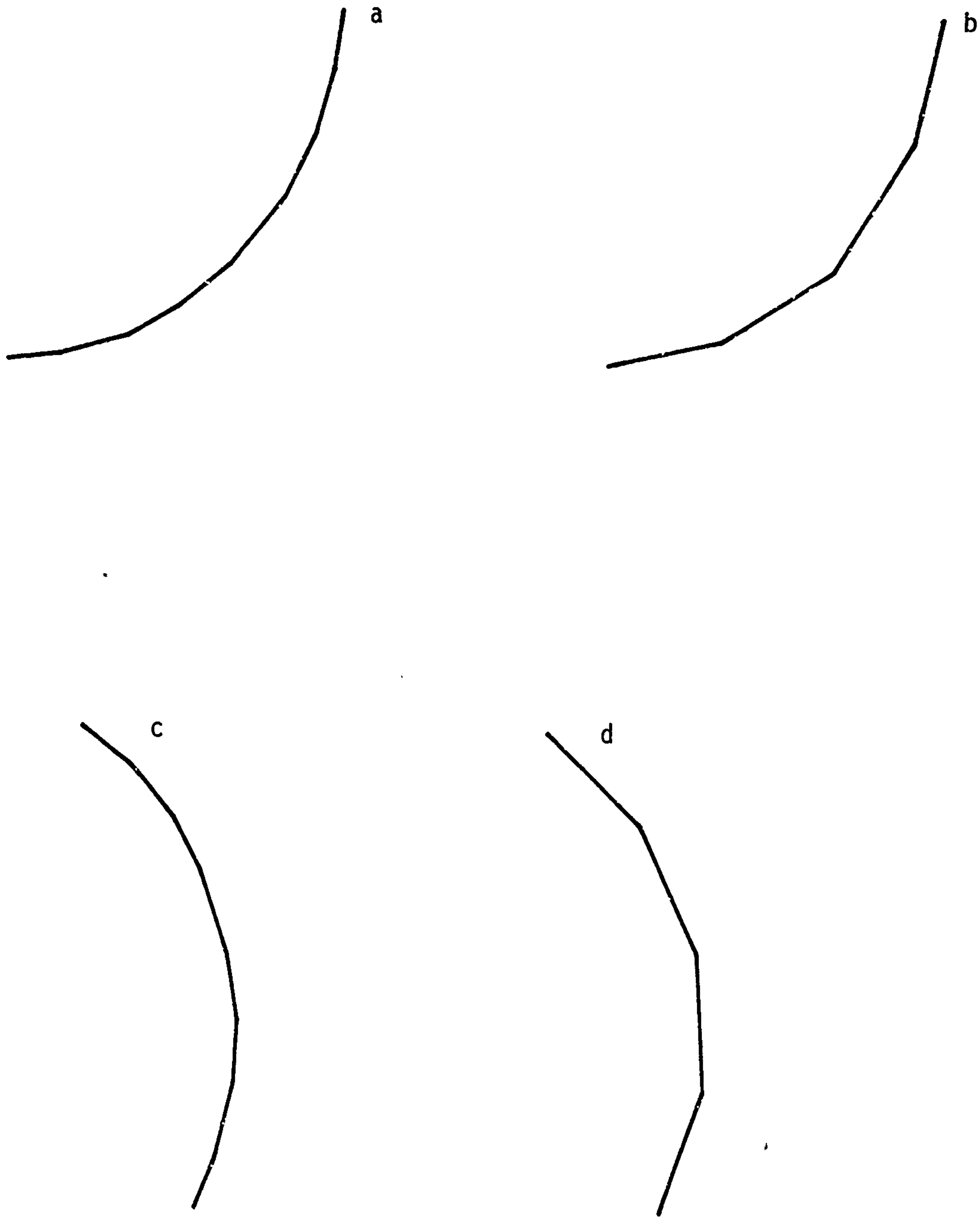


FIG. 40

PROGRAM RESULTS FOR ROTATION

$f_{w_a} = 5.41 < 7$ ; $f'_{w_a} = 6.23 < 7$

$f_{w_\ell} = 5.8 < 7$ ; $f'_{w_\ell} = 6.35 < 7$

$f_{w_{S.E.}} = 4.66 < 7$ ; $f'_{w_{S.E.}} = 4.71 < 7$

$f_c = 5$ ; $f_{m_a} = 31.15 < 35$

$f_{m_\ell} = 31.75 < 35$ ; $f_{m_{S.E.}} = 23.25 < 35$

B) Intermediate Approach

Figs. 41a, 41b, 41c, 41d show, respectively, the drawing L, its quantized version $L^*$, and the transformed L and $L^*$. The transformation is a non-isotropic scaling by a factor of 1 in the X direction and a factor of 2.3 in the Y direction. (Then we have $B_2 = 2.3$ and $B_2^2 = 5.29$). Precision parameters $\ell$, $\theta$, T, n were chosen as follows:

$$\ell = 19.1$$
$$\theta = 10^\circ \text{ (0.17 rad)}$$
$$T = 1$$
$$n = 0.15$$

They lead to the following values for the precision parameters

$k = 0.36$ ; $\bar{\alpha}_{min} = 17^\circ$ (0.33 rod)

$k_\alpha = 1.84$ ; $p_\ell = 0.036$

$k_\ell = 1.072$ ; $p_) = 0.42$

Input and output figures of noise, cost and merit are

$f_{w_a} = 5.41 < 7$ ; $f'_{w_{S.E.}} = 28.5 < 37.03$

$f_{w_\ell} = 5.8 < 7$ ; $f_c = 5$

$f_{w_{S.E.}} = 4.65 < 7$ ; $f_{m_a} = 65.05 < 80.5$

$f'_{w_a} = 13.01 < 16.1$ ; $f_{m_\ell} = 71.5 < 80.5$

$f'_{w_\ell} = 14.3 < 16.1$ ; $f_{m_{S.E.}} = 142.5 < 185.15$

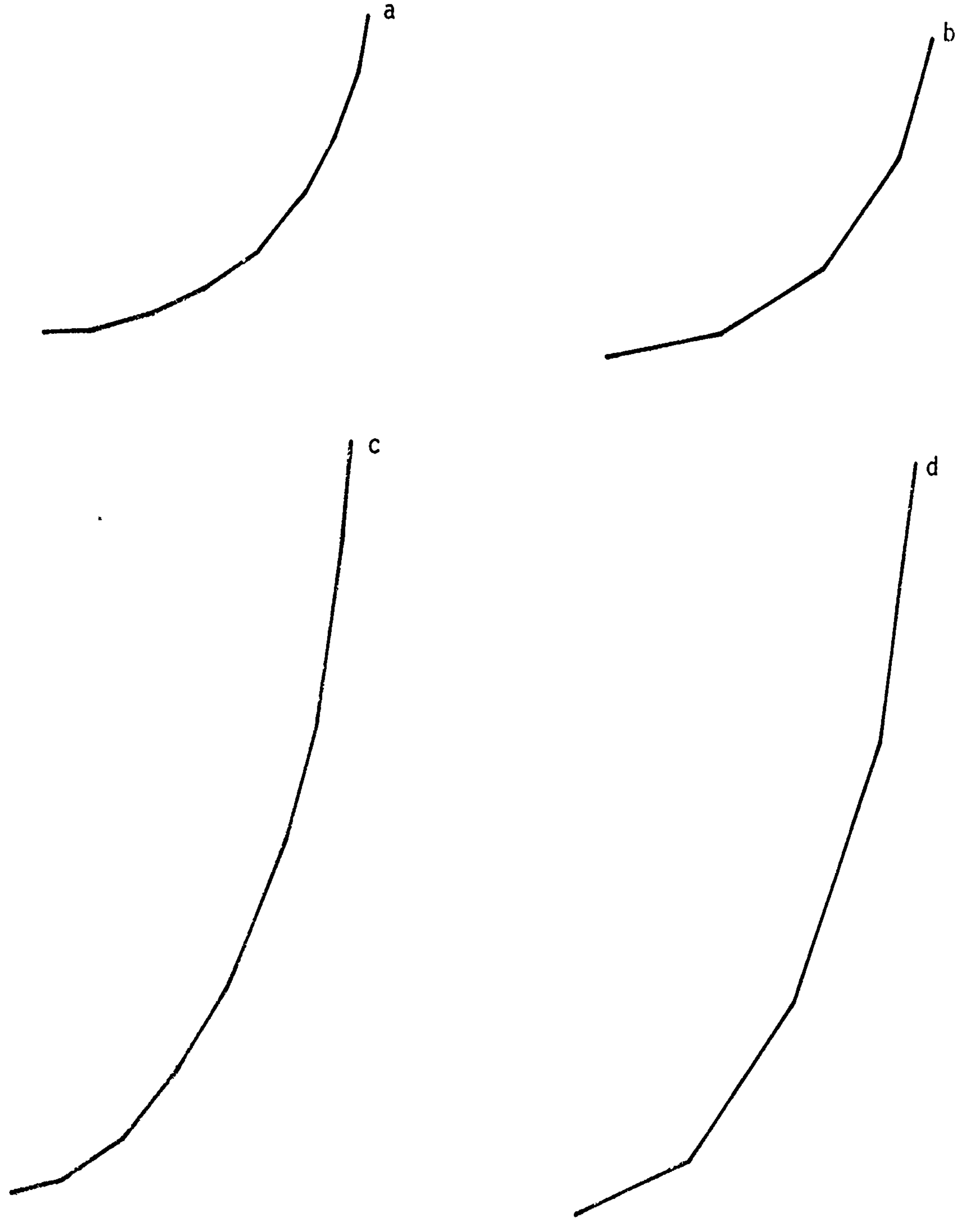


FIG. 41

PROGRAM RESULTS FOR NON-ISOTROPIC SCALINGS

As can be easily seen all constraints predicted by the theory are satisfied.

C) Inverse Approach

Figs. 42a, 42b, 42c, 42d show respectively L, $L^*$, TL, $TL^*$. The transformation is a Mercator Projection defined by the following constants R=150, F=150, ALP=0, P=450 respectively the radius of the sphere, the focal length of the camera, the latitude of the satellite from which the picture was taken (the longitude is assumed to be zero) and the distance of the center of projection from the center of the sphere.

The bound on the output noise was chosen as B=20. Since the transformation is characterized by $B_2=1.8$ ($B_2^2=3.24$) then we have $n=0.16 (1/n=6)$.

Two cycles were necessary for finding a stable solution. We had the following:

Cycle #1

| Predicted Value | Measured Value | Error in % |
|---|---|---|
| $\ell=30$ | $\ell=23$ | 21 |
| $\theta=24^\circ$ (0.41 rad) | $\theta=18^\circ$(0.31 rad) | 20 |

The computed value for T was $T = 3$

Cycle #3

| Predicted Value | Measured Value | Error in % |
|---|---|---|
| $\ell=23$ | $\ell=22.5$ | 2 |
| $\theta=18^\circ$(0.31 rad) | $\theta=17^\circ$(0.29 rad) | 5 |

The computed value for T was $T = 1$

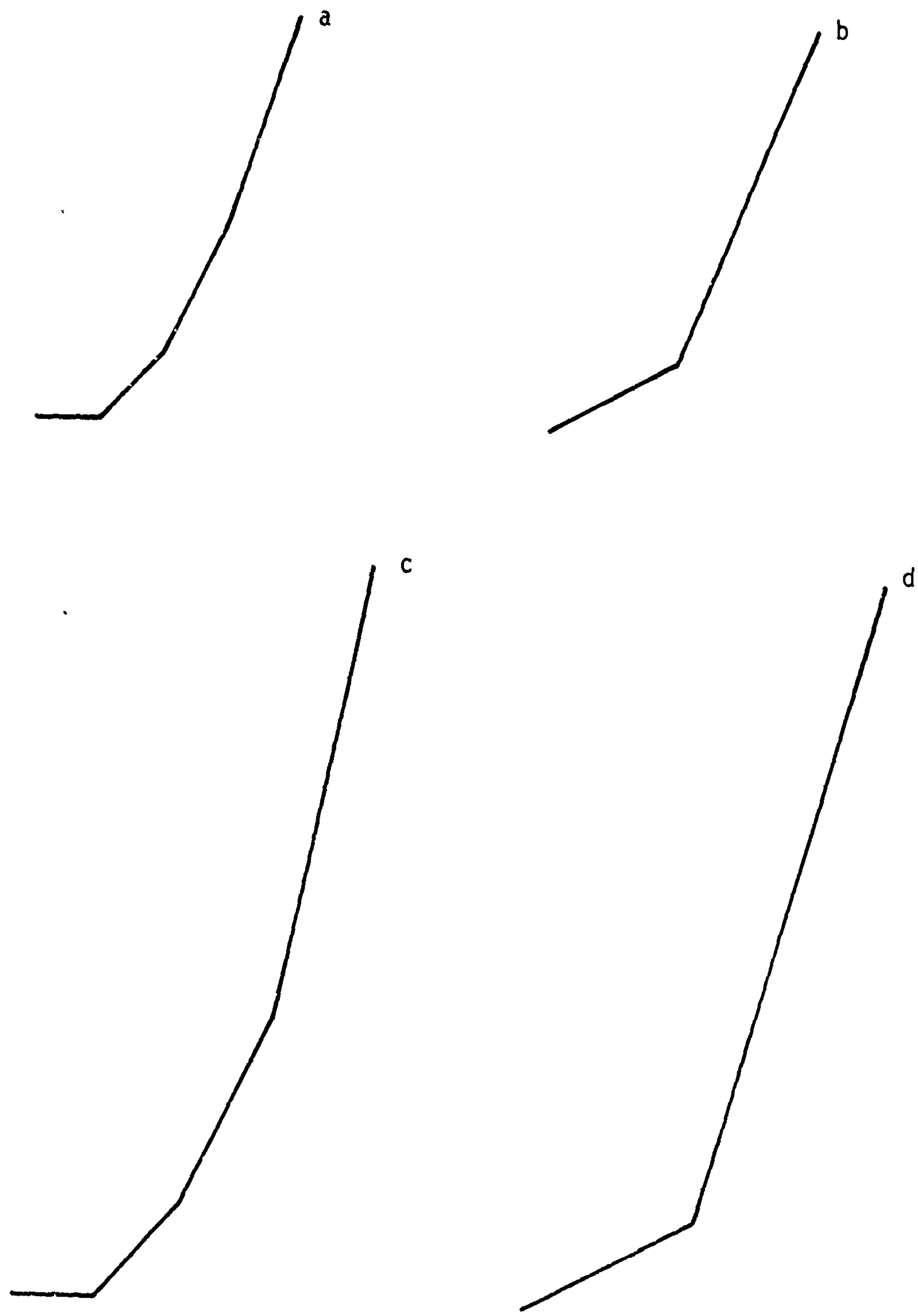


FIG. 42

PROGRAM RESULTS FOR MERCATOR PROJECTION

The precision parameters are

$$k = 0.26 \qquad \bar{\alpha}_{min} = 24^{\circ}(0.418 \text{ rod})$$

$$k_{\alpha} = 1.06 \qquad p_{\ell} = 0.03$$

$$k_{\ell} = 1.4 \qquad p_{\theta} = 0.2$$

and the input and output figures of noise, cost and merit are:

$$f_{w_a} = 4.81 < 6 \quad ; \quad f'_{w_{S.E.}} = 15.7 < 20$$

$$f_{w_\ell} = 5.32 < 6 \quad ; \quad f_c = 3$$

$$f_{w_{S.E.}} = 4.57 < 6 \quad ; \quad f_{m_a} \;\; 27.9 < 60$$

$$f'_{w_a} = 9.3 < 20 \quad ; \quad f_{m_\ell} = 33.0 < 60$$

$$f'_{w_\ell} = 11.0 < 20 \quad ; \quad f_{m_{S.E.}} = 47.1 < 60$$

D) Concluding Remarks

Finally the following example shows the effect of changing n on both $L^*$ and the figures of noise. The drawing L is shown in Fig. 43 (it represents the coastline of the island of Sicily as seen from the Nimbus I satellite). In Fig. 44 a Quantized version is presented which was computed by setting:

$$\ell = 3$$

$$\theta = 10^{\circ} \text{ (0.17 rad)}$$

[illegible] = 1

$$n = 0.16 \; (1/n=6)$$

These values specify the following input figures of noise

$$f_{w_a} = 5.4 < 6 \qquad f_{w_{S.E.}} = 4.57 < 6$$

$$f_{w_\ell} = 4.81 < 6$$

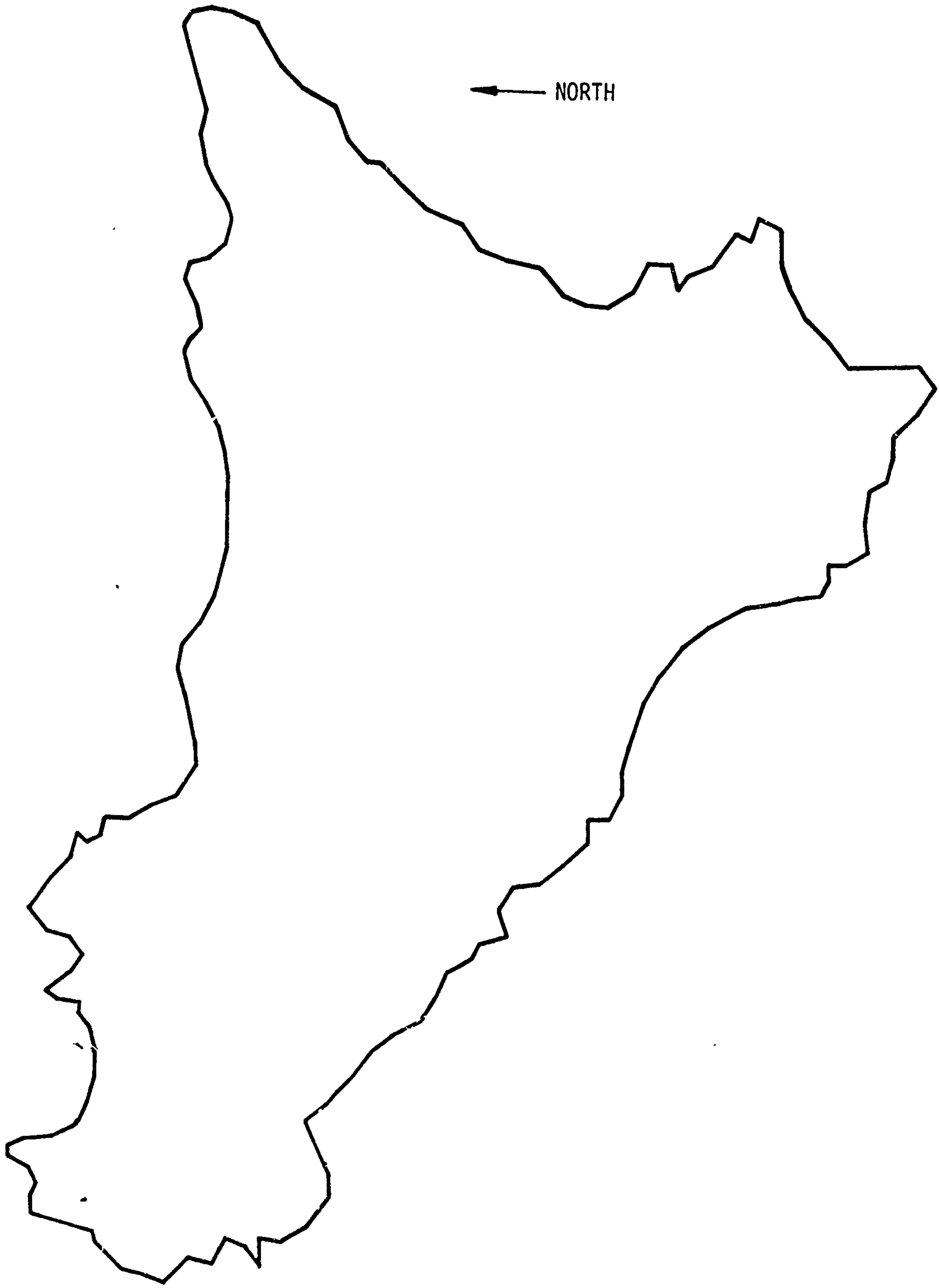


FIG. 43

COASTLINE


FIG. 44

QUANTIZED COASTLINE

However if the following values are chosen

$$\ell = 1$$

$$\theta = 5^\circ \text{ (0.08 rad)}$$

$$T = 1$$

$$n = 5$$

then all the points of L are selected for the quantized version and $L^*$ becomes identical to L. Since there is neither area nor displacement difference between L and $L^*$ it should not come as a surprise that

$$f_{v_a} = 0 \quad ; \quad f_{v_\ell} = 0$$

whereas there is still a nonzero staircase-effect noise due to the fact that L consists of a finite number of points. We have:

$$f_{w_{S.E.}} = 0.1$$

Figs. 45 and 46 show the result of applying a linear transformation to L and to the quantized version of Fig. 44. The transformation consists of an isotropic scaling by a factor of 0.5 followed by a rotation of $60^\circ$. As can be seen the output figures of noise are smaller than the input since the reversible contribution to the figure of noise has been multiplied by a factor smaller than one. This is an obvious result since it only means that in the new drawing (output) the average distance between arc and chord is smaller than for the input drawing. The same is true for $f_{w_a}$ since it is defined in terms of a ratio of areas and lengths; this also holds for $f_{w_{S.E.}}$ which is defined in terms of products of lengths.

FIG. 45

TRANSFORMED COASTLINE

FIG. 46

TRANSFORMED QUANTIZED COASTLINE

We have:

$$f'_{w_a} = 2.94 < 6 \quad ; \quad f_{m_a} = 476.33 < 960$$

$$f'_{w_\ell} = 2.15 < 6 \quad ; \quad f_{m_\ell} = 410.52 < 960$$

$$f'_{w_{S.E.}} = 2.26 < 6 \quad ; \quad f_{m_{S.E.}} = 355.91 < 960$$

$$f_c = 160$$

# IX. SUMMARY AND CONCLUSIONS

## 9.1 General

In previous chapters the problem of how to quantize an irregular line drawing, defined as an abstraction of an image, has been presented and a parametric quantization scheme proposed. Such a scheme generates different results when for the same drawing, a better quality description is required. It has been shown that the qualities of the description of a drawing before and after a regular transformation are directly related. Hence it has been possible to obtain meaningful guidelines for quantizing a given input drawing.

An encoding scheme has been proposed which has the advantage of leading to a code which is both shorter than the standard chain code and easier to manipulate when the applied transformation falls into a certain class. Decomposition of general regular transformations into sets of elementary transformations have been presented and the special case of Mercator Projections has been considered to show how to simplify a transformation problem once the peculiar characteristics of the given transformation are known.

Figures of noise which describe various aspects of quantization noise have been proposed and their relations with the precision parameters ruling the quantization scheme have been studied. Also the effect of a regular transformation on each of the proposed figures of noise has been studied and bounds on their values after a transformation have been obtained.

In order to give a complete presentation of the transformation problem, a figure of cost of a transformation was proposed and a set of figures of merit defined. Such figures of merit specify how much has been spent (figure of cost) in order to achieve a certain quality after a transformation (figure of noise).

In this chapter the specific contributions of this research are pointed out to the reader and possible future extensions are indicated.

## 9.2 Specific Contributions of This Research

A) A new quantization scheme for irregular line drawings has been presented which offers new insight into the problem of quantizing multi-dimensional data. In this presentation an approach, different from a classical one described by Freeman and Glass[17] is introduced. The irregular line drawing is assumed to be an abstraction of an image, that is, an ideal signal. A quantization scheme is then seen as a set of rules which enables one to describe such abstraction in an approximated form. Therefore, it is in the abstracting process that one defines the features of the drawing and chooses the resolution of the quantization scheme so that the features of interest are represented in the quantized version with the desired precision. According to the Freeman and Glass[17] approach the quantization scheme is chosen on the basis of a general curvature criterion and then the features observable in the quantized version of the drawing are determined in terms of the resolution of the quantization scheme. Since the transformation problem is the one of rendering the transformed features of a drawing, a different approach for quantizing drawings has been taken here.

B) Patterns for chain encoded straight line segments have been found by applying the techniques of mathematics of integers and residue arithmetic to the study of special chains. Also a new encoding scheme has been presented which is more efficient than the standard chain code and simplifies the transformation of encoded data.

C) A measure for staircase effect noise has been introduced. Although many claims can be found in the literature about algorithms which reduce the staircase effect, no scheme for measuring it has ever been given before.

D) Simple formulae for evaluating the cost and merit of a quantization scheme have been proposed. In particular, the figure of cost offers insight into the problem of evaluating the cost of transforming one point and the number of points in the quantized drawing.

E) A scheme has been proposed for solving the problem of how to quantize a given drawing so that after a transformation applied to its quantized version the results will have a specified minimum quality.

F) As a practical application, the proposed scheme offers a means for evaluating the quality of computer generated Mercator Maps. This is something which has not been possible in the past.

G) A scheme for non-linearly transforming pictorial data by applying rotations and scalings on a local basis has been presented, together with a theory for decomposing any general transformation into sets of elementary transformations.

H) This thesis has shown that a direct relation exists between the number of chain elements and the percentage length and angle distortion in quantized straight line segments.

I) The advantage of requantizing on finer grids has been shown indirectly, by studying the grid contributions to the transformed figures of noise. Also a systematic way for investigating requantization distortions has been described in terms of geometric regions which depend both on the type of transformation and on the type of quantization scheme used for the transformed data.

## 9.3 Future Extensions

As a possible extension of the work described here it is suggested that a new quantization scheme be studied in which higher-order curves, not only straight line segments, are used in the approximation of an irregular line drawing. The properties of such a quantization scheme and a suitable encoding scheme should be analyzed. The manner and cost of transforming curves encoded in this way would be of considerable interest.

REFERENCES


1. L.J. Bodin, "A Computer Program for the Analysis of Chain Encoded Planar Curves", Technical Note 400-8, New York University, Department of Electrical Engineering, October 1961.

2. H. Blum, "A Transformation for Extracting New Descriptors of Shape", Models for the Perception of Speech and Visual Form, Weiant Wathen-Dunn Editor, Proceedings of a Symposium Sponsored by the Data Science Laboratory, November 1964.

3. J.E. Bresenham, "Algorithm for Computer Control of a Digital Plotter," IBM System Journal, Vol. 4, No. 1, 1965.

4. B.E. Butt and W.J. Snively Jr., "The PAX II Picture Processing System", University of Maryland, Computer Science Center, College Park, Maryland, Technical Report 68-69, May 1968, revised version edited by E.G. Johnson and R. Lipsett.

5. B.E. Butt, E.G. Johnson, P. Kolmus, Y.H. Lee, A. Rosenfeld, E.B. Troy and T. Wells, "Studies in Visual Texture Manipulation and Synthesis 2", University of Maryland, Computer Science Center, College Park, Maryland, Technical Report 69-94, June 1969.

6. L. Calabi and W.E. Hartnett, "Shape Recognition, Prairie Fires, Convex Deficiencies and Skeletons", Amer. Math. Monthly 75, pp. 335-342, 1968.

7. G. Cheng and R. Ledley, "A Theory of Picture Digitization and Applications", Pictorial Pattern Recognition, Proceedings of Symposium of Automatic Photointerpretation, edited by G. Cheng, R. Ledley, B. Polloch, A. Rosenfeld, 1968, Thomson Book Company, Washington, D.C.

8. J. Feder and H. Freeman, "Digital Curve Matching Using a Contour Correlation Technique", IEEE International Convention Record, part 3, 1966.

9. H. Freeman, "On the Encoding of Arbitrary Geometric Configurations", IRE Transactions on Electronic Computers, vol. EC-10, No. 2, June 1961.

10. H. Freeman, "Techniques for the Digital Computer Analysis of Chain Encoded Arbitrary Planar Curves", Proceedings of the National Electronic Conference, Vol. 17, pp. 421-432, 1961.

11. H. Freeman, "On the Digital Computer Classification of Geometric Line Patterns", Proceedings of the National Electronic Conference, Chicago, Illinois, Vol. 18, October 1962.

12. H. Freeman, "Algorithm for Generating a Circle in the Chain Code", New York University, March 1967.

13. H. Freeman, "On the Classification of Line Drawing Data", Pictorial Pattern Recognition, Proceedings of Symposium of Automatic Photointerpretation, edited by G. Cheng, R. Ledley, D. Pollock, A. Rosenfeld, 1968, Thomson Book Company, Washington, D.C.

14. H. Freeman and J. Glass, "On the Quantization of Line Drawing Data", IEEE Transactions on System Science and Cybernetics, Vol. SSC 5, No. 1, January 1969.

15. H. Freeman, "A Review of Relevant Problems in the Processing of Line Drawing Data", Automatic Interpretation and Classification of Images, 1969, Academic Press Inc., New York.

16. H. Freeman, "Boundary Encoding and Processing", Department of Electrical Engineering, New York University.

17. J. Glass, "A Note on the Quantization of Two Dimensional Line Drawings", Technical Report 400-66, New York University, Department of Electrical Engineering, February 1963.

18. R.A. Huber (editor), "Proceedings of the Symposium on Map and Chart Digitizing", Washington, D.C., October 1969, sponsored by: Topographic Division, Geological Survey, U.S. Department of the Interior and Experimental Cartography Unit, Natural Environment Research Council, Royal College of Art, London.

19. J.R. Lourie, "The Computation of Connected Regions in Interactive Graphics", IBM Data Proxessing Division, New York Scientific Center, Technical Report 320-2975, June 1969.

20. U. Montanari, "On Limit Properties in Digitization Schemes, Technical Report, Instituto di Elaborazione dell'Informazione, CNR, Pisa, Italy, 1968.

21. U. Montanari, "A Method for Obtaining Skeletons Using a Quasieuclidean Distance", Journal of the ACM, 15, pp. 600-624, 1968.

22. U. Montanari, "A Note on Minimal Length Polygonal Approximation to a Digitized Contour", Internal Report B68/12, Instituto di Elaborazione dell'Informazione, CNR, Pisa, Italy, 1968.

23. U. Montanari, "Continuous Skeletons from Digitized Images", Journal of the ACM, 16, pp. 534-549, 1969.

24. J. Pfaltz and A. Rosenfeld, "Computer Representation of Planar Regions by Their Skeletons", Communications of the ACM, Vol. 10, No. 2, February 1967.

25. O. Philbrick, "Shape Description with the Medial Axis Transformation", Pictorial Pattern Recognition, Proceedings of Symposium of Automatic Photointerpretation, edited by G. Cheng, R. Ledley, D. Pollock, A. Rosenfeld, 1968, Thomson Book Company, Washington, D.C.

26. A. Pilipchuk, "Mechanical Scanner for Off-Line Picture Digitization", University of Maryland, Computer Science Center, College Park, Maryland, Technical Report 69-92, April 1969.

27. J. Raudseps, "Some Aspects of the Tangent-Angle vs. Arc Length Representation of Contours", Technical Report 1301-6, Ohio State University, Research Foundation, Columbus Ohio, March 1965.

28. A. Rosenfeld, "Connectivity in Digital Pictures", University of Maryland, Computer Science Center, College Park, Maryland, Technical Report 68-81, November 1968.

29. A. Rosenfeld, R.B. Thomas, Y.H. Lee, "Edge and Curve Enhancement in Digital Pictures", University of Maryland, Computer Science Center, College Park, Maryland, Technical Report 69-93, May 1969.

30. A. Rosenfeld, C.M. Park, and J.P. Strong, "Noise Cleaning in Binary Valued Digital Pictures Using Propagation Processes", University of Maryland, Computer Science Center, College Park, Maryland, Technical Report 69-91, May 1969.

31. A. Rosenfeld, "Picture Processing by Computer", Academic Press, New York 1968.

32. D. Rutowitz, "Data Structures for Operations on Digital Images", Pictorial Pattern Recognition, Proceedings of Symposium of Automatic Photointerpretation, edited by G. Cheng, R. Ledley, D. Pollock, A. Rosenfeld, 1968, Thomson Book Company, Washington, D.C.

33. M. Schwartz, "Information, Transmission, Modulation and Noise", McGraw-Hill, New York 1959.

34. G.S. Sebestyen, "Decision Making Processes in Pattern Recognition, ACM Monograph Series, MacMillan Company, New York, 1962.

35. E.B. Socci, "A Study of the Chain Difference Correlation Technique for Contour Line Patterns", Technical Note 400-22, Laboratory for Electroscience Research, Department of Electrical Engineering, New York University, March 1964.

36. W.R. Tobler, "An Experiment in the Computer Generalization of Maps", University of Michigan, Department of Geography, Technical Report 1, Ann Arbor, Michigan, 1964.

37. L. Toralballa, "Calculus with Analytic Geometry and Linear Algebra", Academic Press Textbooks in Mathmatics, New York, N.Y. 1967.